LIGAND-BRIDGED DINUCLEAR CARBONYL COMPOUNDS OF RUTHENIUM AND OSMIUM

Dissertation presented for the degree of Master of Science
in the Department of Chemistry

UNIVERSITY OF CAPE TOWN

by

Paul Mushonga
BSc. (Hons) (UZ)

November 2008

Declaration

I hereby certify that this research is a result of my own investigation and that it has not already been accepted in substance for any degree.

Signed:_____

Paul Mushonga

I hereby certify that this statement is correct.

Signed:_____

Professor J. R. Moss

(Supervisor)

Signed:_____

Professor R. J. Haines

(Co-supervisor)

Department of Chemistry

University of Cape Town

Rondebosch

Cape Town

South Africa

November 2008

Dedication

To my wife Shuvai and my daughter Charity Nyasha,
The LORD richly bless you.

Acknowledgements

I would like to thank the LORD God for directing my footsteps. He is in total control of all things.

My sincere gratitude and appreciation are extended to Professors John R. Moss and Raymond J. Haines for their expert advice and excellent supervision of this work. Thank you very much.

I am also grateful to the following:

- Professor Alan T. Hutton for assisting me with the electrochemistry experiments
- Messrs Peter Roberts and Noel W. Hendricks for recording the NMR spectra and Mr. P. Benincasa for carrying out microanalyses.
- Dr. Hong Su for the determination of the X-ray crystal structures
- The Organometallic Research Group members for all their support.
- The Chemistry Department, UCT for the enabling environment.

I would also like to thank Anglo Platinum and the National Research Foundation (NRF) for financial support.

My wife Shuvai and my precious daughter Charity, your love and support are greatly cherished. Many thanks also go to my parents for their support and encouragement.

Abstract

Ligand-bridged dinuclear carbonyl compounds of ruthenium and osmium have been successfully prepared and characterised by various analytical and spectroscopic techniques. X-ray crystal structures have been determined for the osmium complexes $[Os_2(CO)_4(\mu\text{-}O_2CC_5H_4FeC_5H_5)_2L_2]$ {L = PPh_3 (**102**), py (**103**)}.

Some of the complexes were then investigated for their catalytic activity in the oxidation of cyclohexane and octane. In this work, hydrogen peroxide was used as an oxidant and acetonitrile as the solvent. A higher selectivity for the alcohol products over the ketones was observed. The average ratio of alcohols to ketones was found to be 4.56 and 1.76 for cyclohexane and octane respectively.

The complexes $[Os_2(CO)_6(\mu\text{-}O_2CMe)_2]$ (**4**) $[Ru(CO)_2(\mu\text{–}O_2CMe)_2]_n$ (**86**), $[Ru_2(CO)_4(\mu\text{-}O_2CMe)(\mu\text{-dppm})_2][PF_6]$ (**117**) and $[Ru_2(CO)_4(\mu\text{-}(O_2CMe)_2(MeCN)_2]$ (**118**), were tested as homogeneous catalysts for the isomerisation of terminal alkenes. Complex **4** was inactive while the complex **118** gave a 100 % conversion. It is proposed that the catalysis proceeded via the displacement of one acetonitrile ligand from the metal centre providing a vacant site onto which the substrate coordinated.

The redox behaviour of the four complexes $[Ru_2(CO)_2(\mu\text{-}CO)_2(\mu\text{-}O_2CEt)(N\text{-}N)_2][PF_6]$ {N-N = 1,10-phen (**110**), 5-Me-1,10-phen (**111**), 4-Me-1,10-phen (**112**), 5-Cl-1,10-phen (**113**)}, $[Os_2(CO)_4(\mu\text{-}O_2CC_5H_4FeC_5H_5)_2L_2]$ {L = PPh_3 (**102**), py (**103**)} and $[Ru_2(\mu\text{-}CO)(CO)_4(dppm)_2]$ (**114**) was investigated by cyclic voltammetry in dichloromethane solutions. The complexes **110-113** displayed a single irreversible anodic wave in the range +0.70 to +0.77 V assigned to the one-electron oxidation of the diruthenium core. The complexes **102-103** containing ferrocenyl substituents underwent the reversible oxidation of the ferrocene units followed by the irreversible two-electron oxidation of the diosmium core. The electron-rich complex $[Ru_2(\mu\text{-}CO)(CO)_4(\mu\text{-dppm})_2)]$ (**114**) displayed two irreversible oxidation waves at potentials of +0.02 V and +0.66 V attributed to the oxidation of the diruthenium core and diphosphine ligands respectively.

Conference contributions

Poster entitled "Low oxidation state dinuclear, trinuclear and tetranuclear compounds of ruthenium and osmium in catalytic reactions", P. Mushonga, J. R. Moss and R. J. Haines, presented at the Cape Organometallic Symposium, Organometallics and their Applications (OATA). Cape Town, South Africa (2006).

Poster entitled "Low oxidation state dinuclear, trinuclear and tetranuclear compounds of ruthenium and osmium in catalytic reactions", P. Mushonga, J. R. Moss and R. J. Haines, presented at the 37th International Conference on Coordination Chemistry. Cape Town, South Africa (2006).

Poster entitled "Low oxidation state dinuclear, trinuclear and tetranuclear compounds of ruthenium and osmium in catalytic reactions" , P. Mushonga, J. R. Moss and R. J. Haines, presented at the 15th International Symposium On Homogeneous Catalysis. Sun City, South Africa (2006).

Poster entitled "Low oxidation state dinuclear, trinuclear and tetranuclear compounds of ruthenium and osmium in catalytic reactions" , P. Mushonga, J. R. Moss and R. J. Haines, presented at the Inorganic Conference (INORG007) Club Mykonos, Western Cape, South Africa 2007.

List of abbreviations and symbols

Å	angstrom
bipy	bipyridyl
Bu	butyl
^{o}C	degrees Celsius
cm	centimeter
DMF	dimethylformamide
dmpm	bis(dimethylphosphino)methane
dppe	bis(diphenylphosphino)ethane
dppm	bis(diphenylphosphino)methane
e.e.	enantiomeric excess
Et	ethyl
Fc	ferrocene
g	gram
h	hour(s)
IR	infra-red
L	ligand
M	transition metal
Me	methyl
mg	milligram
mL	millilitre
mmol	millimole
NCMe	acetonitrile
MPa	megapascal
NMR	nuclear magnetic resonance
Ph	phenyl
phen	phenanthroline
Py	pyridine
pyNP	2-(2-pyridyl)-1,8-napththyridine
Pr	propyl
R	alkyl group
THF	tetrahydrofuran

Contents

CHAPTER 2: SYNTHESIS AND CHARACTERIZATION OF CARBOXYL-ATO-BRIDGED COMPLEXES OF RUTHENIUM AND OSMIUM

CHAPTER 1
INTRODUCTION

1.1 Dinuclear ruthenium and osmium carbonyl complexes

Metal clusters are discrete compounds containing three or more metal atoms in which there are substantial and direct interactions between the metal atoms [1a]. Such clusters have interesting structural, chemical and catalytic properties that can often be intermediate between those of mononuclear metal complexes and the bulk metal [1b]. Although they are not considered metal clusters according to the definition, dinuclear compounds receive considerable attention as they are the prototypes of metal cluster compounds.

Binary dinuclear carbonyl derivatives of the iron triad have the general formula $M_2(CO)_9$ [M = Fe, Ru, Os]. Moss *et al.* were the first to successfully prepare the diosmium enneacarbonyl compound $[Os_2(CO)_9]$ as well as report the evidence for the formation of the ruthenium analogue $[Ru_2(CO)_9]$ [2]. These compounds are very unstable. For example, heptane solutions of $[Os_2(CO)_9]$ were reported to decompose to $[Os_2(CO)_8]$ that was thought to be an intermediate in the formation of $[Os_3(CO)_{12}]$ from $[Os_2(CO)_9]$ [2].

Bridging ligands are utilized to stabilize dinuclear and metal cluster compounds to fragmentation. Their function is to maintain the integrity of the metal core during chemical and homogeneous catalytic reactions [3, 4]. Several organic moieties have been used as bridging ligands and these include carboxylato [5], carboxamido [6], pyrazolato [7,8], phosphinato [9], oximato [10], sulphonato [11], pyridine-2-olato [12], 2-diphenylphosphinopyridine [13], 2-diphenylphosphinoquinoline [13], 6-diphenylphosphino-2,2′-bipyridine [13], diphosphines [14] and diphosphazanes [15]. A common feature of these donor ligands is that their atoms are linked through a single atom.

The next sections will focus mainly on carboxylato-bridged dinuclear carbonyl complexes.

1.2 Synthetic routes to the carboxylato-bridged dinuclear carbonyl complexes of ruthenium and osmium

There are three commonly used synthetic routes [16] to the carboxylato-bridged dinuclear compounds of ruthenium and osmium: a) reactions of lower oxidation state complexes with carboxylic acids, b) starting from higher oxidation state complexes and (c) substitution reactions of the dinuclear complexes.

1.2.1 Reactions of lower oxidation state complexes with carboxylic acids

The trinuclear clusters $[Ru_3(CO)_{12}]$ (**1**) and $[Os_3(CO)_{12}]$ (**2**) are used extensively in the synthesis of carboxylato-bridged dinuclear ruthenium(I) and osmium(I) compounds respectively. The synthesis involves the reaction of the clusters with appropriate carboxylic acids at high temperatures for prolonged periods of time [5]. The reaction is an oxidative process and yields insoluble polymeric compounds in the case of ruthenium that are assigned the molecular formula of $[Ru(CO)_2(\mu\text{-}O_2CR)]_n$ and a hexacarbonyl dimer in the case of osmium of the formula $[Os_2(CO)_6(\mu\text{-}O_2CR)_2]$ (R = H (**3**), Me (**4**), Et (**5**), Ph (**6**), etc) [5]. Shvo and coworkers reported that the stabilities of the different carboxylato- complexes that are prepared via this route depend on the nature of the carboxylate ligand [17]. The researchers noted that aliphatic carboxylates have a higher rate of polymerization than aromatic ones attributable to the fact that the aliphatic carboxylates carry a higher electron density. This kinetic effect strongly supports an associative mechanism for the polymerization reaction.

1.2.2 Reduction of higher oxidation state complexes

Kepert *et al.* [18] have developed a facile synthetic route for the synthesis of carboxylato-bridged diruthenium(I) complexes. Polymeric dicarbonyldichloro-ruthenium(II) $[Ru(CO)_2(Cl)_2]_n$ (**7**), prepared from readily available $RuCl_3.xH_2O$, is reduced by reaction with carboxylate salts ($RCO_2^-Na^+$). The target diruthenium(I) complex is then formed by the addition of a two electron donor ligand (**Scheme 1.1**).

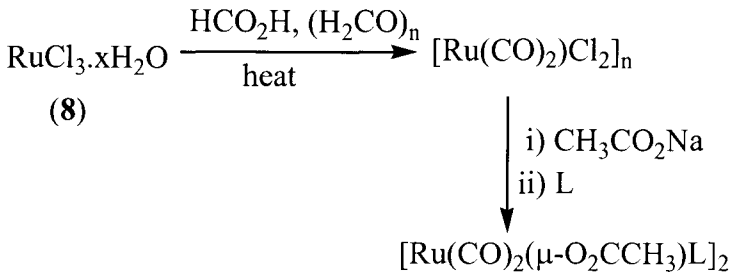

Scheme 1.1

1.2.3. Substitution reactions of the dinuclear complexes

New dinuclear complexes can be synthesized from existing ones through either terminal or bridging ligand substitution. These transformations are discussed in detail in the next section on the reactivities of the dinuclear complexes.

1.3 Chemical reactivities of the carboxylato-bridged dinuclear complexes of ruthenium and osmium

The carboxylato-bridged dinuclear complexes of ruthenium and osmium undergo two modes of reactions that afford a series of new complexes.

1.3.1 Substitution of terminal ligands

The polymer $[Ru(CO)_2(\mu\text{-}O_2CR)]_n$ and the hexacarbonyl dimer $[Os_2(CO)_6(\mu\text{-}O_2CR)_2]$ react with two-electron donor ligands yielding complexes of the type $[M_2(CO)_4(\mu\text{-}O_2CR)_2L_2]$ (M = Ru, Os) in which the axial positions are occupied by new ligands [5, 19, 20]. Mono-substituted osmium complexes of the formula $[Os_2(CO)_5(\mu\text{-}O_2CR)_2L]$ (L = PPh_3 or PMe_2Ph) have been synthesized by using ligand L under mild conditions to displace the coordinated THF ligand from the pentacarbonyl $[Os_2(CO)_5(\mu\text{-}O_2CR)_2(THF)]$ complex prepared from $[Os_2(CO)_6(\mu\text{-}O_2CR)_2]$ in refluxing THF [20].

1.3.2. Substitution of bridging ligands

Bridging ligands and carboxylato-bridges in particular can be replaced by three-electron donor anionic bridging ligands such as diamides, thiolates or other carboxylate ligands. Sherlock *et al.* [21] reported the synthesis of dinuclear ruthenium complexes $Ru_2(CO)_4(\ -L)_2(PPh_3)_2$ [L = $NC_3H_4S_2^-$ (**9**), $NC_5H_4O^-$ (**10**)] from the reactions of appropriate sodium salts with $[Ru_2(CO)_4(\ -O_2CCH_3)_2(PPh_3)_2]$ (**11**). Ros and co-workers [22] also reported the displacement of the carboxylato-bridge in **11** using thiolate ligands.

The polymeric complex $[Ru(CO)_2(\mu\text{-}O_2CR)]_n$ reacts with pyrazole or 3,5-dimethylpyrazole to afford a diruthenium derivative containing either homo- or heterobridges, $[Ru_2(CO)_4(\mu\text{-}Pz)_2(HPz)_2]$ (**12**) and $[Ru_2(CO)_4(\mu\text{-}Pz')(\ -O_2CCH_3)(HPz')_2]$ (**13**) respectively [23]. The heterobridged complex **13** was further shown to undergo displacement of the carboxylato-bridge by anionic σ-donor ligands such as the thiolate or pyrazolate ligands affording the respective heterobridged complexes. The less flexible bidentate ligands such as 2,2′-bipyridyl and phenanthroline selectively cleave the carboxylato-bridge to give the cationic complex $[Ru_2(\mu\text{-}Pz')_2(\ -CO)_2(CO)_2(N\text{-}N)_2]^+$.

The formate complex $[Ru_2(CO)_4(\ -O_2CH)_2(PPh_3)_2]$ (**14**) reacts with primary alcohols *iso*-pentanol or *n*-butanol [24] in refluxing toluene for 24h to yield carboxylato-bridged complexes (**Scheme 1.2**)

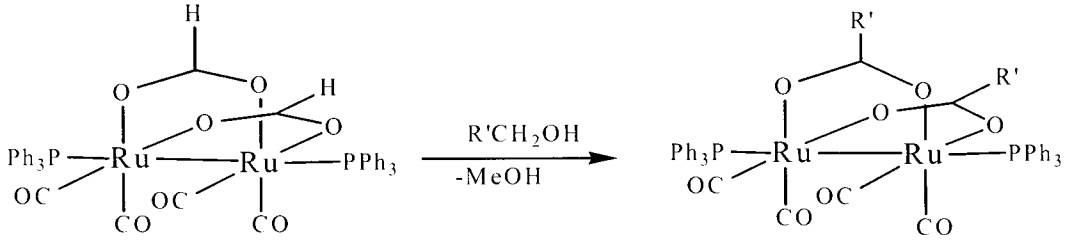

(**14**)

R' = $(CH_3)_2CHCH_2$ (**15a**)
or $CH_3CH_2CH_2$ (**15b**)

Scheme 1.2

1.4 Factors influencing the ruthenium-ruthenium bond distance in ligand bridged diruthenium(I) complexes

The metal-metal bond distances in ligand bridged diruthenium(I) complexes depend upon the nature and proximity of the axial ligands. Using 1,8-naphthyridine-based ligands with hydrogen, furyl, thiazolyl, pyridyl and pyrolyl substituents at the 2-position, Patra *et al.* showed that the gradual increase in the Ru-Ru distances was directly related to the increasing donor strength of the ligands. [25] (see **Table 1.1**). The longest Ru-Ru distance of 2.6969(10) was observed for complex **16e** while the shortest distance of 2.6071(9) was observed for complex **16a.** The complexes **16c** and **16d** with thiazolyl and pyridyl substituents at the 2-position respectively that are of comparable donor abilities had similar Ru-Ru bond distances. **Figure 1.1** shows the typical manner in which the 1,8-naphthyridine-based ligands coordinate to the diruthenium unit.

Table 1.1 Ru-Ru and Ru-L bond distances for diruthenium complexes with 1,8-naphthyridine-based ligands [25]

Compound	**Interatomic distances,**		
	Ru-Ru	**Ru-O(axial)**	**Ru-N(axial)**
$[Ru_2(3\text{-}MeNP)_2(CO)_4(OTf)_2]$ **(16a)**	2.6071(9)	2.267(4)	
$[Ru_2(fuNP)_2(CO)_4][BF_4]_2$ **(16b)**	2.6261(9)	2.300(5)	
		2.294(5)	
$[Ru_2(tzNP)_2(CO)_4][ClO_4]_2$ **(16c)**	2.6734(7)		2.183(2)
$[Ru_2(pyNP)_2(CO)_4][OTf]_2$ **(16d)**	2.6792(9)		2.171(4)
			2.179(4)
$[Ru_2(prNP)_2(CO)_4]$ **(16e)**	2.6969(10)		2.142(5)
			2.142(5)

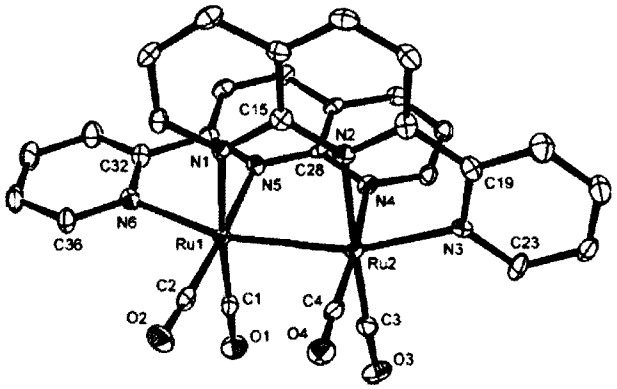

Figure 1.1 ORTEP diagram of the di-cation $[Ru_2(pyNP)_2(CO)_4]^{2+}$ in compound $[Ru_2(pyNP)_2(CO)_4][OTf]_2$ (**16d**) [25] .

Results from electronic studies of complexes of the type $[Ru_2(CO)_4(\mu\text{-}O_2CR)_2L_2]$ have been used to explain the varying sensitivities of the metal-metal bond lengths to axial coordination and the inductive effect of the R group of the bridging carboxylate ligand (see **Table 1.2**) [26]. When π-acid ligands occupy the axial positions, electron transfer from the filled M-M antibonding orbitals to the axial ligand antibonding orbitals strengthens the M-M bonding interaction by increasing the M-M bond order. In the presence of strong σ-donor ligands with or without π-accepting ability in axial positions such as pyridine, the M-M bond order decreases by bonding interactions through the M-M antibonding orbitals.

Table 1.2 Selected bond distances for complexes of the formula $[Ru_2(CO)_4(\mu\text{-}O_2CR)_2L_2]$ [26]

Compound		Average interatomic distances,			
R	**2L**	**Ru-O**	**Ru-CO**	**Ru-L**	**Ru-Ru**
Me	2 CO	2.094	1.845	1.976	2.689
Me	2 py	-	1.84	-	2.678
Me	2 PPh_3	2.119	1.834	2.451	2.736
CF_3	2 PPh_3	2.149	1.836	2.446	2.728
Pr^n	2 P^tBu_3	2.13	1.83	2.622	2.728
4-F-C_5H_4	{CO, H_2O}	2.119	1.851	1.999 [a], 2.999 [b]	2.649
Ph	2 $PhCO_2H$[c]	2.134	1.834	2.265	2.637
Ph	2 $PhCO_2$[d]	2.130	1.829	2.299	2.639
Ph	2 CO	2.108	1.840	2.013	2.704
Ph	2 PPh_3	2.116	1.834	2.437	2.741

[a] Ru–CO distance, [b] Ru–OH_2 distance, [c] There exists two intramolecular hydrogen bonds between $PhCO_2H$ and one bridging PhCOO ligand, [d] Oxygen atoms of the neighbouring bridging carboxylates coordinate with the Ru atoms in the axial positions

1.5 Reactions of carboxylato-bridged complexes with bidentate ligands

Using different starting materials, Sherlock *et al.* [27] reported the influence of solvent in the reactions of the carboxylato-bridged complexes of ruthenium with bidentate ligands. On the one hand, when the acetonitrile dimer $[Ru_2(CO)_4(\mu\text{-}O_2CCH_3)_2(NCCH_3)_2]$ (**17**), reacts with two equivalents of the diphosphine in refluxing THF, the bidentate ligand coordinates to the metal centers in a ^{1}-fashion trans to the metal-metal bond.

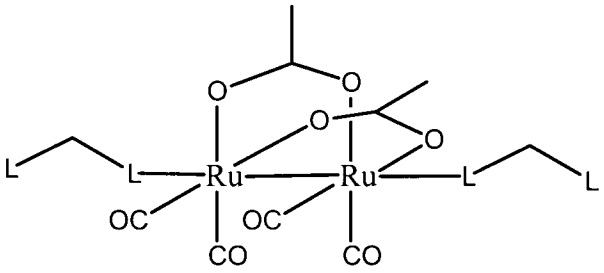

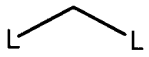

= dppm (**18**)
dmpm (**19**),

On the other hand, a cationic di-substituted complex is formed when the polymer reacts with two molar equivalents of the bidentate ligand in refluxing alcohols. This is a result of the displacement of an anionic ligand by the incoming ligands. The researchers reported that dppm formed a diphosphine-bridged complex and dppe formed a diphosphine-chelated complex consistent with the known bridging properties of dppm and the chelating properties of dppe [27].

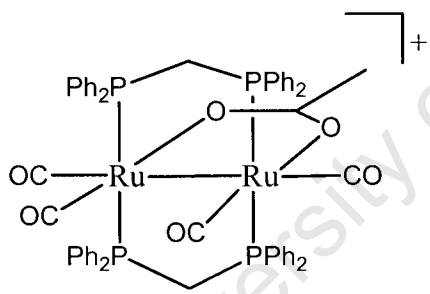

(**20**)

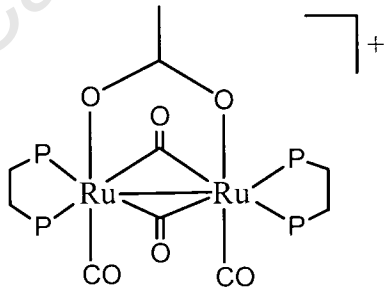

(**21**)

1.6 Some catalytic applications of binuclear, trinuclear and tetranuclear ruthenium and osmium compounds

Low oxidation state compounds of ruthenium and osmium are emerging as important catalysts in several industrial processes. Catalysis by these compounds affords the possibility of multi-site interactions with substrate molecules [1b]. This opens up mechanistic pathways that are not available to mononuclear complexes [28, 29].

The presence of ligands that are capable of stabilizing the metal framework is considered to be important in catalytic reactions [15, 30]. The ligands can allow for

reversible metal-metal bond cleavage which can be an important step in homogeneous catalytic processes [31, 32].

A survey of some reactions catalyzed by binuclear, trinuclear and tetranuclear ruthenium and osmium compounds is given below.

1.6.1. Isomerisation of alkenes

Migration of the carbon-carbon double bond in alkenes is a well-studied catalytic reaction. Salvini *et al.* [33] reported that the non-hydridic phosphine substituted ruthenium carbonyl carboxylato-bridged dinuclear complexes $[Ru_2(CO)_4(\ -O_2CMe)_2(PBu_3)_2]$ (**22**) and the tetranuclear complex $[Ru_4(CO)_8(\mu\text{-}O_2CMe)_4(PBu_3)_2]$ (**23**) were active catalysts for the isomerisation of 1-hexene. In the presence of complex **23** in n-heptane solution at 80°C, terminal olefins are activated through the opening of the oxygen bridge linking the two $[Ru_2(CO)_4(\ -O_2CMe)_2(PBu_3)]$ moieties affording the complex $[Ru_2(CO)_4(olefin)(\ -O_2CMe)_2(PBu_3)]$ (**24**) (see **Scheme 1.3**). Isomerisation to give an internal olefin takes place reducing its coordinating ability and its subsequent replacement by another terminal olefin takes place. The tetranuclear complex is only regenerated at low terminal olefin concentrations [33].

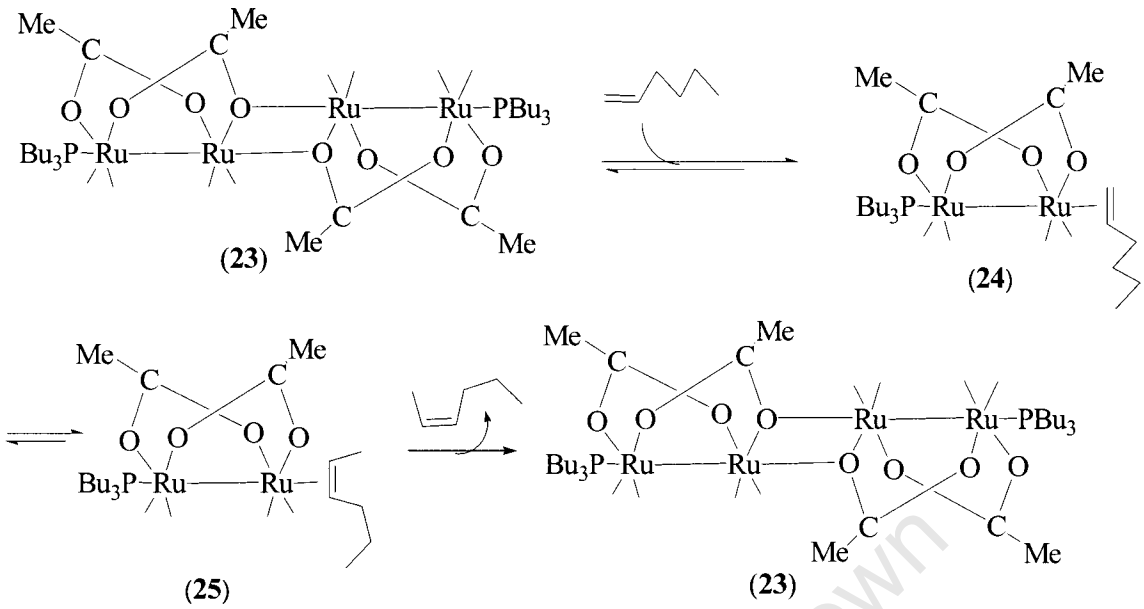

Scheme 1.3

The catalysis by complex **22** was reported to proceed via the displacement of one phosphine ligand by 1-hexene affording the ruthenium complex **24**.

The trinuclear ruthenium carbonyl derivative $[Ru_3(CO)_{10}(dppm)]$ (**26**) catalyzes the isomerisation of 1-hexene at low hydrogen pressures (0.7 MPa) affording *cis*-2-hexene as the major product (Eqn.1.1) [34].

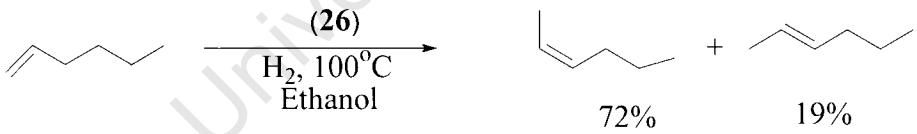

Eqn. 1.1

The isomerisation is effected by the dppm substituted cluster on the basis of the observed turnover frequencies that increase with increasing amount of the cluster. The tetra-substituted ruthenium carbonyl derivative $[Ru_3(CO)_8(dppm)_2]$ (**27**) also catalyses the isomerisation of 1-hexene affording high yields of the *cis*-2-hexene as the major product at low hydrogen pressures and in polar solvents [35]. Its catalytic activity has been reported to be less than that of complex **26** with only one bidentate ligand and this was attributed to steric effects.

The chiral tri-osmium cluster $[(\mu\text{-H})Os_3(\mu\text{-X})(CO)_{10}]$(X = OCNHMe) (**28**) catalyzes the isomerisation of the *N*-allylic substrate N-2-propenylacetamide to N-1-propenylacetamide at room temperature (Eqn. 1.2) [36].

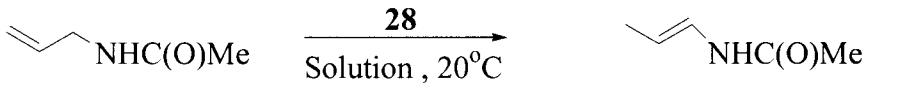

Eqn. 1.2

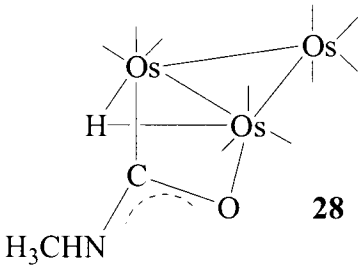

28

The nature of the bridging μ-X ligand is important in the catalytic system as no conversion is detected for complexes with other 3-electron μ-X donor ligands (X= $OOCCH_3$ (**29**), $NHCH_2CHCH_2$ (**30**), Br (**31**)). The reaction proceeds via the insertion of an alkene into the Os-O bond with the coordination of the double bond to Os. This is followed by hydrogen bond formation between the α C-H and the acyl oxygen affording a five-membered ring. Subsequent cleavage of the C-H bond takes place resulting in protonation of the acyl oxygen. A [1,2]-double bond shift occurs and the acyl oxygen is deprotonated followed by the release of the alkene and the regeneration of the cluster (see **Scheme 1.4** in which the catalyst is a carboxamido complex **28** or **30** and carbonyl ligands are omitted for clarity).

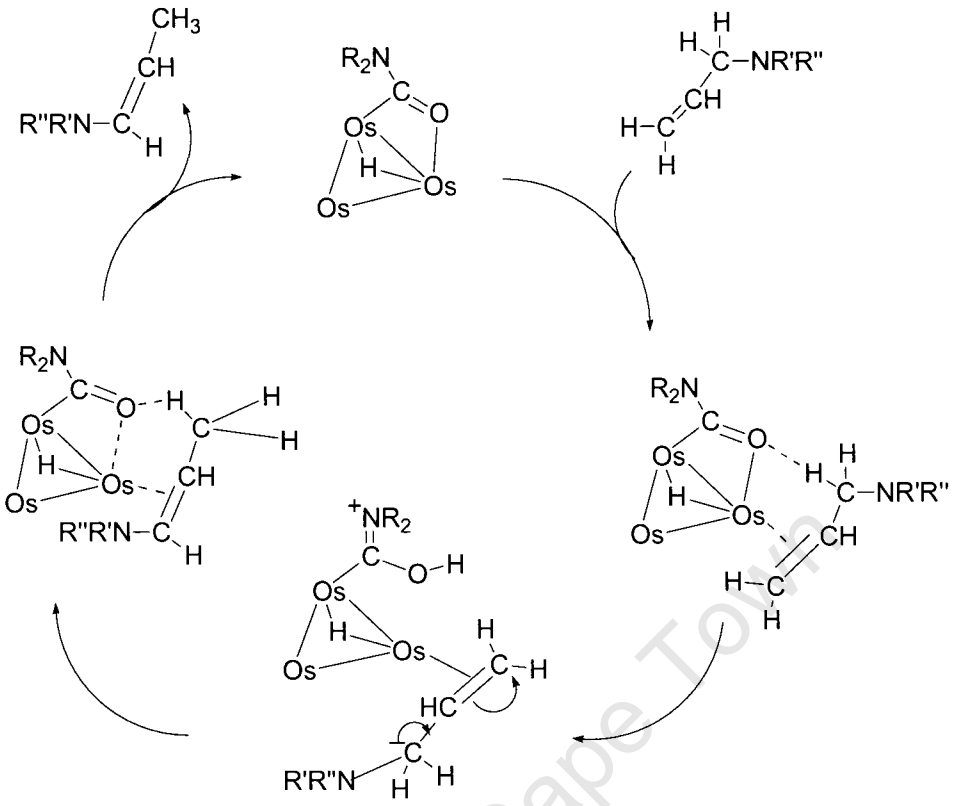

Scheme 1.4

1.6.2 Hydrogenation of alkenes and alkynes

The selective hydrogenation of alkenes and alkynes remains an important issue in catalysis. The ruthenium carbonyl carboxylato-bridged complex with nitrogen-containing ligands $[Ru_2(CO)_4(\ -O_2CCH_3)(bipy)_2][CH_3CO_2]$ (**32**) catalyses the hydrogenation of phenylethyne to styrene (18 %) and ethylbenzene(3 %) in the presence of water or polar solvents with low catalytic activity [37]. The complex $[Ru_2(CO)_4(\ -O_2CCH_3)(phen)_2][CH_3CO_2]$ (**33**) also catalyses the same reaction.

The diphenylphosphido-bridged triruthenium cluster $[Ru_3(CO)_9(\ -H)(\ -PPh_2)]$ (**34**) catalyzes the hydrogenation of an alkyne substrate. The process involves the loss of a CO ligand and the formation of a $[Ru_3(\ ^2\text{-PhC=CHPh})(CO)_8(\ -H)(PHPh_2)]$ (**35**) vinyl hydride resting state [38]. The reaction is affected by the polarity of the solvent with a more polar solvent facilitating the elimination of the alkene from the catalytic intermediate. No cluster fragmentation was observed in this system.

Gervasio *et al.* [39] reported the catalytic hydrogenation of acetylene by $[Ru_3(CO)_9L_3]$ (L= PPh_3 (**36**) or PEt_3 (**37**)) with activity being influenced mainly by the chemical reactivity of the clusters, that is their tendency to fragment or disproportionate. The triphenylphosphine-substituted complex was reported to be more catalytically active than the triethylphosphine-substituted derivative indicating that the electron donor ability of the phosphine ligand plays a role in catalytic activity. The electron-withdrawing triphenylphosphine weakens the cluster framework and favours catalysis by fragments and this was confirmed by the decrease in turnover numbers with a decrease in substrate/cluster ratios for the two derivatives.

The triruthenium hydride derivative $[HRu_3(CO)_9(\ _3-\ ^3$-1,3 dithiacyclohexane)] (**38**) acts as a moderately active catalyst in 1-hexene hydrogenation to hexane [40]. The catalytic cycle is given in **Scheme 1.7**:

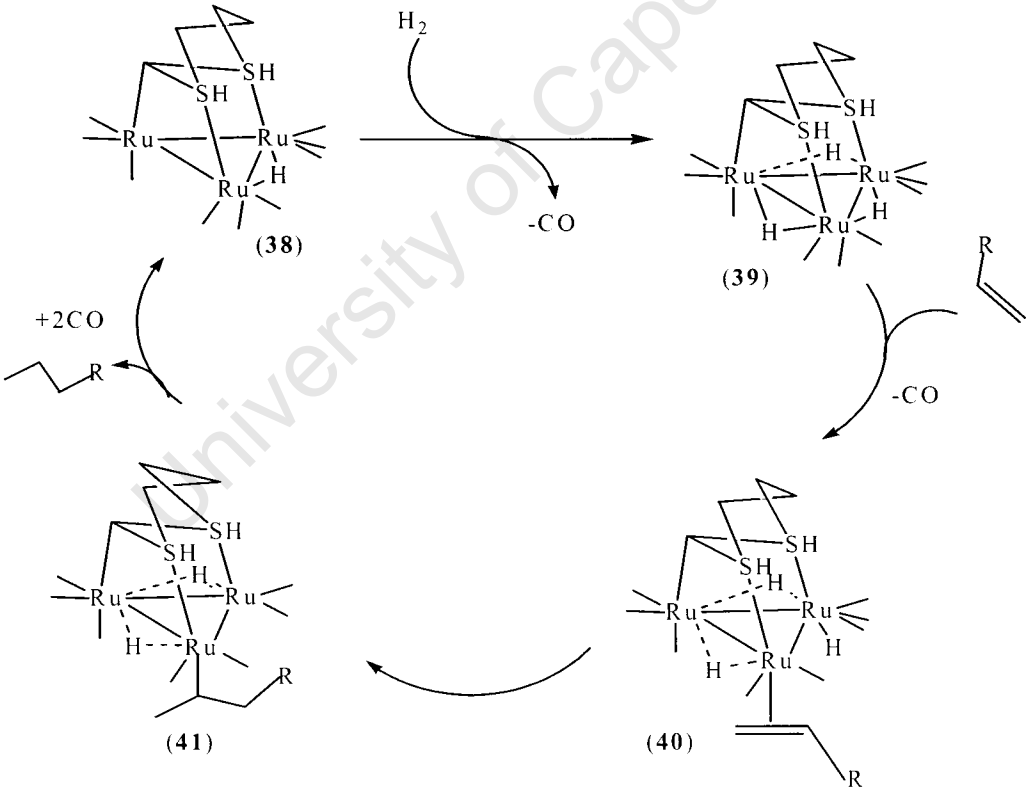

Scheme 1.7

The water soluble ruthenium carbonyl clusters $[Ru_3(CO)_{12-x}(TPPTN)_x]$ {x = 1 (**42**); 2 (**43**) or 3 (**44**) (TPPTN = tris(3-sulfonatophenyl)phosphine tri-sodium salt)} are catalyst precursors for the hydrogenation of non-activated alkenes under biphasic conditions and pressures of 6 MPa at 60°C with catalytic activity increasing with

increasing number of phosphine ligands [41]. Repeated use of the catalysts results in loss of catalytic activity. The tetranuclear cluster $[H_4Ru_4(CO)_{11}(TPPTN)]$ (**45**) also acts as a catalyst precursor for the hydrogenation process [41].

The benzyne-substituted clusters $[Ru_3(CO)_7(\mu\text{-}PPh_2)_2(C_6H_4)]$ (**46**) and $[Ru_4(CO)_{11}(\mu_4\text{-}PPh)(C_6H_4)]$ (**47**) as well as the alkyne-substituted analogues $[Ru_3(CO)_7(\mu\text{-}PPh_2)_2(HC_2Ph)]$ (**48**) and $[Ru_4(CO)_{11}(\mu_4\text{-}PPh)(C_2Ph_2)]$ (**49**) catalyze the homogeneous hydrogenation of alkynes and of 1,4-cyclohexadiene [32]. The benzyne substituted clusters show the highest hydrogenation activity towards the alkynes, with the activity related to the nature of the alkyne substrates (C_2Et_2< EtC_2Ph < C_2Ph_2). Cluster catalysis in these systems is supported by the recovery of large amounts of clusters after the reactions as well as the observed dependence of the catalytic activity on the substrate and cluster concentrations and the high selectivity towards cis-stilbene when C_2Ph_2 is used as a substrate.

The triphenylphosphine-substituted clusters $[Ru_3(CO)_{12-x}(PPh_3)_x]$ {x = 1 (**50**) or 2 (**51**)} complexes act as catalysts for the hydrogenation of alkenes and alkynes [42]. Blazina *et al.* reported that whether catalysis was by intact or fragmented clusters depended on the polarity of the solvent. In non-polar solvents, the catalyst fragments to $[Ru(H)_2(CO)_2(PPh_3)(substrate)]$ (**52**), while in polar solvents the catalyst undergoes rapid CO loss to yield a vacant coordination site that reacts with C_2Ph_2 with fast hydride transfer and subsequently generating the cis-stilbene.

The catalytic activity of the cluster complex $[Ru_3(\mu\text{-}H)(\mu_3\text{-}ampy)(CO)_8(PPh_3)]$ (**53**) (Hampy = 2-amino-6-methylpyridine) in the homogeneous hydrogenation of diphenylacetylene under mild conditions of 80 ^oC and hydrogen pressure of <1atm giving *cis*- and *trans*-stilbene (catalytic turnover frequency 10.9 h^{-1}) has been reported [43]. A kinetic study of the reaction showed it to be first order in cluster and hydrogen concentration and negative or zero order in substrate concentration supporting the idea of cluster catalysis. The cationic cluster $[Ru_3(\mu\text{-}H)(\mu_3\text{-}ampy)(\mu,\eta^1\text{:}\eta^2\text{-}PhC{=}CHPh)(CO)_8][BF_4]$ (**54**) also catalyses the hydrogenation of diphenylacetylene to *cis*- and *trans*-stilbene under very mild conditions of less than 1 atm at 60 ^oC [44].

The trinuclear osmium cluster $[Os_3(CO)_{12}]$ (**2**) and its anionic hydride derivative $[PPN][HOs_3(CO)_{11}]$](PPN = $[(Ph_3P)_2N]^+$) (**55**) [28] are effective catalyst precursors in the hydrogenation of cyclohexene to cyclohexane under moderate conditions with the activity of the anionic catalyst being considerably less than that of the neutral one.

The tetranuclear osmium clusters [28] $[H_4Os_4(CO)_{12}]$ **(56)**, $[PPN][H_3Os_4(CO)_{12}]$ (PPN = $[(Ph_3P)_2N]^+$) (**57**), $[H_3Os_4(CO)_{12}I]$ (**58**), $[H_3Os_4(CO)_{12}(NO)]$ (**59**) and $[H_3Os_4(CO)_{12}(MeCN)_2][BF_4]$ (**60**), are efficient catalysts for olefin hydrogenation under moderate conditions with the coordinatively unsaturated species with butterfly structures (complexes **58-60**) exhibiting higher catalytic activity than the closed saturated species with closed structures (complexes **56** and **57**).

The hydrido tetranuclear ruthenium clusters $[H_4Ru_4(CO)_{12}]$ (**61**) and $[H_2Ru_4(CO)_{13}]$ (**62**) were shown to hydrogenate 1,3-cyclohexadiene to cyclohexene with 100 % selectivity, but with relatively low turnover numbers that only increased with time [45]. Higher turnover numbers and low selectivity were observed when the isomer 1,4-cyclohexadiene was the substrate.

1.6.3 Hydrogenation of ketones and unsaturated carboxylic acids

The acetate-bridged ruthenium carbonyl complexes with nitrogen-containing ligands, $[Ru_2(CO)_4(\ -O_2CCH_3)(bipy)_2](CH_3CO_2)$ (**32**) and $[Ru_2(CO)_4(\ -O_2CCH_3)(phen)_2]$-$(CH_3CO_2)$ (**33**) catalyse the hydrogenation of acetone to propan-2-ol under conditions of 10 MPa of hydrogen pressure at 100 °C with catalytic activity increasing with the polarity of the solvent [37]. Higher activity for the hydrogenation of the C=C bonds compared to the C=O bonds is observed in unsaturated ketones. Cyclohex-2-en-1-one is hydrogenated to cyclohexanone (56 %) and cyclohexanol (44 %) in the presence of catalytic amounts of **32** under the same conditions. The complexes $[Ru_2(CO)_4(\ -O_2CMe)_2(PBu_3)_2]$ (**22**) and $[Ru_4(CO)_8(MeCO_2)_4(PBu_3)_2]$ (**23**) catalyze the hydrogenation of acetic acid to ethyl acetate at temperatures of 140 °C and 160 °C respectively [46].

The water-soluble and air-stable triruthenium carbonyl cluster $[Ru_3(CO)_9(TPPMS)_3]$ (**63**) (TPPMS = sodium diphenylphosphinobenzene-*m*-sulphonate) acts as a catalyst

precursor in the hydrogenation of acrylic acid and phenyl ethylene yielding propionic acid (94 %) and phenylethane (85 %) respectively (see Eqns. 1.3 and 1.4) [47].

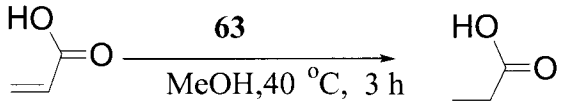

Eqn. 1.3

94 % , Turnover = 780 h^{-1}

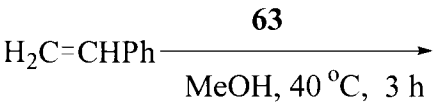

CH_3CH_2Ph Eqn. 1.4

85 % , Turnover = 712 h^{-1}

Both IR and XPS studies of the catalyst before and after the reaction show that the cluster remains intact throughout the reaction indicating cluster catalysis [47].

The hydrogenation of styrene to ethylbenzene in decalin solution is effectively catalyzed by the tetranuclear osmium complexes $[H_4Os_4(CO)_{12}]$ **(56)**, $[PPN][H_3Os_4(CO)_{12}]$ **(57)**, $[H_3Os_4(CO)_{12}I]$ **(58)** and $[PPN][H_2Os_4(CO)_{12}I]$ **(64)** (PPN = $[(Ph_3P)_2N]^+$) at ambient or sub-ambient pressures [48]. These complexes are known to be both thermally and oxidatively stable reducing the probability of facial fragmentation processes taking place under experimental conditions. Homogeneity tests have established that the hydrogenation reactions are truly homogeneous [48].

1.6.4 Asymmetric and transfer hydrogenation

The tetranuclear carbonyl hydrido clusters consisting of enantiomeric pairs, $[H_4Ru_4(CO)_{10}\{$ -1,2-(R/S,R/S)-BDPP$\}]$ **(65)** and $[H_4Ru_4(CO)_{10}\{$ -1,1-(R/S,R/S)-BDPP$\}]$ **(66)** catalyze the asymmetric hydrogenation of trans-2-methyl-2-butenoic acid under relatively mild reaction conditions of 5 MPa hydrogen and 100 °C with high conversion rates (75-100 %) [49]. The predominating enantiomeric form of the hydrogenated product strongly depends upon the enantiomeric form of the ligand.

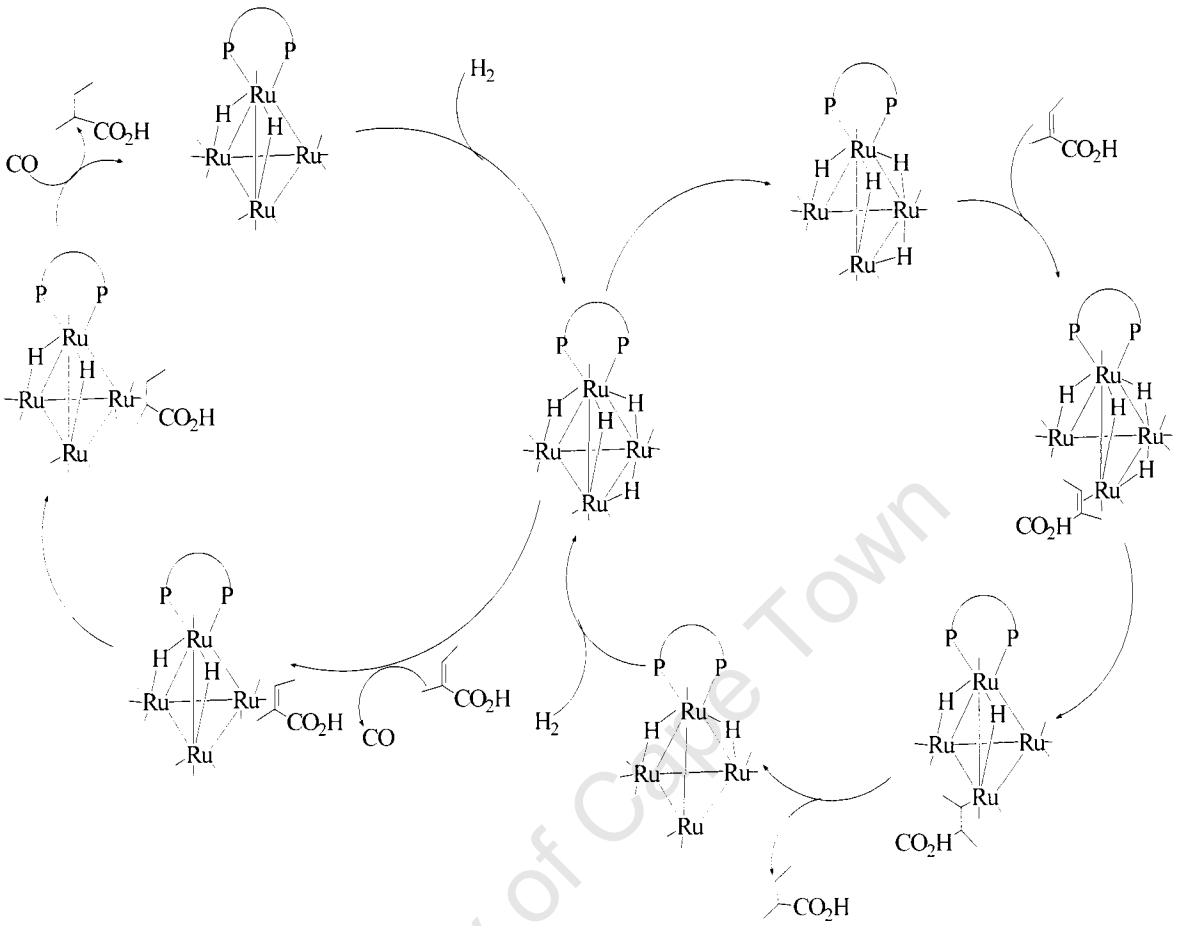

Scheme 1.8

The researchers Homanen *et al.* proposed that a mechanism involving heterolytic cleavage of a Ru-Ru bond to form a two-electron deficient 60-electron intermediate was more likely as a way of introducing the substrate into the ligand sphere of the cluster catalyst when the expected low partial pressure of CO is taken into account (see **Scheme 1.8**). The low partial pressure makes CO re-association unlikely (for the cycle involving dissociation of carbonyl).

The transfer hydrogenation of alkynes (Ph_2C_2, PhC_2Me, Et_2C_2 and Pr_2C_2) in the presence of a diruthenium complex $[Ru_2(\mu\text{-}CO)(CO)_4(\mu\text{-}dppm)_2]$ (**67**) using formic acid as a hydrogen donor has been reported [50]. The internal alkynes react with HCOOH in acetone at room temperature for one day affording the pure cis-alkene with no trace of trans-alkene or further hydrogenation to alkane. The reaction proceeds via the fast decomposition of formic acid to give CO_2 and H_2 followed by

the slow hydrogenation of the alkyne to afford the cis-alkene. The authors Gao *et al.* reported that excess HCOOH is required to supply excess H_2 for the slow second step.

The chiral ruthenium cluster $[H_4Ru_4(CO)_8[(-)\text{-DIOP}]_2]$ {DIOP = 2,3-(isopropyl-idenedioxy)-2,3-dihydroxy-l,4-bis(diphenylphosphanyl)butane)} (**68**) catalyzes the asymmetric hydrogenation of α, β unsaturated mono- and dicarboxylic acids achieving up to 68 % e.e. for the unsaturated monocarboxylic acids and 10 % e.e. for unsaturated dicarboxylic acids [51]. Severe reaction conditions of 90-120 °C and 13 MPa hydrogen are required. The reduction of the carbon-carbon double bond is achieved with high selectivity.

The transfer hydrogenation of ketones [52] with secondary alcohols as hydrogen source affords low optical yields of the products (see Eqn. 1.5).

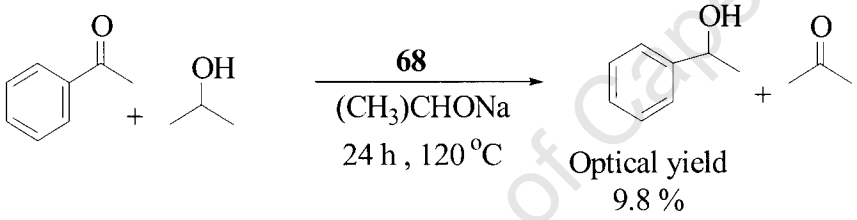

Eqn. 1.5

The chiral tetranuclear ruthenium complexes $[H_4Ru_4(CO)_8[(+)(-)\text{-DIOP}]_2]$ (**69**) and $[(-)\text{-}Ru_4(CO)_8[glu]_2[(+)\text{-DIOP}]_3]$ (**70**) have been reported as catalysts in the reduction of prochiral -nitroketones [53].

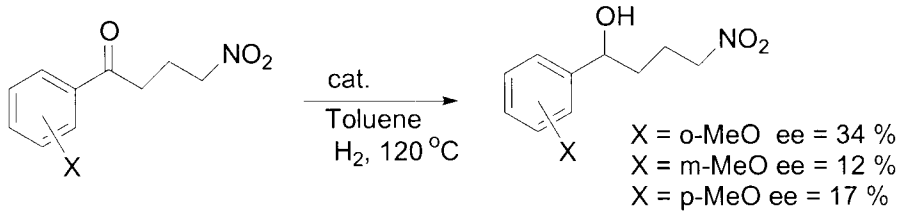

Eqn. 1.6

1.6.5 Hydroformylation reactions

The hydroformylation of alkenes is an important commercial application of homogeneous catalysis involving transition metal catalysts. The tetranuclear ruthenium carbonyl cluster $[H_4Ru_4(CO)_{12}]$ (**61**) selectively catalyzes the

hydroformylation of olefins with CO_2 as a reactant in the presence of the salt LiCl affording the corresponding alcohols in high yields (Eqn. 1.7) [54,55].

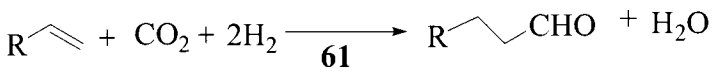

Eqn. 1.7

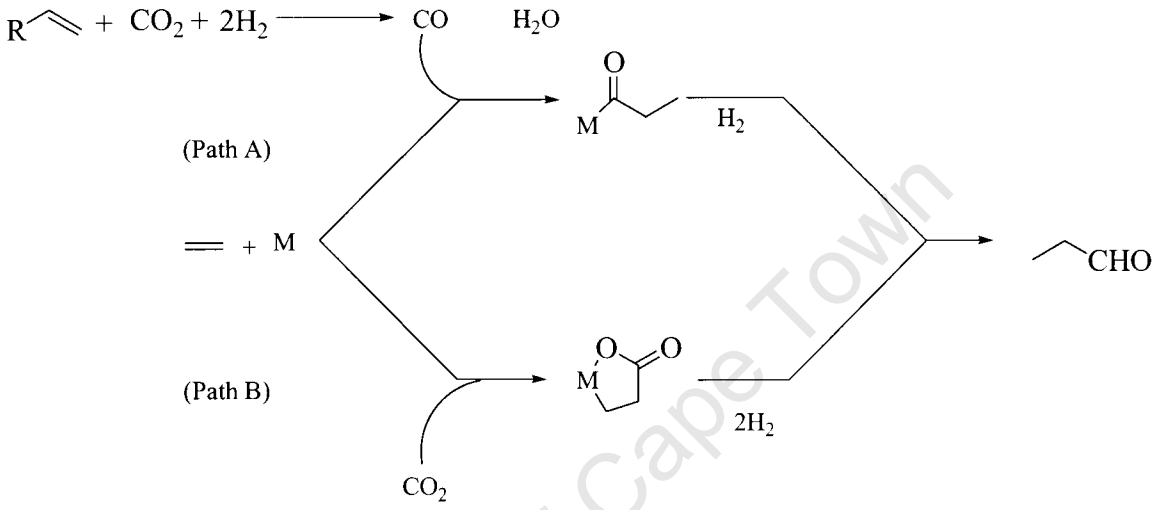

Scheme 1.9

Two possible pathways for the synthesis of aldehydes from alkenes, CO_2 and H_2 have been proposed (see **Scheme 1.9**). Path A involves the hydroformylation of the alkene with the CO formed by the hydrogenation of CO_2 while Path B involves the hydrocarboxylation reaction. The contribution from Path B was reported to be very small as no formation of metallocyclic complex was observed. The activity of the tetranuclear ruthenium complex towards the hydrogenation of CO_2 to CO (Path A) is strongly dependent on the nature of added salts. When halide salts are used, hydroformylation proceeds while the use of non-halide salts results only in hydrogenation taking place (see **Table 1.3**). In the absence of the halide salts, the ruthenium carbonyl complex $[H_4Ru_4(CO)_{12}]$ (**61**) decomposes with loss of carbonyl groups and precipitation of the metal (run 1 in **Table 1.3**).

The reaction proceeds via the formation of CO, followed by the hydroformylation and then the hydrogenation of the aldehyde to alcohol.

Table 1.3 Effects of salts on hydroformylation of cyclohexene using CO_2 [a] [55]

Run	Salt	Conversion (%)	Yield (%)		
			Alcohol	Aldehyde	Alkane
1	None[b]	100	0	0	92
2	LiCl	100	88	2	6
3	LiCl[c]	100	82	3	4
4	LiBr	100	76	1	13
5	LiI	100	29	0	61
6	[PPN]Cl	100	82	0	15
7	NaCl	99	72	8	18
8	KCl	97	66	11	13
9	Li_2CO_3	18	0	0	14
10	LiOAc	73	0	0	68

[a]Conditions: $[H_4Ru_4(CO)_{12}]$ (**61**) (0.1 mmol), salt (0.4 mmol), cyclohexene (5.0 mmol), NMP (N-methyl-2-pyrrolidone) (8.0 mL), CO_2 (4.0 MPa), H_2 (4.0 MPa), 140 ^oC, 30 h. [b] Reaction time was 5 h. [c]This reaction used CO (4.0 MPa) in place of CO_2

The researchers reported that only ruthenium carbonyl complexes could be catalyst precursors for carbonylation with CO_2, although a variety of ruthenium complexes including mononuclear complexes and clusters are able to catalyze the conventional hydroformylation with CO (see runs 1-6 in **Table 1.4**) [55].

Table 1.4 Catalytic activities of various kinds of ruthenium complexes for the hydroformylation of cyclohexene using carbon dioxide [a] [55]

Run	Complex	Conversion (%)	Yield (%)		
			Alcohol	Aldehyde	Alkane
1	$[H_4Ru(CO)_{12}]$ (**61**)	100	88	2	6
2	$[Ru_3(CO)_{12}]$ (**1**)	100	86	0	12
3	$[PPN][Ru(CO)_3Cl_3]$ (**71**)	100	82	7	7
4	$[Ru_3(CO)_{10}(bipy)]$ (**72**)	94	31	2	56
5	$[Ru_3(CO)_{10}(dppm)]$ (**26**)	92	66	0	23
6	$[Ru_2(CO)_4Cp^*_2]$ (**73**)	32	2	0	28
7	$[RuCl_3.3H_2O]$ (**8**)	100	0	0	100
8	$[RuCl_2(PPh_3)_3]$ (**74**)	100	0	0	92

[a] Conditions: complex (0.1 mmol), LiCl (0.4 mmol), cyclohexene (5.0 mmol), NMP (N-methyl-2-pyrrolidone) (8.0 mL), CO_2 (4.0 MPa), H_2 (4.0MPa), 140 °C, 30 h.

The cluster $[Ru_3(CO)_{12}]$ (**1**) catalyses the reaction of ethylene with CO and hydrogen in supercritical CO_2 ($scCO_2$) over a temperature range of 70-125 °C (Eqn. 1.8) [56].

$$C_2H_4 + H_2 + CO \xrightarrow[scCO_2]{Ru_3(CO)_{12}} CH_3CH_2CHO \qquad \text{Eqn. 1.8}$$

The catalytic activity of the cluster **1** in $scCO_2$ (TON 190, 115 °C, 24 h) is better than in dimethylformamide as solvent (10 mL, TON 157, 10 bar CO, 10 bar H_2, 80 °C, 24 h).

The hydroformylation of propylene in the presence of catalytic amounts of $[Ru_3(CO)_{12}]$ (**1**) and 1,10-phenanthroline under 8 MPa CO and hydrogen at 120 °C in an amide solvent to afford C_4–aldehydes in high yield with high selectivity for *n*-butyraldehyde (Eqn. 1.9) has been reported [57].

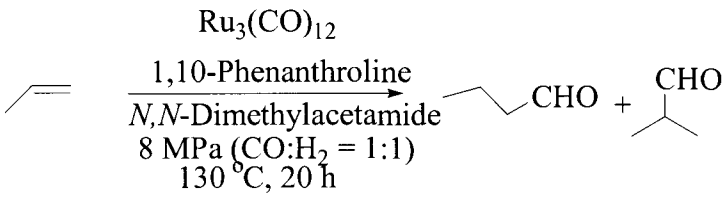

Eqn. 1.9

The researchers examined the effects of ligands on the hydroformylation reaction (see **Table 1.5**). Use of pyridine in place of 1,10-phenanthroline gave high yields of C_4–aldehydes but with low *n*-selectivity. When triphenylphosphine was used, the reaction was completely suppressed.

Table 1.5 Effects of ligands on $Ru_3(CO)_{12}$-catalyzed hydroformylation of propylene [a] [57].

Run	Ligand	Total Yield (%)	*n*-Selectivity [b] (%)
1	None	25	84
2	1,10-phenanthroline	73	95
3	2,9-dimethyl-1,10-phenanthroline	76	92
4	$Me_2N(CH_2)_2NMe_2$	31	95
5	$Me_2N(CH_2)_3NMe_2$	33	96
6	$Me_2N(CH_2)_4NMe_2$	57	96
7	$Me_2N(CH_2)_6NMe_2$	62	96
8	2,2-Bipyridyl	24	93
9	PPh_3	0	-
10	Pyridine	79	91
11[c]	1,10-phenanthroline	93	95

[a] $[Ru_3(CO)_{12}]$ (**1**) (0.11 mmol), propylene (40 mmol), *N,N*-dimethylacetamide (10 mL), bidentate ligand (1.33 mmol) or monodentate ligand (2.66 mmol), CO (4 MPa), H_2 (4 MPa), 120 °C, 20 h. [b] *n*-Selectivity = *n*-butyraldehyde / C_4 – aldehyde. [c] At 130 °C.

Styrene [58] is hydroformylated under 100 atm of synthesis gas at 120 °C in the presence of catalytic amounts of $[Ru_3(CO)_{12}]$ (**1**) and 1,10-phenanthroline in DMF giving corresponding aldehydes in high yield (80 %). The hydroformylation of methyl acrylate and ethyl acrylate at 80 °C gives the corresponding 4-alkoxy-4-methyl-δ-valerolactones in very poor yields. When the 1,10-phenanthroline ligand is replaced

by the triphenylphosphine ligand, hydroformylation of methyl acrylate at 100 °C gives an open chain aldehyde in 18 % yield. The formation of 4-methoxy-4-methyl-δ-valerolactone proceeds via the hydroformylation of methyl acrylate to give methyl-2-formylpropionate. Michael addition between this intermediate and methyl acrylate follows giving dimethyl-2-formyl-2-methylglutarate which subsequently undergoes reduction of the carbonyl functionality and lactonization affording the product (see Eqn. 1.10).

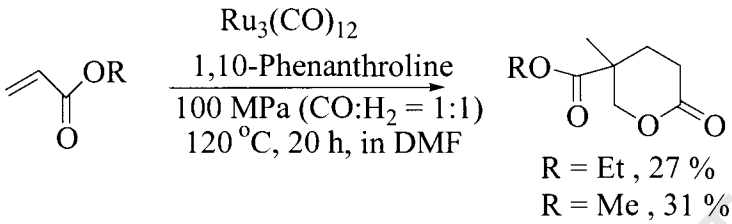

Eqn. 1.10

The ruthenium carbonyl complexes $[Ru_3(CO)_{12}]$ (**1**), $[H_4Ru_4(CO)_{12}]$ (**61**) and $[Ru(CO)_3Cl_2]_2$ (**75**) catalyze the hydroformylation of 1-hexene using CO_2 and H_2 as reactants in the presence of Groups 1 and 2 metal halide promoters [59]. The presence of the promoters reduces the excessive hydrogenation of the substrate to hexane. In this study, they also showed that the cluster is not the key to the hydroformylation reaction. The chloride is necessary either as an ion originating from an added salt or as a ligand in the catalyst precursor itself in which case a suitable cation is needed for a positive promoting effect.

The hydroformylation of propylene [47] with CO/H_2 in water in the presence of the complex $[Ru_3(CO)_9(TPPMS)_3]$ (**63**) as a catalyst at 120 °C under a total gas pressure of 4.7 MPa gives 1-butanal (90 %) and other side products with high TON (490). Addition of halide or alkali metal cation promoters in the hydroformylation of ethylene increases the catalytic activity and leads to formation of more of the side-product 3-pentanone.

The ruthenium clusters with bulky diphosphine ligands bis(dicyclohexyl-phosphino)methane (dcpm) and bis(perfluorodiphenylphosphino)-ethane (F-dppe); $[Ru_3(CO)_{10}(dcpm)]$ (**76**), $[Ru_3(CO)_{10}(F\text{-}dppe)]$ (**77**), $[Ru_3(CO)_8\text{-}(dcpm)_2]$ (**78**), and $[Ru_3(CO)_8(F\text{-}dppe)_2]$ (**79**) act as catalysts in the hydroformylation of ethylene and propylene [60] affording corresponding aldehydes with the di-substituted clusters being less active but more selective than the mono-substituted clusters (**Table 1.6**).

Table 1.6: Catalytic activity of **76-80** and of **1** for the hydroformylation [a] of ethylene and propylene

Catalyst [b]	Ethylene pressure (MPa)	Propylene pressure (MPa)	TON [c]	Selectivity [d]
76	1	-	274	-
	-	0.9	130	71/29
77	1	-	429	-
	-	0.9	145	57/41
78	1	-	127	-
	-	0.9	72	83/17
79	1	-	143	-
	-	0.9	130	67/33
1	1	-	157	-
	-	0.9	63	85/5
$[Ru_3(CO)_{10}(dppe)]$(**80**)	1	-	289	-
	-	0.9	128	63/37

[a] Conditions: 10mL DMF, 1 MPa H_2, 80 °C, 24 h. [b] 0.01mmol. [c] mol product/mol catalyst. [d] *n*-Propionaldehyde/*i*-propionaldehyde (%)

The complex $[Ru_3(\mu\text{-}H)(\mu_3\text{-}MeNpy)(CO)_9]$ (**81**) (MeNpy = 2-(methylamino)pyridyl) acts as a catalyst for the hydroformylation of diphenylacetylene to α-phenylcinnam-aldehyde [61].

1.6.6 Olefin cyclopropanation reactions

The cyclopropane unit is common in many natural products and biologically active compounds [62,63]. An example of biologically active molecules containing the cyclopropane unit is decamethrin, a very important insecticide [64]. The development of methods that allow for the synthesis of cyclopropane-containing molecules is receiving increasing attention [65]. The dinuclear ruthenium(I) carboxylato complexes $[Ru_2(CO)_4(\mu\text{-}O_2CR)_2]_n$ {R = C_3H_7 (**81**), H (**83**), CF_3 (**84**)} are effective catalysts for

cyclopropanation of alkenes with methyl diazoacetate [66]. The cyclopropanation of 2-methyl-2-butene with methyl diazoacetate affords the corresponding cyclopropane in good yield (61 %).

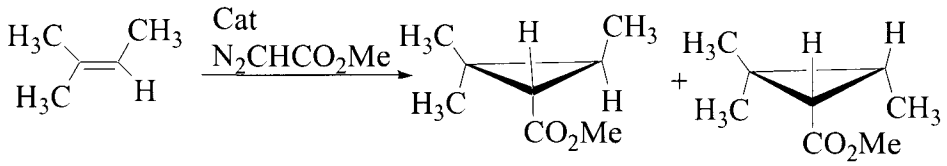

Eqn. 1.11

The 2-pyridonate complex $[Ru_2(CO)_4$ (-2-pyridonate$)_2]_n$ (**85**) was also shown to be an efficient catalyst for olefin cyclopropanation reactions.

1.7 Focus of this Project

The chemistry of ligand bridged ruthenium and osmium complexes remains interesting. The survey done on the reactions catalyzed by polynuclear compounds of ruthenium and osmium (see Section 1.6) has shown that catalytic investigations have been dominated by the trinuclear clusters and their derivatives. Very few examples of reactions catalyzed by dinuclear carboxylato-bridged complexes have been reported in literature (see Section 1.6). A lot of work still needs to be done in finding catalytic applications for this class of organometallic compounds.

The focus of this work was therefore to extend the chemistry of the carboxylato-bridged complexes of ruthenium and osmium and test some of the complexes for catalytic activity. This involved the synthesis of carboxylato-bridged complexes. This was achieved by varying the ligand L in complexes of the type $[Ru_2(CO)_4($ -$O_2CR)_2L_2]$. Various R groups (H, Me, Et and Fc) were also used in this regard.

Some of the complexes were then tested for catalytic activity in the isomerisation of 1-alkenes. We have also made preliminary investigations into the catalytic oxidation of some alkanes.

1.8 References

1. a). F. A. Cotton, G. Wilkinson, C. A. Murillo, M. Bochmann, *Advanced Inorganic Chemistry, 6th ed., Wiley-Interscience, New York,* 1999, Chapter 16; b). B. H. S. Thimmappa, *Coord. Chem. Rev.,* 1995, **143**, 1.
2. a). J. R. Moss, W. A. G. Graham, *J. Chem. Soc. D,* 1970, 13, 835; b). J. R. Moss, W. A. G. Graham, *J. Chem. Soc., Dalton Trans.*, 1977, 95
3. a). G. M. Ferrence, P. E. Fanwick, C. P. Kubiak, R. J. Haines, *Polyhedron,* 1997, **16**, 1453; b). J. Kuncheria, H. A. Mirza, H. A. Jenkins, J. J. Vittal, R. J. Puddephatt, *J. Chem. Soc., Dalton Trans.,* 1998, 285
4. G. De Leeuw, J. S. Field, R. J. Haines, B. McCullouch, E. Meintjies, C. Monberg, K. G. Moodley, G. M. Olivier, C. N. Sampson, N. D. Steen, *J. Organomet. Chem.*, 1982, **228**, C66
5. G. R. Crooks, B. F. G. Johnson, J. Lewis, I. G. Williams, G. Gamlen, *J. Chem. Soc. A,* 1969, 2761
6. F. Neumann, H. Stoeckli-Evans, G. Süss-Fink, *J. Organomet. Chem.,* 1989, **379**, 139
7. J. A. Cabeza, C. Landazuri, L. A. Oro, A. Tiripicchio, M. Tiripicchio-Camellini, *J. Organomet. Chem.,* 1987, **322**, C16
8. a). F. Neumann, G. Süss-Fink, *J. Organomet. Chem.,* 1989, **367**, 175; b). F. Neumann, H. Stoeckli-Evans, G. Süss-Fink, *J. Organomet. Chem.,* 1989, **379**, 15; c). J. A. Cabeza, C. Landázuri, L. A. Oro, D. Belletti, A. Tiripicchio, M. T. Camellini, *J. Chem. Soc., Dalton Trans.,* 1989, 1093
9. D. S. Bohle, H. Vahrenkamp, *Inorg. Chem.,* 1990, **29**, 1097
10. M. Langenbahn, H. Stoeckli-Evans, G. Süss-Fink, *Helv. Chim. Acta,* 1991, **74**, 549
11. G. Rheinwald, H. Stoeckli-Evans, G. Süss-Fink, *J. Organomet. Chem.,* 1992, **441**, 295
12. T. Werle, L. Schäffler, G. Maas, *J. Organomet. Chem.,* 2005, **690**, 5562
13. J S. Field, R. J. Haines, C. J. Parry, *J. Chem. Soc., Dalton Trans.*, 1997, 2843
14. I. Albers, E. Alvarez, J. Cámpora, C. M. Maya, P. Palma, L. J. Sánchez, E. Passaglia, *J. Organomet. Chem.,* 2004, **689**, 833.
15. G. M. G. Hossain, Md. I. Hyder, S. E. Kabir, K. M. A. Malik, Md. A. Miah, T. A. Siddiquee, *Polyhedron,* 2003, **22**, 633.

16. J. A. Cabeza, J. M. Fernández-Colinas, *Coord. Chem. Rev.,* 1993, **126**, 319
17. M. Rotem, I. Golberg, U. Shmueli, Y. Shvo, *J. Organomet. Chem.,* 1986, **314**, 185.
18. C.M. Kepert, G.B. Deacon, L. Spiccia, G.D. Fallon, B.W. Skelton, A.H. White, *J. Chem. Soc., Dalton Trans.,* 2000, 2867.
19. J. G. Bullitt, F. A. Cotton, *Inorg. Chim. Acta,* 1971, **5**, 406
20. A. J. Deeming, N. P. Randle, M. B. Hursthouse, R. L. Short, *J. Chem. Soc., Dalton Trans.,* 1987, 2473
21. S. J. Sherlock, M. Cowie, E. Singleton, M. M. de V. Steyn, *J. Organomet. Chem.,* 1989, **361**, 353
22. J. Soler, J. Ros, M. R. Carrasco, A. Ruiz, A. Alvearez-Larena, J. F. Piniella, *Inorg. Chem.,* 1995, **34**, 6211
23. K.-B. Shiu, W. -M. Lee, C. -L. Wang, S. -L. Wang, F. -L. Liao, J. -C. Wang, L. -S. Liou, S. -M. Peng, G. -H. Lee, M. Y. Chiang, *Organometallics,* 1996, **15**, 2979
24. J. Soler, I. Moldes, E. de la Encarnación, J. Ros, *J. Organomet. Chem.,* 1999, **580**, 108
25. S. K. Patra, N. Sadhukhan, J. K. Bera, *Inorg. Chem.,* 2006, **45**, 4007
26. K. -B Shiu, S. -M. Peng, M. -C. Cheng, *J. Organomet. Chem.,* 1993, **452**, 143
27. S. J. Sherlock,, M. Cowie, E. Singleton, M. M. de V. Steyn, *Organometallics,* 1988, **7**, 1663
28. R. A. Sanchez-Delgado, J. Puga, M. Rosales, *J. Mol. Catal.,* 1984, **24**, 221.
29. K. Whitmire, D.F. Shriver, *J. Am. Chem. Soc.,* 1980, **102**, 1456
30. B. Fontal, M. Reyes, T. Suárez, F. Bellandi, N. Ruiz, *J. Mol. Catal. A: Chem.,* 1999, **149**, 87
31. E. Sappa, A. Tiripicchio, P. Braunstein, *Coord. Chem. Rev.,* 1985, **65**, 219
32. M. Castiglioni, S. Deabate, R. Giordano, P. J. King, S. A. R. Knox, E. Sappa, *J. Organomet. Chem.,* 1998, **571**, 251
33. A. Salvini, P. Frediani, F. Piacenti, *J. Mol. Catal. A: Chem.,* 2000, **159**, 185
34. B. Fontal, M. Reyes, T. Suarez, F. Bellandi, J. C. Diaz, *J. Mol. Catal. A: Chem.,* 1999, **149**, 75
35. Fontal B, Reyes M, Suárez T, Bellandi F, Ruiz N, *J. Mol. Catal. A: Chem.,* 1999, **149**, 87

36. V. A. Ershova, A. V. Golovin, V. M. Pogrebnyak, *J. Organomet. Chem.*, 2002, **658**, 147
37. P. Frediani, M. Bianchi, A. Salvini, R. Guarducci, L. C. Carluccio, F. J. Piacenti, *J. Organomet. Chem.*, 1995, **498**, 187
38. D. Blazina, S. B. Duckett, P. J. Dyson, J. A. B. Lohman, *Dalton Trans.*, 2004, 2108
39. G. Gervasio, R. Giordano, D. Marabello, E. Sappa, *J. Organomet. Chem.*, 1999, **588**, 83
40. K. O. Kallinen, T. T. Pakkanen, T. A. Pakkanen, *J. Mol. Catal. A: Chem.*, 1995, **99**, 29
41. D. J. Ellis, P. J. Dyson, D. G. Parker, T. Welton, *J. Mol. Catal. A: Chem.*, 1999, **150**, 71
42. D. Blazina, S. B. Duckett, P. J. Dyson, J. A. B. Lohman, *Angew. Chem., Int. Ed. Engl.*, 2001, **40**, 3874
43. J. A. Cabeza, J. M. Fernandez-Colinas, A. Llamazares, V. Riera, *Organometallics,* 1993, **12**, 4141
44. J. A. Cabeza, I. del Rio, J. M. Fernandez-Colinas, V. Riera, *Organometallics,* 1996, **15**, 449
45. M. Castiglioni, R. Giordano, E. Sappa, *J. Organomet. Chem.*, 1995, **491**, 111
46. A. Salvini, P. Frediani, C. Giannelli, L. Rosi, *J. Organomet. Chem.*, 2005, **690**, 371
47. J. Gao, P. Xu, X. Yi, H. Wan, K. Tsai, *J. Mol. Catal. A: Chem.*, 1999, **147,** 99
48. R. A. Sanchez-Delgado, A. Andriollo, J. Puga, G. Martin, *Inorg. Chem.*, 1987, **26**, 1867
49. P. Homanen, R. Persson, M. Haukka, T. A. Pakkanen, E. Nordlander, *Organometallics,* 2000, **19**, 5568
50. Y. Gao, M. C. Jennings, R. J. Puddephatt, *Can. J. Chem.*, 2001, **79**, 915
51. C. Botteghi, S. Gladiali, M. Bianchi, U. Matteoli, P. Frediani, P. G. Vergamini, E. Benedetti, *J. Organomet. Chem.*, 1977, **140**, 221
52. M. Bianchi, U. Matteoli, G. Menchi, P. Frediani, S. Pratesi, F. Piacenti, C. Botteghi, *J. Organomet. Chem.*, 1980, **198,** 73
53. D. Scarpi, G. Menchi, Occhiato, A Guarna, *J. Mol. Catal. A: Chem.*, 1996, **110**, 129
54. K. Tominaga, Y. Sasaki, *Catal. Comm.*, 2000, **1**, 1

55. K. Tominaga, Y. Sasaki, *J. Mol. Catal. A: Chem.,* 2004, **220**, 159
56. C. Erkey, E. L. Diz, G. Süss-Fink, X. Dong, *Catal. Comm.,* 2002, **3**, 213
57. T. Mitsudo, N. Suzuki, T. Kondo, Y. Watanabe, *J. Mol. Catal. A: Chem.,* 1996, **109**, 219
58. T. Mitsudo, N. Suzuki, T. Kobayashi, T. Kondo, *J. Mol. Catal. A: Chem.,* 1999, **137**, 253
59. S. Jääskeläinen, M. Haukka, *Applied Catal. A: General,* 2003, **247**, 95
60. E. L. Diz, A. Neels, H. Stoeckli-Evans, G. Süss-Fink, *Polyhedron,* 2001, **20**, 2771
61. P. Nombel, N. Lugan, B. Donnadieu, G. Lavigne, *Organometallics,* 1999, **18**, 187
62. A. Hartikka, A. T. Ślósarczyk, P. I. Arvidsson, *Tetrahedron: Asymmetry,* 2007, **18**, 1403
63. W. A. Donaldson, *Tetrahedron,* 2001, **57**, 8589
64. J. Clayden, N. Greeves, S. Warren, P. Wothers, *Organic Chemistry, Oxford University Press, New York,* 2006, Chapter 40
65. H. Lebel, J. –F. Marcoux, C. Molinaro, A. B. Charette, *Chem. Rev.,* 2003, **103**, 977
66. T. Werle, T. Schaffler, G. Maas, *J. Organomet. Chem.,* 2005, **690**, 5562

CHAPTER 2
SYNTHESIS AND CHARACTERIZATION OF CARBOXYLATO-BRIDGED COMPLEXES OF RUTHENIUM AND OSMIUM

2. Introduction

The first chapter of this thesis provided details on the different synthetic routes that are available for the preparation of carboxylato-bridged complexes of ruthenium and osmium. It also gave a review on the catalytic application of low oxidation state compounds of ruthenium and osmium.

In pursuance of the aims of this project (see Section 1.7), dinuclear carboxylato-bridged complexes of Ru and Os have been synthesized. This chapter now describes the synthesis and characterization of these complexes.

2.1 Synthesis of polymers $[Ru(CO)_2(\mu\text{-}O_2CR)]_n$ {R = H (83), Me (86), Et (87)} and of the dimer $[Os_2(CO)_6(\mu\text{-}O_2CMe)_2]$ (4) .

The ruthenium(I) carboxylate polymers of the general formula $[Ru(CO)_2(\mu\text{-}O_2CR)]_n$ {R = H (**83**), Me (**86**), Et (**87**)} were first synthesized by Lewis *et al.* [1] in 1969 by the reaction of the trinuclear cluster $[Ru_3(CO)_{12}]$ (**1**) with the appropriate carboxylic acid under refluxing conditions. These polymers have been shown to be excellent precursors for the synthesis of carboxylato-bridged diruthenium complexes affording products of the formula $[Ru_2(CO)_4(\mu\text{-}O_2CR)_2(L)_2]$ on treatment with donor ligands such as CO, pyridine, acetonitrile and tertiary phosphines [1,2].

In this study, the procedure developed by Lewis *et al.* as shown in **Scheme 2.1** was followed for the synthesis of $[Ru(CO)_2(\mu\text{-}O_2CR)]_n$ {R = H (**83**), Me (**86**), Et (**87**)}.

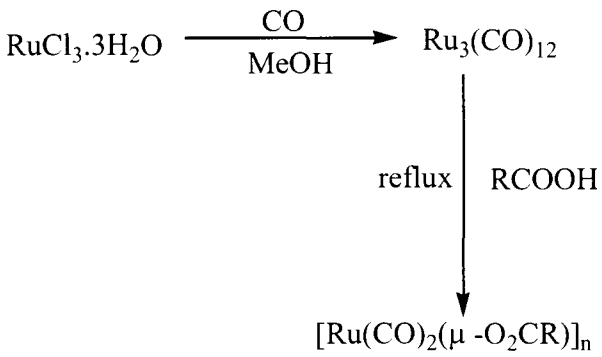

Scheme 2.1

For the synthesis of $[Ru(CO)_2(\mu\text{-}O_2CH)]_n$ (**83**), the starting material $[Ru_3(CO)_{12}]$ (**1**), synthesized from $RuCl_3.3H_2O$ in a high pressure autoclave reaction, was suspended in excess neat formic acid and then heated under reflux for 6 h. The compound **83** separated as an orange product in good yield (68 %). For the synthesis of $[Ru(CO)_2(\mu\text{-}O_2CMe)]_n$ (**86**) and $[Ru(CO)_2(\mu\text{-}O_2CEt)]_n$ (**87**), neat acetic acid and propionic acid were used respectively. The osmium dimer $[Os_2(CO)_6(\mu\text{-}O_2CMe)_2]$ (**4**) was synthesized from the reaction of $[Os_3(CO)_{12}]$ (**2**) with neat acetic acid at 180 °C for 8 h in a sealed tube.

Rotem *et al.* [3] reported that the reaction between the cluster **1** and the carboxylic acid gives the dimer $[Ru_2(CO)_6(\mu\text{-}O_2CR)_2]$ as the initial product. Due to its instability, the dimer subsequently undergoes polymerization by losing CO ligands to yield the stable polymer $[Ru(CO)_2(\mu\text{-}O_2CR)]_n$. The bonding interactions in the polymer are believed to involve the Ru–O bridges that connect adjacent dimeric units. The researchers [3] proposed that the structure of $[Ru_2(sec\text{-}C_4H_9CO_2)_2(CO)_4(sec\text{-}C_4H_9CO_2H)]_2$ (**88**) elucidated by X-ray crystallography (**Figure 2.1**) represented the possible mode of polymerization with the removal of the end acids in the complex inducing polymerization via the additional Ru–O bridges. A similar tetranuclear complex, $[Ru_4(CO)_8(MeCO_2)_4(PBu_3)_2]$ (**23**), reported by Salvini *et al.* [4] as an alkene isomerization catalyst (See Section 1.6.1), also possesses these oxygen bridges that connect two $[Ru_2(CO)_4(MeCO_2)_2(PBu_3)_2]$ moieties.

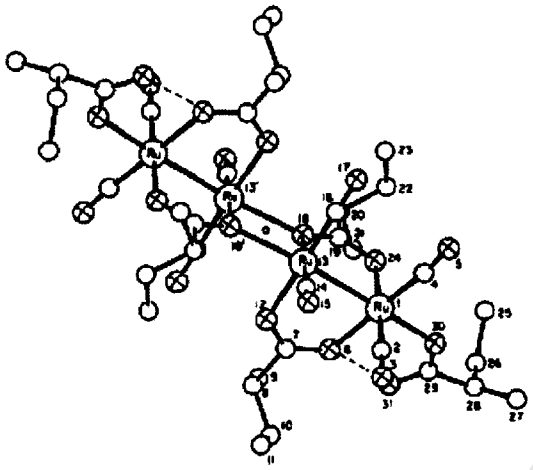

Figure 2.1 Molecular structure of $[Ru_2(sec\text{-}C_4H_9CO_2)_2(CO)_4(sec\text{-}C_4H_9CO_2H)]_2$ (**88**) (the crossed circles represent oxygen atoms)

Due to their polymeric nature and insolubility, the compounds could not be analyzed by ^1H NMR spectroscopy. However, they all were characterized by both elemental analysis and IR spectroscopy. The elemental analyses agreed with the formulation of the complexes.

2.1.1 IR spectroscopic analysis of complexes 83, 86, 87 and 4.

The IR spectroscopic data for the complexes were all in agreement with literature data [1]. The spectra showed three (CO) bands in the region 2100-1900 cm^{-1} as well as bands in the region 1600-1400 cm^{-1} that were assigned to bridging carboxylate groups.

2.2 Synthesis and characterization of tertiary phosphine-substituted dimers of the formula $[M_2(CO)_4(\mu\text{-}O_2CR)_2(L)_2]$ (M = Ru, Os); (L = PPh_3, PCy_3)

The dinuclear carboxylato-bridged complexes were synthesized following literature procedures [1]. The ruthenium-based complexes were synthesized from the polymers

$[Ru(CO)_2(\mu\text{-}O_2CR)]_n$ {R = H (**83**), Me (**86**)} while their osmium analogues were prepared from the dimeric complex $[Os_2(CO)_6(\mu\text{-}O_2CMe)_2]$ (**4**).

The complex $[Ru_2(CO)_4(\mu\text{-}O_2CMe)_2(PPh_3)_2]$ (**11**) was prepared by refluxing a suspension of $[Ru(CO)_2(\mu\text{-}O_2CMe)]_n$ (**86**) and triphenylphosphine in diethyl ether and the product was obtained as a yellow solid in good yield (70 %). This complex has also been prepared by Kepert *et al.* [5] from the salt $RuCl_3.3H_2O$ via the preparation of a dicarbonyldichlorodiruthenium(II) polymer $[Ru(CO)_2(Cl)_2]_n$ (**7**).

A new tricyclohexylphosphine substituted dimer $[Ru_2(CO)_4(\mu\text{-}O_2CH)_2(PCy_3)_2]$ (**89**) was prepared by the reaction of the formate polymer with an excess of the tricyclohexylphosphine ligand in diethyl ether. The reaction was performed under refluxing conditions for 2h during which time a yellow product formed. The formate polymer was also reacted with triphenylphosphine under refluxing conditions in diethyl ether. The reaction was carried out for five hours during which time the orange formate polymer was converted to a yellow solid, the triphenylphosphine substituted dimer $[Ru_2(CO)_4(\mu\text{-}O_2CH)_2(PPh_3)_2]$ (**14**).

The osmium dimer $[Os_2(CO)_4(\mu\text{-}O_2CMe)_2(PCy_3)_2]$ (**90**) was obtained by reaction of the osmium dimer $[Os_2(CO)_6(\mu\text{-}O_2CMe)_2]$ (**4**) with an excess of tricyclohexylphosphine. This reaction was carried out in benzene under refluxing conditions and it gave a new tricyclohexylphosphine-substituted complex **90** as a yellow powder in moderate yield (46 %). The elemental analysis of this complex agreed with the formulation of the compound. When triphenylphosphine was used as the monodentate ligand, a known compound $[Os_2(CO)_4(\mu\text{-}O_2CMe)_2(PPh_3)_2]$ (**91**) was obtained. The reaction was carried out under similar conditions but petroleum ether was added to precipitate the white complex. The elemental analysis of this complex also agreed with the formulation.

A new ruthenium dimer $[Ru_2(CO)_4(\mu\text{-}O_2CCHPh_2)_2(PPh_3)_2]$ (**92**) was prepared from the reaction of a suspension of the cluster $[Ru_3(CO)_{12}]$ (**1**) and diphenyl-acetic acid in

tetrahydrofuran under reflux conditions for 3h followed by the addition of the ligand triphenylphosphine. The dimer was obtained as a light brown solid in 56 % yield.

2.2.1 IR spectroscopic data

All the phosphine-substituted dimers showed the same pattern of absorption bands in the terminal carbonyl region (2100-1900 cm^{-1}) that is consistent with sawhorse-type complexes with C_{2v} symmetry (**Figure 2.2**). The data obtained for the known complexes $[Ru_2(CO)_4(\mu\text{-}O_2CMe)_2(PPh_3)_2]$ (**14**) and $[Os_2(CO)_4(\mu\text{-}O_2CMe)_2(PPh_3)_2]$ (**91**) agreed very well with literature data [1]. Comparison of the carbonyl infrared stretching frequencies of complexes showed that increasing the basicity of the ligand from PPh_3 to PCy_3 leads to a decrease in the carbonyl stretching frequencies due to increased π back donation (see **Table 2.1**). The bands in the region 1600-1400 cm^{-1} were attributed to the bridging carboxylate ligands.

Table 2.1 Comparison of the infrared carbonyl stretching frequencies (CO) of the complexes [a,b]

Complex	(CO) / cm^{-1}		
$[Ru_2(CO)_4(\mu\text{-}O_2CH)_2(PCy_3)_2]$ (**89**)	2018	1972	1945
$[Ru_2(CO)_4(\mu\text{-}O_2CH)_2(PPh_3)_2]$ (**14**)	2031	1988	1961
$[Ru_2(CO)_4(\mu\text{-}O_2Cme)_2(PPh_3)_2]$ (**11**)	2027	1983	1956
$[Os_2(CO)_4(\mu\text{-}O_2Cme)_2(PCy_3)_2]$ (**90**)	2008	1962	1931
$[Os_2(CO)_4(\mu\text{-}O_2Cme)_2(PPh_3)_2]$ (**91**)	2018	1975	1945
$[Ru_2(CO)_4(\mu\text{-}O_2CCHPh_2)_2(PPh_3)_2]$ (**92**) [c]	2024	1980	1952

[a] Only the carbonyl stretching frequencies tabulated.
[b] Solvent CCl_4.
[c] Solvent CH_2Cl_2

2.2.2 ^{1}H NMR spectroscopic data

The ^{1}H NMR spectra of the di-substituted triphenylphosphine complexes **11** and **91** showed two characteristic resonances for the thirty protons of the triphenylphosphine ligands in the aromatic region. The signal for the methyl protons of the bridging acetate ligands appeared as singlets at 1.67 and 1.61 ppm for the complexes **11** and **91** respectively. These signals integrated for the six protons relative to the phenyl protons. The signals for the two protons of the formate bridges appeared at 8.16 and 8.18 ppm for the complexes **14** and **89** respectively.

The ^{1}H NMR spectrum for the complex $[Ru_2(CO)_4(\mu\text{-}O_2CCHPh_2)_2(PPh_3)_2]$ (**92**) exhibited four signals in the aromatic region. The two resonances attributed to the thirty protons of the triphenylphosphine ligands at 7.43 and 7.34 ppm are downfield with respect to the resonances (7.12 and 6.88 ppm) attributed to the twenty protons of the phenyls groups on the carboxylato-bridges.

2.2.3 ^{31}P NMR spectroscopic data

The ^{31}P NMR spectra for all complexes revealed a single peak, consistent with the two equivalent phosphines bonded to two metal centers *trans* to the metal-metal bond [6]. The triphenylphosphine substituted complexes showed peaks at 14.67 and 18.01 ppm for $[Ru_2(CO)_4(\mu\text{-}O_2CMe)_2(PPh_3)_2]$ (**11**) and $[Os_2(CO)_4(\mu\text{-}O_2CMe)_2(PPh_3)_2]$ (**91**) respectively.

In the formate bridged complexes $[Ru_2(CO)_4(\mu\text{-}O_2CH)_2(PPh_3)_2]$ (**14**) and $[Ru_2(CO)_4(\mu\text{-}O_2CH)_2(PCy_3)_2]$ (**89**), the resonances appear at 13.15 and 25.71 ppm respectively. The observation that the signal for the di-substituted tricyclohexylphosphine complex occurs more downfield with respect to that of the di-substituted triphenylphosphine complex was attributed to the fact that there is more negative charge on the phosphorus atom in tricyclohexylphosphine than in triphenylphosphine.

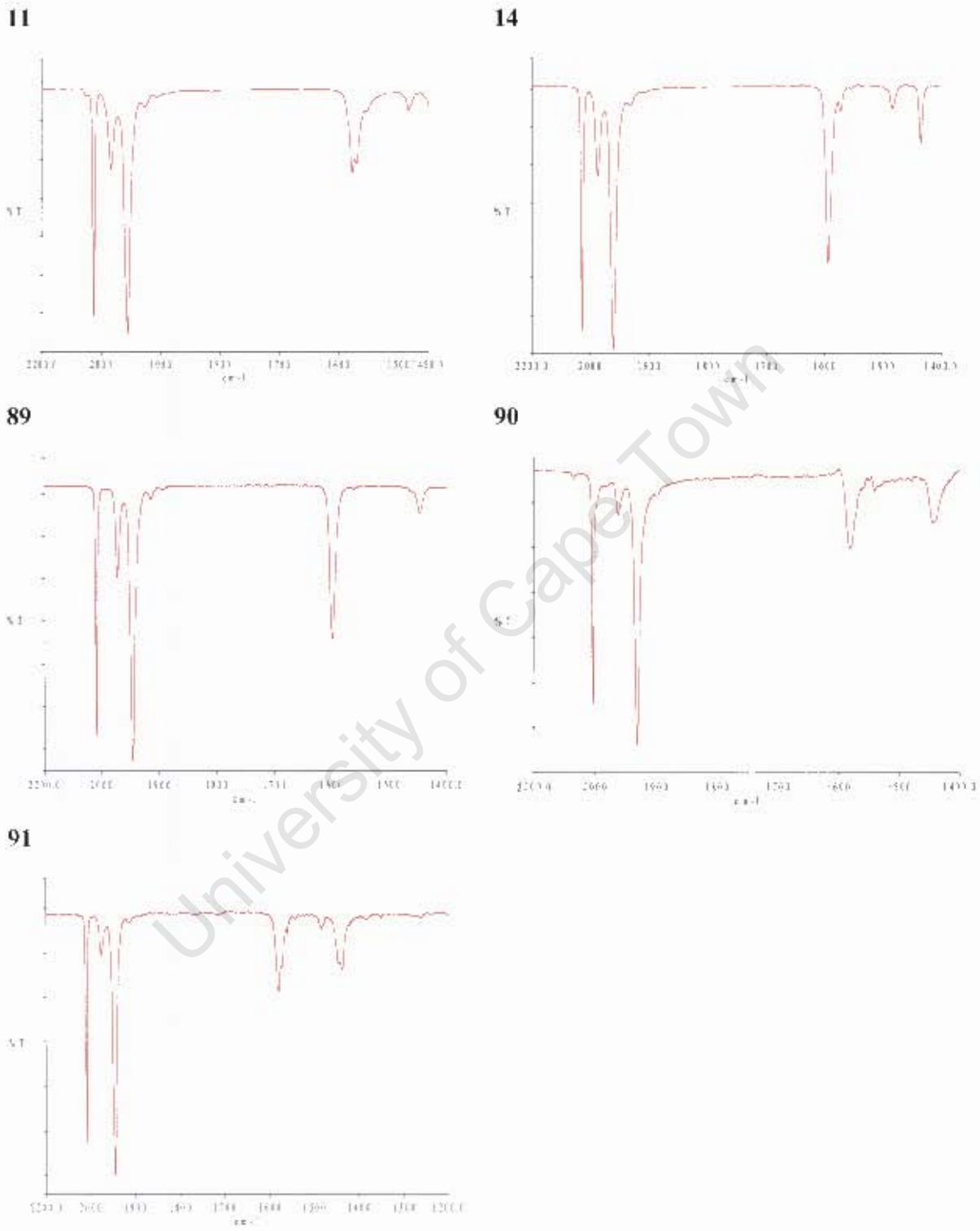

Figure 2.2 IR Spectra for $[M_2(CO)_4(\mu\text{-}O_2CR)_2(L)_2]$ {**M** – Ru, L– PPh_3, R = Me (**11**), H (**14**); L – PCy_3, R – H (**89**)}, {M – Os, R– Me, L– PCy_3 (**90**), PPh_3 (**91**)} in the region 2200-1400 cm^{-1}.

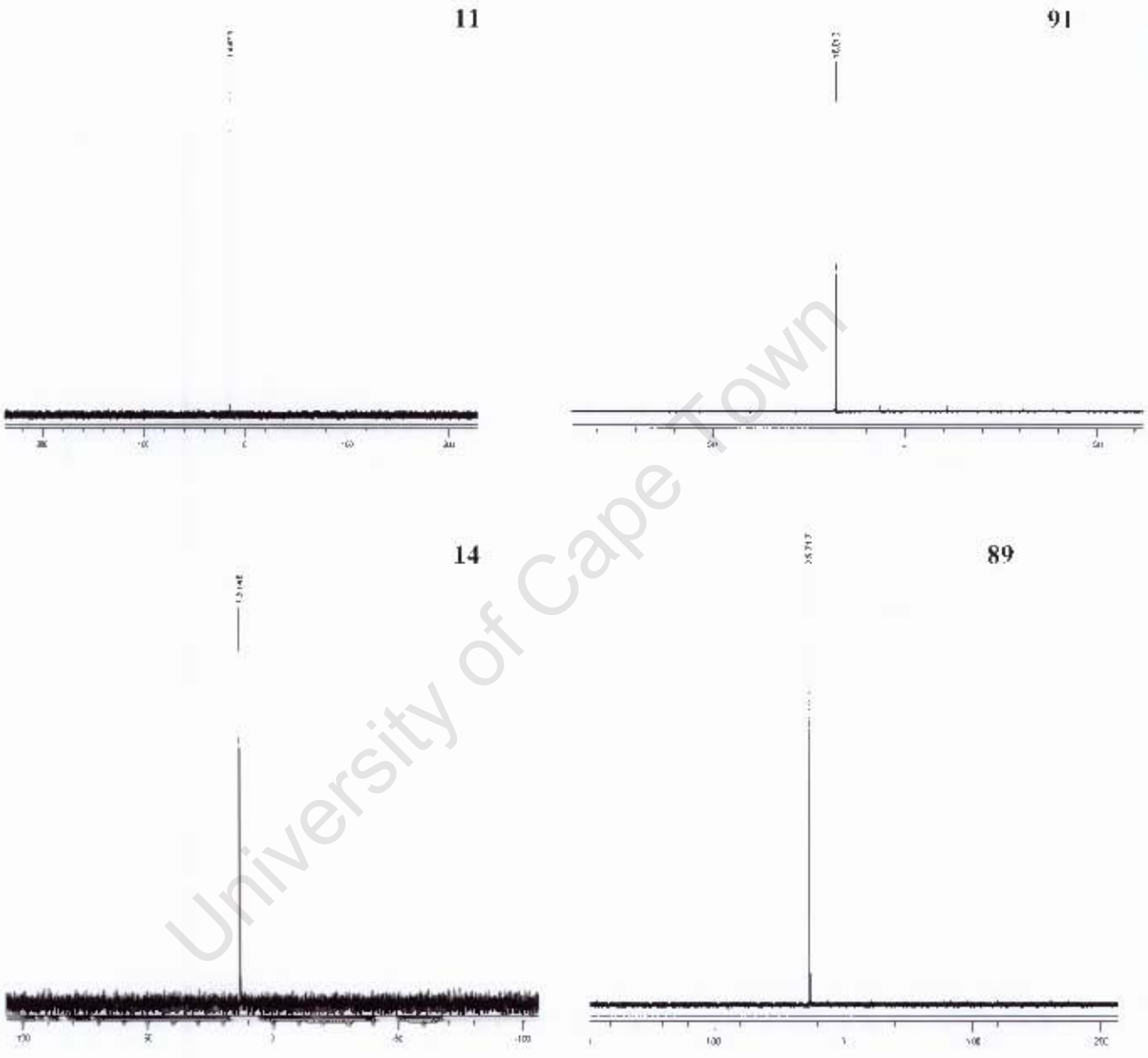

Figure 2.3 ^{31}P NMR spectra for $[Ru_2(CO)_4(\mu\text{-}O_2CMe)_2(PPh_3)_2]$ (**11**), $[Os_2(CO)_4(\mu\text{–}O_2CMe)_2(PPh_3)_2]$ (**91**), $[Ru_2(CO)_4(\mu\text{-}O_2CH)_2(PPh_3)_2]$(**14**) and $[Ru_2(CO)_4(\mu\text{-}O_2CH)_2(PCy_3)_2]$ (**89**)

2.3 Synthesis and characterization of pyridine and substituted pyridine dimers of the formula $[M_2(CO)_4(\mu\text{-}O_2CR)_2(L)_2]$ {M = Ru, L= py, R = H (93), Me (94), Et (95); L = 4-Phpy,R = H (96), Et (97); L = 4-Me_2Npy, Me (98), Et (99)} {M = Os, R= Me, L= 4-Phpy (100), 4-H_2Npy (101)}

The pyridine substituted complexes of the formula $[M_2(CO)_4(\mu\text{-}O_2CR)_2(L)_2]$ (M = Ru, Os) (L= py, 4-Phpy, 4-Me_2Npy, 4-H_2Npy) were prepared from the polymeric precursors (for the ruthenium-based complexes) and from the dimeric complex $[Os_2(CO)_6(\mu\text{-}O_2CMe)_2]$ (**4**) (for the osmium complexes). Refluxing conditions were applied to effect the depolymerisation of the ruthenium polymers as well as the substitution of the axial carbonyl ligands in the osmium dimer. The complexes were analysed by NMR and IR spectroscopic techniques (see **Section 2.3.1** and **2.3.2**).

2.3.1 IR spectroscopic data

All the complexes display patterns for the IR absorptions similar to those shown by their phosphine substituted analogues which are characteristic of complexes with the $(CO)_2$Ru-Ru$(CO)_2$ core structure. Substitution in the *para*-position of pyridine had no effect in the carbonyl stretching frequencies of the complexes (see **Table 2.2**).

The R group in $[Ru_2(CO)_4(\mu\text{-}O_2CR)_2L_2]$ has a mild inductive effect on the carbonyl stretching frequencies of the complexes. As the alkyl chain length increases from the methyl to the ethyl group, the positive inductive effect increases, resulting in increased electron density on the metal centers available for back donation into CO $\pi*$ orbitals. This leads to a slight decrease in the carbonyl stretching frequencies (see **Table 2.2**).

Table 2.2 Comparison of the IR carbonyl stretching frequencies (CO) of pyridine and substituted pyridine dimers [a,b]

Complex	(CO) / cm^{-1}		
$[Ru_2(CO)_4(\mu\text{-}O_2CH)_2(py)_2]$ (**93**)	2029	1977	1945
$[Ru_2(CO)_4(\mu\text{-}O_2CMe)_2(py)_2]$ (**94**)	2024	1972	1939
$[Ru_2(CO)_4(\mu\text{-}O_2CEt)_2(py)_2]$ (**95**)	2023	1971	1938
$[Ru_2(CO)_4(\mu\text{-}O_2CH)_2(4\text{-}Phpy)_2]$ (**96**)	2028	1977	1945
$[Ru_2(CO)_4(\mu\text{-}O_2CEt)_2(4\text{-}Phpy)_2]$ (**97**)	2023	1971	1938
$[Os_2(CO)_4(\mu\text{-}O_2CMe)_2(4\text{-}Phpy)_2]$ (**100**)	2008	1956	1921
$[Ru_2(CO)_4(\mu\text{-}O_2CMe)_2(4\text{-}Me_2Npy)_2]$ (**98**)	2019	1966	1932
$[Ru_2(CO)_4(\mu\text{-}O_2CEt)_2(4\text{-}Me_2Npy)_2]$ (**99**)	2018	1965	1931
$[Os_2(CO)_4(\mu\text{-}O_2CMe)_2(4\text{-}H_2Npy)_2]$ (**101**)	1994	1943	1906

[a] Only the carbonyl stretching frequencies tabulated.
[b] Solvent CH_2Cl_2.

A comparison of carbonyl stretching frequencies for the triphenylphosphine substituted dimers and their pyridine substituted analogues shows that the carbonyl stretching frequencies in the triphenylphosphine substituted dimers are higher. This is due to the fact that triphenylphosphine is a stronger π–acceptor than pyridine. This means that there is less electron density on the metal centre in triphenylphosphine substituted dimers. This results in decreased back donation into CO π^* orbitals and hence higher carbonyl stretching frequencies.

2.3.2 ^{1}H NMR spectroscopic data

The ^{1}H NMR spectrum of $[Ru_2(CO)_4(\mu\text{-}O_2CH)_2(py)_2]$ (**93**) showed three resonances in the aromatic region consistent with two pyridine rings in chemically equivalent environments. A singlet that appeared at 8.36 ppm was attributed to the two protons from the bridging formate ligands. The integration was in agreement with the number of protons.

The complex $[Ru_2(CO)_4(\mu\text{-}O_2CMe)_2(py)_2]$ (**94**) also exhibited three peaks in the aromatic region for the pyridine ligands. The methyl protons of the acetate bridges appeared at 2.07 ppm as a singlet with the correct integration for six protons relative to the protons of the two pyridine rings. The protons in complex $[Ru_2(CO)_4(\mu\text{-}O_2CEt)_2(py)_2]$ (**95**) appeared at 2.30 ($-CH_2$) and 1.06 ppm ($-CH_3$) as a quartet and triplet respectively. The peaks integrated for the ten protons of the ethyl groups relative to the protons of the pyridine ligands.

The ^1H NMR spectrum of $[Ru_2(CO)_4(\mu\text{-}O_2CEt)_2(4\text{-}Phpy)_2]$ (**97**) exhibited four peaks in the aromatic region in agreement with the presence of 4-phenyl pyridine ligands in identical environments. In this complex the ethyl protons appeared at 2.34 ($-CH_2$) and 1.10 ppm ($-CH_3$) as a quartet and triplet respectively integrating for the ten protons of the two ethyl groups.

In the 4-dimethylaminopyridine-substituted derivatives $[Ru_2(CO)_4(\mu\text{-}O_2CMe)_2(4\text{-}Me_2Npy)_2]$ (**100**) and $[Ru_2(CO)_4(\mu\text{-}O_2CEt)_2(4\text{-}Me_2Npy)_2]$ (**99**), the six protons of the dimethylamine substituent appeared at 3.06 ppm as a singlet integrating for the 12 protons of the two ligands. The methyl protons in the acetate bridges of complex **100** appeared at 2.04 ppm as a singlet integrating for the six protons of the two acetate bridges. In the propionate bridged complex **99**, the ethyl protons appeared at 2.28 ($-CH_2$) and 1.07 ppm ($-CH_3$) as a quartet and a triplet respectively. The protons of the amine substituent in $[Os_2(CO)_4(\mu\text{-}O_2CMe)_2(4\text{-}H_2NPy)_2]$ (**101**) appeared at 6.11 ppm as a singlet while a singlet observed at 1.96 ppm was attributed to six protons of the two acetate bridges.

.

2.4 Synthesis and characterization of $[Os_2(CO)_4(\mu\text{-}O_2CC_5H_4FeC_5H_5)_2L_2]$ {L = PPh_3 (102), py (103)}

The ferrocenecarboxylato-bridged complexes $[Os_2(CO)_4(\mu\text{-}O_2CC_5H_4FeC_5H_5)_2L_2]$ {L = PPh_3 (**102**), py (**103**)} were synthesized from the reaction of a trinuclear osmium cluster

$[Os_3(CO)_{12}]$ (**2**) with ferrocene carboxylic acid in tetrahydrofuran followed by the addition of the appropriate monodentate ligand. These complexes were obtained as brown crystalline solids. The ruthenium analogues of these complexes have been reported in literature [7].

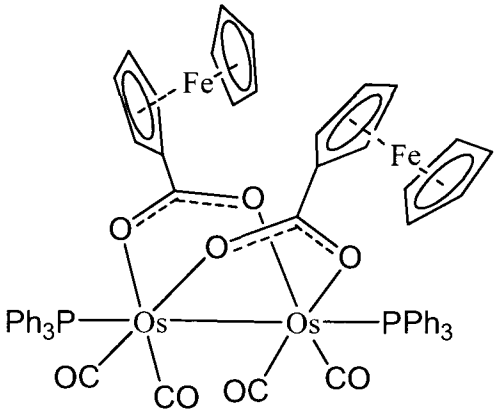

102

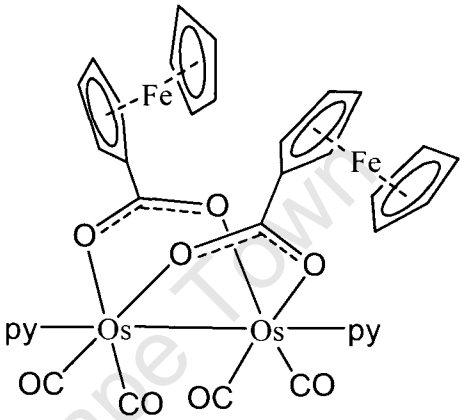

103

The two complexes were characterised by ^{1}H NMR and IR spectroscopic techniques.

2.4.1 IR spectroscopic analysis of complexes 102 and 103

The IR spectra of the two complexes **102** and **103** showed absorption bands characteristic of the sawhorse-type complexes with C_{2v} symmetry. They contained three peaks in the terminal carbonyl region (2100 - 1900 cm^{-1}); two very sharp bands and a medium peak between them. The stretching frequencies for the bridging ferrocene carboxylate ligands were observed in the region 1600 – 1400 cm^{-1}. The triphenylphosphine ligand is a better π-acid ligand than the pyridine ligand. It therefore reduces the electron density on the $Os_2(CO)_4$ core and hence decreases back donation to the terminal carbonyl groups. This phenomenon explains why the carbonyl stretching frequencies of complex **102** were at slightly higher frequencies than those of complex **103**.

2.4.2 NMR spectroscopic data for complexes 102 and 103

The ^{1}H NMR spectrum of complex **102** showed two characteristic resonances for the thirty protons of the triphenylphosphine ligands. The signals of ferrocenyl protons of the ferrocene carboxylato-bridge were observed at 4.06 (t, 4H), 3.97 (t, 4H) and 3.91 (s, 10H). The ^{31}P-NMR spectrum of the complex **102** exhibited a singlet at 17.68 ppm which is in agreement to two PPh_3 ligands bonded to the osmium atoms in a *trans* arrangement (see **Figure 2.4**).

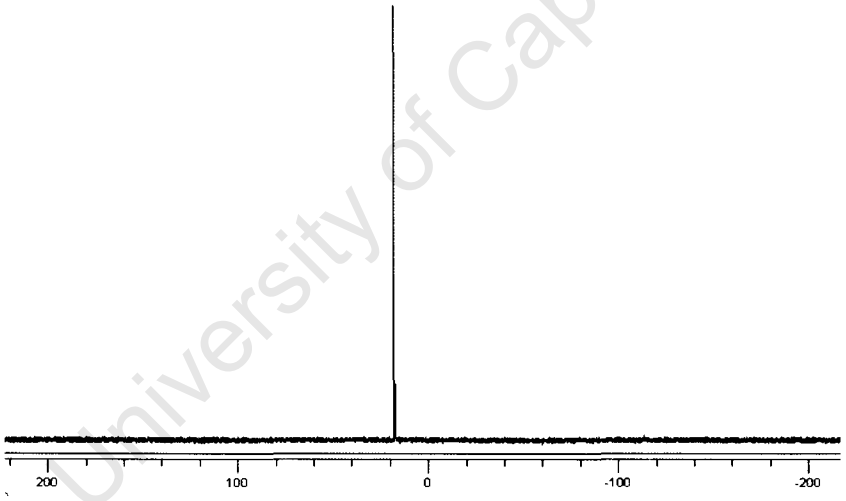

Figure 2.4 ^{31}P NMR spectrum of complex **102**

The ^{1}H-NMR spectrum of complex **103** showed three resonance signals in the aromatic region which were in the ratio of 2:1:2. The signals were attributed to the 2- and 6-H, 4-H and the 3- and 5-H protons of the pyridine ring.

2.4.3 Crystal structures of complexes 102 and 103

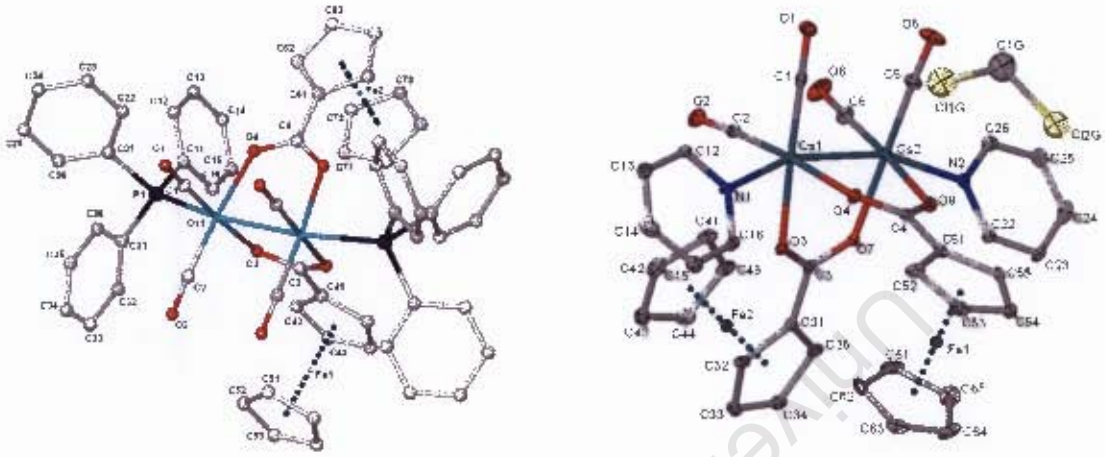

102 **103**

Figure 2.5 Crystal structures of **102** and **103** showing the atomic numbering.

The two dimeric osmium(I) complexes **102** and **103** have also been characterised by X-ray crystallography. Crystals suitable for X-ray diffraction were obtained by recrystallisation from dichloromethane-methanol mixtures. Complex **103** gave dichloromethane-solvated crystals. Crystallographic data for both complexes are summarized in **Table 2.3**.

Both complexes adopt a sawhorse structure in which two CO groups on each metal centre are mutually cis and opposite the bridging ferrocenyl carboxylate groups with two axial ligands (see **Figure 2.5**). Each osmium atom is octahedrally surrounded by two carbon atoms from the terminal carbonyl ligands, two oxygen atoms from the carboxylato-bridges, the other osmium atom and phosphorus (for **102**) or nitrogen (for **103**) atom from the axial ligands.

The structures are similar to those of the analogous ruthenium complexes reported by Auzias *et al.* [7]. The two ferrocenyl substituents at the two carboxylato-bridges adopt an

endo / exo orientation. The Os–Os distances (**102**: 2.7603(5)Å, **103**: 2.7076(4)Å are in the range of an Os–Os single bond [8,9,10] (see also **Tables 2.4 and 2.5** for selected bond length and angles). The Os–Os distance is longer in complex **102** than in **103**. This is probably due to the steric effects of the bulky triphenylphosphine ligands.

The OCO bond angles of the two carboxylato-bridges (**102**: 124.1(8) and 124.6(8)°, **103**: 125.6(8) and 125.3(8)°) are comparable to those of the analogous ruthenium complexes [7].

The pyridine rings in **103** are displaced away from the carbonyl groups and towards the middle of the two carboxylato-bridges with N1–Os1–Os2 and N2–Os2–Os1 angles of 161.00(17) and 162.34(18)° respectively. Such behaviour is a result of the dihedral angle between the planes of the equatorial ligands around each metal center being open towards the equatorial carbonyl groups and that the osmium-nitrogen bond is perpendicular to the plane of the equatorial ligands [11]. The acetate groups are slightly twisted with respect to the Os1–Os2 bond as shown by the O3–Os1–Os2–O7 and O4–Os1–Os2–O8 torsion angles (7.4(2) and 4.3(2) respectively).

Table 2.3 Crystallographic data for complexes **102** and **103**

Chemical formula	$C_{62}H_{48}Fe_2O_8P_2Os_2$ **(102)**	$C_{37}H_{29}Cl_2Fe_2N_2O_8Os_2$ **(103)**
Formula weight	1475.04	1192.62
Crystal system	Monoclinic	Monoclinic
Space group	$P2_1/m$	$P2_1$
Crystal colour and shape	Red needle	Red needle
Crystal size	0.16 x 0.05 x 0.04	0.13 x 0.13 x 0.12 mm
a( )	11.8407(3)	10.3611(2)
b( )	17.8596(9)	16.7872(3)
c( )	12.6968(7)	11.1389(25)
α(°)	90	90
β(°)	102.753(3)	106.9480(10)
(°)	90	90
V(^{3})	2618.8(2)	1853.29(6)
Z	2	2
T(K)	173(2)	223(2)
D_{calc} (gcm^{-3})	1.871	2.137
(mm^{-1})	5.499	7.800
Scan range (2θ)	2.88 – 25.65	4.83 – 25.65
Unique reflections	4938	6976
Reflections used [$I > 2\sigma(I)$]	25897	32268
R_{int}	0.0942	0.0552
Final R indices [$I > 2\sigma(I)$]	0.0339, wR_2 0.0640	0.0327 wR_2 0.0687
R indices (all data)	0.0636, wR_2 0.0775	0.0421, wR_2 0.0727
Goodness-of-fit	1.017	1.045
Maxi , minimum Δ / $^{-3}$	0.8100, 0.4732	0.4546, 0.4304

Table 2.4 Selected interatomic distances and angles for complex **103**

Interatomic distances (Å)

Os(1)-C(1)	1.824(11)	Fe(1)-C(52)	2.057(9)
Os(1)-C(2)	1.833(9)	Fe(2)-C(42)	2.017(10)
Os(1)-O(4)	2.114(5)	Fe(2)-C(31)	2.028(8)
Os(1)-O(3)	2.137(6)	Fe(2)-C(45)	2.031(10)
Os(1)-N(1)	2.217(6)	Fe(2)-C(43)	2.037(9)
Os(1)-Os(2)	2.7076(4)	Fe(2)-C(44)	2.039(9)
Os(2)-C(5)	1.822(10)	Fe(2)-C(33)	2.047(10)
Os(2)-C(6)	1.823(10)	Fe(2)-C(32)	2.049(8)
Os(2)-O(7)	2.109(6)	Fe(2)-C(35)	2.054(9)
Os(2)-O(8)	2.132(6)	Fe(2)-C(34)	2.055(9)
Os(2)-N(2)	2.193(7)	Fe(2)-C(41)	2.060(9)
Fe(1)-C(51)	2.013(8)	O(1)-C(1)	1.169(11)
Fe(1)-C(62)	2.026(10)	O(2)-C(2)	1.178(10)
Fe(1)-C(65)	2.027(11)	O(3)-C(3)	1.263(10)
Fe(1)-C(61)	2.029(10)	O(4)-C(4)	1.269(9)
Fe(1)-C(55)	2.035(8)	O(5)-C(5)	1.165(11)
Fe(1)-C(64)	2.042(10)	O(6)-C(6)	1.151(11)
Fe(1)-C(54)	2.045(9)	O(7)-C(3)	1.280(10)
Fe(1)-C(63)	2.047(11)	O(8)-C(4)	1.271(10)
Fe(1)-C(53)	2.049(9)		

Bond Angles (deg)

C(1)-Os(1)-C(2)	88.8(4)	C(6)-Os(2)-N(2)	96.9(3)
C(1)-Os(1)-O(4)	96.2(3)	O(7)-Os(2)-N(2)	82.4(2)
C(2)-Os(1)-O(4)	175.0(3)	O(8)-Os(2)-N(2)	83.9(2)
C(1)-Os(1)-O(3)	177.0(3)	C(5)-Os(2)-Os(1)	93.8(3)
C(2)-Os(1)-O(3)	91.1(3)	C(6)-Os(2)-Os(1)	94.6(3)
O(4)-Os(1)-O(3)	83.9(2)	O(7)-Os(2)-Os(1)	83.73(15)
C(1)-Os(1)-N(1)	98.9(3)	O(8)-Os(2)-Os(1)	83.84(15)
C(2)-Os(1)-N(1)	97.3(3)	N(2)-Os(2)-Os(1)	162.34(18)
O(4)-Os(1)-N(1)	81.3(2)	C(3)-O(3)-Os(1)	122.5(5)
O(3)-Os(1)-N(1)	84.0(2)	C(4)-O(4)-Os(1)	124.5(5)
C(1)-Os(1)-Os(2)	93.6(3)	C(3)-O(7)-Os(2)	123.9(5)
C(2)-Os(1)-Os(2)	97.2(3)	C(4)-O(8)-Os(2)	123.1(5)
O(4)-Os(1)-Os(2)	83.15(14)	O(1)-C(1)-Os(1)	179.2(8)
O(3)-Os(1)-Os(2)	83.51(15)	O(2)-C(2)-Os(1)	175.7(8)
N(1)-Os(1)-Os(2)	161.00(17)	O(3)-C(3)-O(7)	124.6(8)
C(5)-Os(2)-C(6)	90.1(5)	O(3)-C(3)-C(31)	118.8(7)
C(5)-Os(2)-O(7)	176.5(4)	O(7)-C(3)-C(31)	116.5(7)
C(6)-Os(2)-O(7)	92.6(4)	O(4)-C(4)-O(8)	124.1(8)
C(5)-Os(2)-O(8)	93.2(4)	O(4)-C(4)-C(51)	116.9(7)
C(6)-Os(2)-O(8)	176.4(4)	O(8)-C(4)-C(51)	119.1(7)
O(7)-Os(2)-O(8)	84.1(2)	O(5)-C(5)-Os(2)	176.5(11)
C(5)-Os(2)-N(2)	99.5(3)	O(6)-C(6)-Os(2)	178.9(10)

Dihedral Angles (deg)			
C(1)-Os(1)-Os(2)-C(5)	10.4(4)	O(4)-Os(1)-Os(2)-O(8)	7.3(2)
C(2)-Os(1)-Os(2)-C(5)	99.6(4)	O(3)-Os(1)-Os(2)-O(8)	-77.3(2)
O(4)-Os(1)-Os(2)-C(5)	-85.4(4)	N(1)-Os(1)-Os(2)-O(8)	-28.0(6)
O(3)-Os(1)-Os(2)-C(5)	-170.1(4)	C(1)-Os(1)-Os(2)-N(2)	149.4(7)
N(1)-Os(1)-Os(2)-C(5)	-120.8(6)	C(2)-Os(1)-Os(2)-N(2)	-121.3(7)
C(1)-Os(1)-Os(2)-C(6)	-80.1(4)	O(4)-Os(1)-Os(2)-N(2)	53.6(6)
C(2)-Os(1)-Os(2)-C(6)	9.2(4)	O(3)-Os(1)-Os(2)-N(2)	-31.0(6)
O(4)-Os(1)-Os(2)-C(6)	-175.9(4)	N(1)-Os(1)-Os(2)-N(2)	18.2(8)
O(3)-Os(1)-Os(2)-C(6)	99.5(4)	C(1)-Os(1)-O(3)-C(3)	-4(7)
N(1)-Os(1)-Os(2)-C(6)	148.7(6)	C(2)-Os(1)-O(3)-C(3)	83.6(7)
C(1)-Os(1)-Os(2)-O(7)	-172.1(3)	O(4)-Os(1)-O(3)-C(3)	-97.2(6)
C(2)-Os(1)-Os(2)-O(7)	-82.9(3)	C(1)-Os(1)-N(1)-C(16)	-140.8(7)
O(4)-Os(1)-Os(2)-O(7)	92.0(2)	Os(2)-Os(1)-N(1)-C(12)	168.7(5)
O(3)-Os(1)-Os(2)-O(7)	7.4(2)	Os(1)-Os(2)-N(2)-C(26)	173.8(5)
N(1)-Os(1)-Os(2)-O(7)	56.7(6)	O(4)-Os(1)-C(1)-O(1)	100(74)
C(1)-Os(1)-Os(2)-O(8)	103.2(3)	O(8)-Os(2)-C(5)-O(5)	12(13)
C(2)-Os(1)-Os(2)-O(8)	-167.6(3)		

Table 2.5 Selected interatomic distances and angles for complex **102**

Interatomic distances (Å)			
Os(1)-C(1)	1.835(7)	Fe(2)-C(62)	2.022(7)
Os(1)-C(2)	1.850(7)	Fe(2)-C(71)#1	2.029(6)
Os(1)-O(4)	2.124(4)	Fe(2)-C(71)	2.029(6)
Os(1)-O(3)	2.131(4)	Fe(2)-C(61)	2.032(10)
Os(1)-P(1)	2.4246(15)	Fe(2)-C(63)	2.035(6)
Os(1)-Os(1)#1	2.7603(5)	Fe(2)-C(63)#1	2.035(6)
Fe(1)-C(41)	2.029(9)	Fe(2)-C(73)	2.052(11)
Fe(1)-C(53)#1	2.038(7)	P(1)-C(21)	1.826(6)
Fe(1)-C(53)	2.038(7)	P(1)-C(11)	1.833(6)
Fe(1)-C(42)	2.040(6)	P(1)-C(31)	1.840(6)
Fe(1)-C(42)#1	2.040(6)	O(1)-C(1)	1.173(8)
Fe(1)-C(51)	2.040(11)	O(2)-C(2)	1.153(8)
Fe(1)-C(52)#1	2.042(8)	O(3)-C(3)	1.267(5)
Fe(1)-C(52)	2.042(8)	O(4)-C(4)	1.273(5)
Fe(1)-C(43)	2.048(7)	C(3)-O(3)#1	1.267(5)
Fe(1)-C(43)#1	2.048(7)	C(3)-C(41)	1.470(12)
Fe(2)-C(72)	2.015(7)	C(4)-O(4)#1	1.273(5)
Fe(2)-C(72)#1	2.015(7)	C(4)-C(61)	1.472(12)
Fe(2)-C(62)#1	2.022(7)		

Bond Angles (deg)			
C(1)-Os(1)-C(2)	89.7(3)	O(3)-Os(1)-Os(1)#1	83.15(10)
C(1)-Os(1)-O(4)	92.2(2)	P(1)-Os(1)-Os(1)#1	165.79(4)
C(2)-Os(1)-O(4)	175.3(2)	O(4)#1-C(4)-O(4)	125.6(8)
C(1)-Os(1)-O(3)	176.1(2)	O(4)#1-C(4)-C(61)	117.2(4)
C(2)-Os(1)-O(3)	92.7(2)	O(4)-C(4)-C(61)	117.2(4)
O(4)-Os(1)-O(3)	85.13(16)	C(3)-O(3)-Os(1)	124.1(4)
C(1)-Os(1)-P(1)	95.75(19)	C(4)-O(4)-Os(1)	123.9(4)
C(2)-Os(1)-P(1)	98.36(19)	O(1)-C(1)-Os(1)	178.7(5)
O(4)-Os(1)-P(1)	85.70(11)	O(2)-C(2)-Os(1)	177.9(6)
O(3)-Os(1)-P(1)	86.99(10)	O(3)#1-C(3)-O(3)	125.3(8)
C(1)-Os(1)-Os(1)#1	93.64(19)	O(3)#1-C(3)-C(41)	117.3(4)
C(2)-Os(1)-Os(1)#1	92.31(19)	O(3)-C(3)-C(41)	117.3(4)
O(4)-Os(1)-Os(1)#1	83.30(10)		

Dihedral Angles (deg)			
C(1)-Os(1)-O(3)-C(3)	37(3)	C(1)-Os(1)-C(2)-O(2)	-117(17)
C(2)-Os(1)-O(3)-C(3)	-90.2(6)	O(4)-Os(1)-C(2)-O(2)	-2(19)
O(4)-Os(1)-O(3)-C(3)	85.6(6)	O(3)-Os(1)-C(2)-O(2)	60(17)
P(1)-Os(1)-O(3)-C(3)	171.6(6)	P(1)-Os(1)-C(2)-O(2)	148(17)
Os(1)#1-Os(1)-O(3)-C(3)	1.8(6)	Os(1)#1-Os(1)-C(2)-O(2)	-23(17)
C(1)-Os(1)-O(4)-C(4)	95.1(6)	Os(1)-O(3)-C(3)-O(3)#1	-3.9(12)
C(2)-Os(1)-O(4)-C(4)	-20(3)	Os(1)-O(3)-C(3)-C(41)	173.7(5)
O(3)-Os(1)-O(4)-C(4)	-82.0(6)	Os(1)-O(4)-C(4)-O(4)#1	-3.7(12)
P(1)-Os(1)-O(4)-C(4)	-169.3(6)	Os(1)-O(4)-C(4)-C(61)	178.5(5)
Os(1)#1-Os(1)-O(4)-C(4)	1.7(5)	O(3)#1-C(3)-C(41)-C(42)	174.4(8)
P(1)-Os(1)-C(1)-O(1)	-166(26)	O(3)-C(3)-C(41)-C(42)#1	-174.4(8)
Os(1)#1-Os(1)-C(1)-O(1)	3(26)		

Symmetry transformations used to generate equivalent atoms:#1 x,-y+1/2,z

Table 2.6 Comparison of the Os–Os distances in dinuclear osmium compounds

Compound	Os–Os	Reference
$[Os_2(CO)_6(MeCO_2)_2]$ (**4**)	2.731(2)	10
$[Os_2(CO)_4(MeCO_2)_2(dppm)_2]$ (**104**)	2.740(1)	12
$[Os_2(\ :\ ^4\text{-}C_{12}H_{10}N_2)(CO)_6]$ (**105**)	2.7998(8)	13
$[Cp^*(CO)_2Os]_2$ (**106**)	2.7668(7)	
$[Os_2(CO)_4(\mu\text{-}O_2CC_5H_4FeC_5H_5)_2(PPh_3)_2]$ (**102**)	2.7603(5)	This work
$[Os_2(CO)_4(\mu\text{-}O_2CC_5H_4FeC_5H_5)_2(py)_2].(CH_2Cl_2)$ (**103**)	2.7076(4)	This work
$[N(PPh_3)_2][Os_2(MeCO_2)_2Cl(CO)_5]$ (**107**)	2.714(4)	
$[Os_2(\mu\text{-}I)(\mu\text{-}PPh_2)(PPh_3)_2(CO)_4]$ (**108**)	2.781(1)	14

Table 2.4 shows the Os–Os bond distances in dinuclear osmium compounds. The bond distance varies from 2.7076(4) Å to 2.7998(8) Å.

2.5 Synthesis and characterization of $[Ru_2(CO)_2(\mu\text{-}CO)_2(\mu\text{-}O_2CEt)(N\text{-}N)_2][PF_6]$ {N-N = bipy (109), 1,10-phen (110), 5-Me-1,10-phen (111), 4-Me-1,10-phen (112), 5-Cl-1,10-phen (113)}

The carboxylato-bridged complexes of the type $[Ru_2(CO)_2(\mu\text{-}CO)_2(\mu\text{-}O_2CEt)(N\text{-}N)_2][PF_6]$ were synthesized from $[Ru_2(CO)_4(\mu\text{-}O_2CEt)_2(py)_2]$ as shown in Scheme **2.2**.

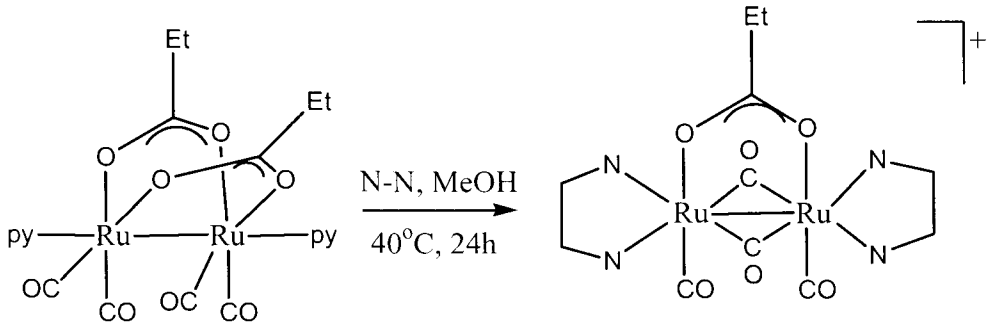

Scheme 2.2

This takes advantage of the ease of synthesis of complex $[Ru_2(CO)_4(\mu\text{-}O_2CEt)_2(py)_2]$ and also the high lability of pyridine ligands [5,8]. The bidentate diimine is added to a methanol suspension of $[Ru_2(CO)_4(\mu\text{-}O_2CEt)_2(py)_2]$ in excess. The suspension is then sonicated for about 5 minutes. The resulting solution is then heated at about 40°C for 24h. NH_4PF_6 is then added precipitating out a solid product of the type $[Ru_2(CO)_2(\mu\text{-}CO)_2(\mu\text{-}O_2CEt)(N\text{-}N)_2][PF_6]$. The complexes **109-113** were obtained as orange powders in moderate to good yields. The complexes were characterised by ^{1}H-NMR and IR spectroscopic techniques.

2.5.1 IR spectroscopic analysis of complexes 109-113

The IR spectra of the complexes **109-113** exhibit two bands in the region 2100-1800 cm^{-1} and two bands at lower frequencies in the region 1800-1700 cm^{-1} (**Figure 2.6**). The bands in the first region were assigned to $\nu(CO_{terminal})$ while those in the second region were assigned to $\nu(CO_{bridging})$. These spectra closely resemble that of the structurally characterised complex $[Ru_2(\mu\text{-}CO)_2(\mu\text{-}O_2CMe)(N\text{-}N)_2][PF_6]$ (N-N = 1,10-phen) synthesized by Frediani *et al.* [9]. This suggests a similar core structure in which one bridging propionate ligand and the two pyridine ligands have been displaced by the two diimine ligands that coordinate to the two metal centers in a chelating fashion.

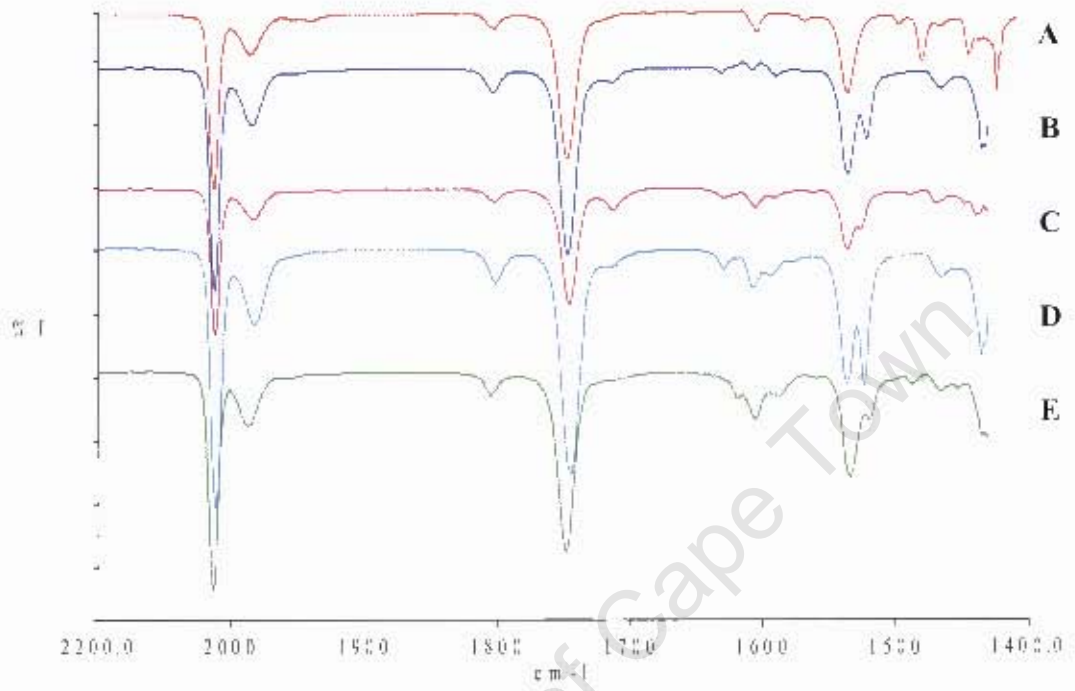

Figure 2.6: IR spectra for complexes $Ru_2(\mu\text{-}CO)_2(\mu\text{-}O_2CEt)(N\text{-}N)_2][PF_6]$ (N-N = bipy (**A**), 1,10-phen (**B**), 5-methyl-1,10-phen (**C**), 4-methyl-1,10-phen (**D**) and 5-chloro-1,10-phen (**E**).

2.5.2 ^{1}H NMR spectroscopic data for complexes 109-113

As reported in literature [8] for similar complexes where R = Me, the ^{1}H NMR spectra show that the complexes are symmetrical. The ethyl group displayed a quartet and a triplet around 1.09 ppm and -0.18 ppm for the CH_2 and CH_3 groups respectively. These signals integrated for the two and three protons.

In the aromatic region (8.17 – 10.08 ppm), the spectrum of $[Ru_2(CO)_4(\mu\text{-}O_2CEt)(bipy)_2][PF_6]$ **109** exhibited four resonance signals that were attributed to the sixteen protons, eight on each of the bipyridine ligands. This is in agreement with two chemically equivalent rings in a bipyridine ligand.

The spectrum of $[Ru_2(CO)_4(\mu\text{-}O_2CEt)(1,10\text{-phen})_2][PF_6]$ **110** also exhibited four resonances in the region 8.47 – 10.63 ppm for the 1,10-phenanthroline ligands in chemically equivalent environments. The 4-methyl-1,10-phenanthroline and 5-methyl-1,10-phenanthroline ligands present in the complexes $[Ru_2(CO)_4(\mu\text{-}O_2CEt)(4\text{-Me-}1,10\text{-phen})_2][PF_6]$ and $[Ru_2(CO)_4(\mu\text{-}O_2CEt)(5\text{-Me-}1,10\text{-phen})_2][PF_6]$ each exhibited a singlet at 3.15 and 3.03 ppm respectively that was attributed to methyl substituent.

2.6 Synthesis and characterization of $[Ru_2(\mu\text{-}CO)(CO)_4(\mu\text{-dppm})_2]$ (114)

The electron rich complex **114** was synthesized from the reaction of a trinuclear ruthenium cluster $[Ru_3(CO)_{12}]$ (**1**) with bis(dimethylphosphino)-methane (dppm) under a high pressure of CO (6.9 MPa). The product was isolated as an air sensitive yellow solid.

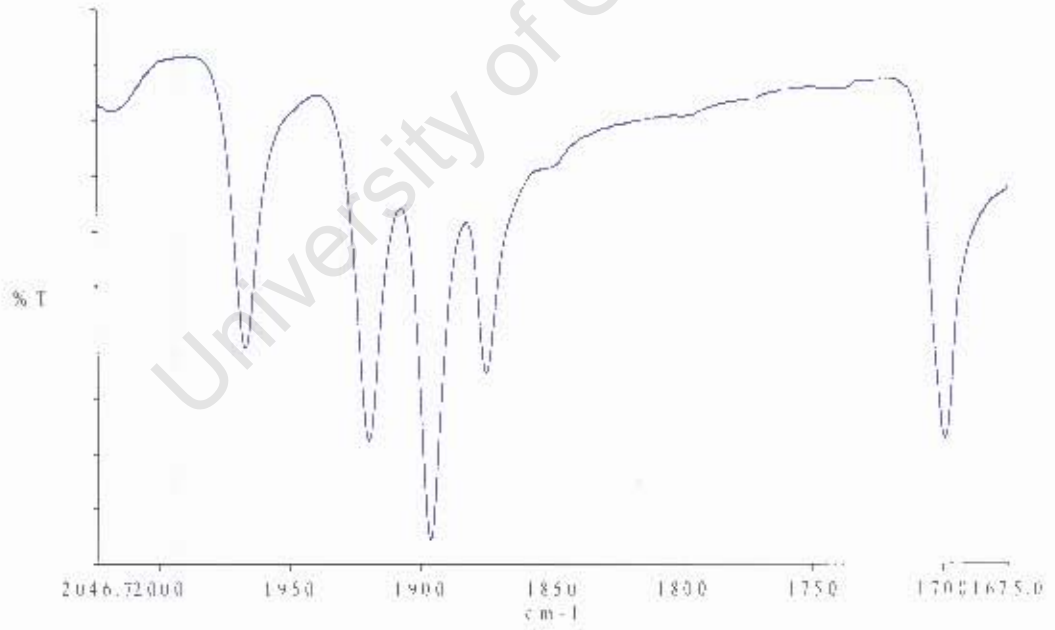

Figure 2.7 IR spectrum of complex (**114**)

The IR spectrum of the complex exhibited four absorption bands in the region 2000 – 1800 cm^{-1} that are attributable to the terminal carbonyl ligands while an absorption at 1699 cm^{-1} was attributed to the bridging carbonyl ligand (see **Figure 2.7**).

The redox behaviour of this complex was also studied by cyclic voltammetry (see Chapter 3).

2.7 Attempted synthesis of $[Os_2(\mu\text{-}CO)(CO)_4(\mu\text{-}dppm)_2]$ (115)

An attempt was made to synthesize an osmium analogue of $[Ru_2(\mu\text{-}CO)(CO)_4(\mu\text{-}dppm)_2]$ (**114**) (see **Scheme 2.3**). A high pressure autoclave reaction of the trinuclear osmium cluster $[Os_3(CO)_{12}]$ (**2**) with dppm yielded orange crystals of the known complex $[Os_3(CO)_8(\mu\text{-}dppm)_2]$ (**116**) [15] in high yield (90 %) instead of the targeted complex. This complex is derived from the parent complex **2** by the substitution of carbonyl groups by the phosphorus atoms of the edge-bridging dppm ligands. The failure to form the electron rich complex **115** could be attributed to the very strong Os-Os bonds.

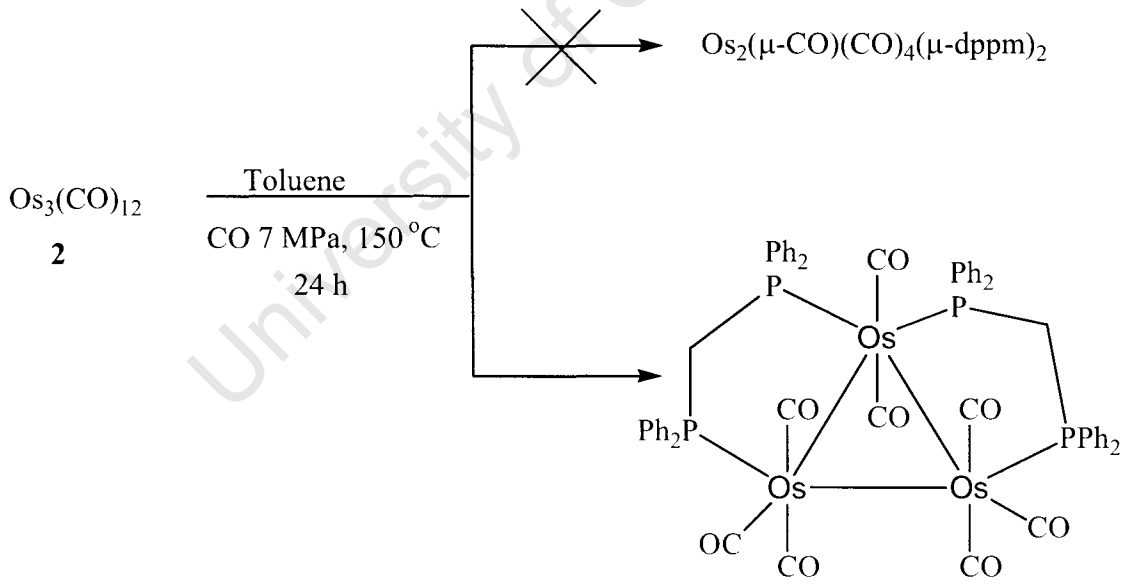

116

Scheme 2.3

2.7.1 IR spectroscopic analysis of $[Os_3(CO)_8(\mu\text{-dppm})_2]$ (116)

The infrared spectrum showed five bands in the region 2100 – 1800 cm^{-1}. The data (2047m, 1990 m, 1963 vs, 1938 m and 1896 w) is in agreement with that previously reported by Cartwright *et al.* (2047 m, 1989 m, 1962 vs, 1937 m, 1895 w and 1887 sh) [15]. The product formulation was also supported by elemental analysis studies.

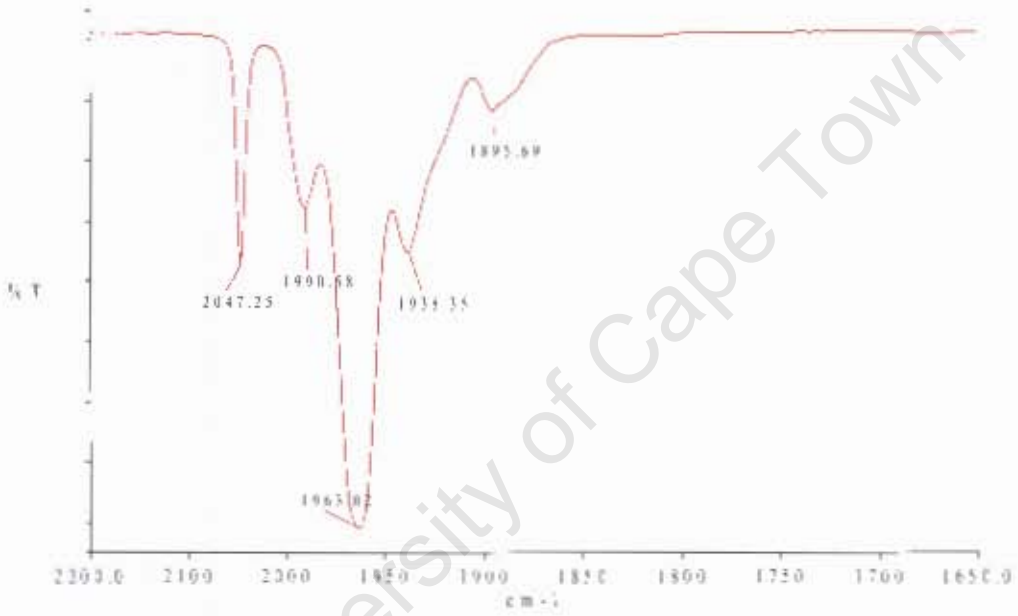

Figure 2.8 IR Spectrum for $[Os_3(CO)_8(\mu\text{-dppm})_2]$

2.7.2 NMR spectroscopic data for 116

The ^1H NMR spectrum of complex **116** showed a triplet signal at 4.80 ppm attributed to the - CH_2 protons of the dppm ligands with a coupling constant (J – 9.80 Hz) that is in agreement with the literature value [15]. The ^{31}P-NMR spectrum exhibited an AA'BB' pattern that was centred at -21.81 ppm (see **Table 2.7**).

Table 2.7 ^1H and ^{31}P NMR spectroscopic data for complex 116

Complex	δ (^1H)	δ ($^{31}P\{^1H\}$)
116	4.8 (t, *J* – 9.8 Hz)	AA'BB' spectrum centered at -21.81

2.8 References

1. G. R. Crooks, B. F. G. Johnson, J. Lewis, I. G. Williams, G. Gamlen, *J. Chem. Soc. A*, 1969, 2761.
2. M. Bianchi, P. Frediani, U. Matteoli, G. Menchi, F. Piacenti, G. Petrucci, *J. Organomet. Chem.,* 1983, **259**, 207.
3. M. Rotem, Y. Shvo, I. Goldberg, U. Shmueli, *Organometallics,* 1984, **3**, 1758.
4. A. Salvini, P. Frediani, F. Piacenti, *J. Mol. Cat. A: Chemical,* 2000, **159**, 185.
5. C. M. Kepert, G. B. Deacon, L. Spiccia, G. D. Fallon, B. W. Skelton, A. H. White, *J. Chem. Soc., Dalton Trans.,* 2000, 2867.
6. J. Soler, I. Moldes, E. de la Encarnación, J. Ros, *J. Organomet. Chem.,* 1999, **580**, 108.
7. M. Auzias, B. Therrien, G. Labat, H. Stoeckli-Evans, G. Süss-Fink, *Inorg. Chim. Acta,* 2006, **359**, 1012.
8. P. Pearson, C. M. Kepert, G. B. Deacon, L. Spiccia, A. C. Warden, B. W. Skelton, A. H. White, *Inorg. Chem.,* 2004, **43**, 683.
9. P. Frediani, M. Bianchi, A. Salvini, R. Guarducci, L. C. Carluccio, F. Piacenti, S. Ianelli, M. Nardelli, *J. Organomet. Chem.,* 1993, **463**, 187
10. J. G. Bullitt, F. A. Cotton, *Inorg. Chim. Acta,* 1971, **5**, 406
11. N. Kanematsu, M. Ebihara, T. Kawamura, *J. Chem. Soc., Dalton Trans.,* 1999, 4413
12. E. Singleton, M. O. Albers, M. M. de V. Steyn, *J. Chem. Soc., Dalton Trans.,* 1989, 2303
13. R. A. Machado, D. Rivillo, A. J.Arce, Y. De Sanctis, A. J. Deeming, L. D'Ornelas, T. González, R. Atencio, *J. Organomet. Chem.,* 2005, **690**, 504
14. A. W. Herlinger, A. L. Rheingold, *Acta Cryst.,* 1997, **C53**, 285
15. S. Cartwright, J. A. Clucas, R. H. Dawson, D. F. Foster, M. M. Harding, A. K. Smith, *J. Organomet. Chem.,* 1986, **302**,403

CHAPTER 3
ALKANE OXIDATION REACTIONS, ALKENE ISOMERISATION REACTIONS AND ELECTROCHEMICAL STUDIES

3.1 C-H Activation

Alkane C-H bond activation is defined as the binding of an alkane C-H bond to a metal normally with the cleavage of the bond by oxidative addition (Eqn 3.1) [1]

$$L_nM + R\text{-}H \longrightarrow L_nM(H\text{-}R) \longrightarrow L_nM(R)(H) \qquad \text{Eqn 3.1}$$

Alkanes from natural gas and petroleum are among the world's most abundant and low cost feedstocks [2, 3, 4, 5]. The petrochemical industry currently relies on heterogeneous catalysts for the production of chemical intermediates from hydrocarbons under severe conditions. C-H activation and functionalization using homogeneous transition metal catalysts offers several advantages such as high selectivity (regio-, stereo-, or enantio-) and very mild conditions [6, 7] and are potentially applicable to the functionalization of alkanes [6, 8, 9]. Thus the direct activation of alkanes to value-added petrochemicals would exploit an inexpensive hydrocarbon feedstock [10, 11]. Direct C-H bond activation requires insertion of a transition metal across a strong C-H bond to form a new carbon-metal bond followed by the generation of a new C-R bond (**Scheme 3.1**)

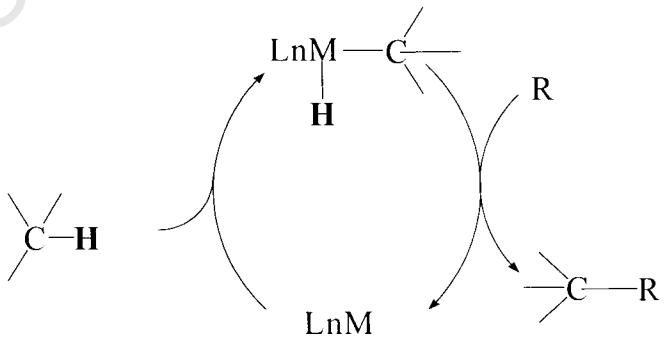

Scheme 3.1

Activation by Group 9 coordinatively unsaturated complexes has been proposed to proceed via two steps. The first step involves the coordination of the hydrocarbon to the

metal centre with the saturated alkane forming a σ-complex through the interaction of the metal with a C-H bond. The second step involves the cleavage of the C-H bond to form a metal alkyl hydride [10, 12, 13, 14, 15]. Crabtree [15] reported that the C-H σ-complexes are relevant to C-H activation because of the degree of acidification of the C-H proton that allows loss of proton and formation of a metal alkyl. The acidification results from the predominant ligand-to-metal charge transfer and minimal back donation. The C-H σ-complexation occurs preferentially at the least hindered CH bond for steric reasons hence the selectivity order of $1^{o} > 2^{o} > 3^{o}$ in many reactions.

Possible bonding modes have been proposed for alkanes and include η^2–C,H, η^2-H,H and η^3-H,H,H interactions [16, 17].

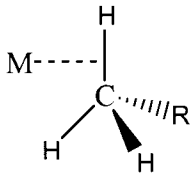

η^2–C,H

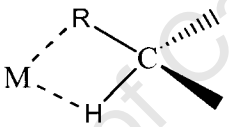

η^2–H,H

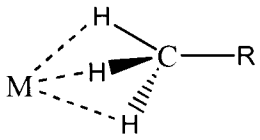

η^3–H,H,H

3.1.1. Classification of C-H bond activation mechanisms

Mechanistic studies have shown that there are five pathways for the activation of C-H bonds under mild conditions [4, 13, 18, 19]: oxidative addition, sigma bond metathesis, electrophilic substitution, metalloradical activation and 1,2 addition / elimination. The first three pathways shall be discussed here.

3.1.1.1. Oxidative addition / reductive elimination

Wayland reported that electronically and coordinatively unsaturated metal centres are required for the oxidative addition of hydrocarbon C-H units [20]. The route is common for electron rich low valent complexes of the late transition metals where this

coordinative unsaturation at the metal centre is readily accessible. Therefore it is necessary to generate the active species by either ligand dissociation from the metal centre or reductive elimination of the substrate [4, 21, 22, 23] (see Eqn. 3.2)

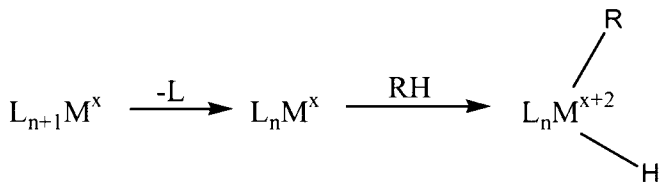

Eqn 3.2

3.1.1.2 Sigma bond metathesis

This route is common for the early transition metals with d^o (or d^of^n) electronic configurations [4, 19, 24 25]. Sigma bond metathesis proceeds via a four-centred transition state (Eqn. 3.3).

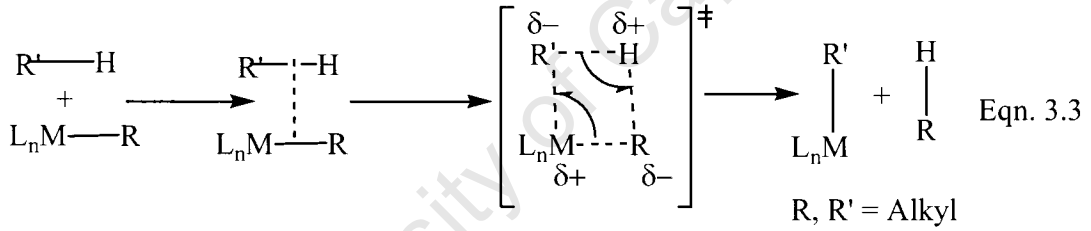

Eqn. 3.3

The sigma bond metathesis method always results in the formation of R-H and not R-R' bonds. Milet *et al.* have extended the concept of sigma bond metathesis to late transition metal through a theoretical assessment of reactions involving palladium(II) hydride and methyl complexes [25].

3.1.1.3 Electrophilic addition

Electrophilic activation usually occurs in a strongly polar medium such as water and anhydrous strong acids (Eqn. 3.4).

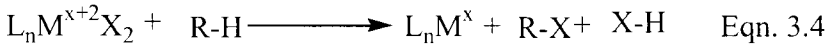

Eqn. 3.4

3.2 Alkane oxidations and alkene isomerisation reactions

The examples of alkane functionalisation include the oxidation of alkanes to their oxygenated products. In this project, cyclohexane and octane were used as models for the hydrocarbon functionalisation. The products, especially from cyclohexane are important raw materials for the industrial synthesis of adipic acid, a precursor in nylon 6 and nylon 66 synthesis. The next sections will detail results on alkane oxidation (Section 3.2) as well as alkene isomerisation (Section 3.3).

3.2.1 Results and discussion on oxidation of alkane substrates

The catalytic activity of the dinuclear carboxylato-bridged complexes of osmium $[Os_2(CO)_4(\mu\text{-}O_2CMe)_2(PCy_3)_2]$ (**90**), $[Os_2(CO)_4(\mu\text{-}O_2CMe)_2(PPh_3)_2]$ (**91**) and $[Os_2(CO)_4(\mu\text{-}O_2CMe)_2(4\text{-}H_2Npy)_2]$ (**101**), was investigated in the oxidation of both linear (octane) and cyclic (cyclohexane) alkanes.

Several oxidants in these reactions have been reported in literature and include hydrogen peroxide [26,27,28], alkyl hydroperoxides [29,30,31], and molecular oxygen.

In the present study, the catalytic reactions were carried using H_2O_2 as the oxidant. The advantage of using hydrogen peroxide as an oxidant is that it gives water as a by-product [32]. The catalyst : substrate : oxidant ratio used was 1:1100:1100 with a catalyst concentration of 7×10^{-4} M. In the runs carried out, a control experiment was conducted with the substrate and the oxidant present but without the catalyst. All the samples were analyzed without workup. Authentic samples of the oxygenated products were used as calibration standards in order to assign peaks in the gas chromatograms by comparison of retention times.

The oxidation of cyclohexane gave cyclohexanol and cyclohexanone as products (see **Table 3.1**). The average ratio of cyclohexanol to cyclohexanone is 4.53:1. In the case of

octane, the alcohol : ketone average ratio is 1.76. These ratios indicate a higher selectivity for the alcohol products over the ketones.

Table 3.1 Oxidation of Cyclohexane [a]

Catalyst	Cy=O [b] (%) [c]	Cy–OH [d] (%) [e]	ol/one	Total yield (%) [f]	TON [g]
90	1.02 ± 0.16	4.49 ± 0.24	4.40	5.52	61
91	0.99 ± 0.07	3.79 ± 0.53	3.83	4.78	53
101	1.16 ± 0.02	6.22 ± 0.20	5.36	7.38	81

[a] Reaction conditions: [catalyst] = 7.0 x 10^{-4} M; oxidant : substrate : catalyst mole ratio of 1100 :1100:1; solvent = acetonitrile; reaction duration = 24 h; Temperature = 80 °C. [b] Cy=O is cyclohexanone. [c] (mol cyclohexanone / mol cyclohexane) x 100 %. [d] Cy–OH is cyclohexanol. [e] (mol cyclohexanol / mol cyclohexane) x 100. [f] Total yield (%) = cyclohexanone + cyclohexanol. [g] Turn over number (TON) = (mol products / mol catalyst).

Table 3.2 Oxidation of Octane [a, b]

Catalyst	3-one (%)	2-one (%)	3-ol (%)	2-ol (%)	1-ol (%)	1-al (%)	Total (%) [c]	TON [d]
90	0.82	0.71	0.96	1.07	0.91	0.65	5.12	53
91	0.93	0.67	1.40	1.42	1.28	0.60	6.31	69
101	0.98	0.64	1.68	1.87	1.48	0.90	7.54	83

[a] Reaction conditions: [catalyst] = 7.0 x 10^{-4} M; oxidant : substrate : catalyst mole ratio of 1100 :1100:1; solvent = acetonitrile; reaction duration = 24 h; Temperature = 80 °C; yield of each product = (mol of product / mol of octane) x 100 %. [b] 3-one = octan-3-one; 2-one = octan-2-one; 3-ol = octan-3-ol; 2-ol = octan-2-ol; 1-ol = octan-1-ol; 1-al = octanal. [c] Total yield (%) = ∑(product yields). [d] Turn over number (TON) = (mol products / mol catalyst).

In the oxidation of cyclohexane, complex **101** gave the best yields for both the alcohol and ketone products.

In the catalytic oxidation of octane, six products were formed which are octanal, 3-octanone, 2-octanone, 3-octanol, 2-octanol and 1-octanol (see **Table 3.2**). These oxygenated products were obtained in very low yields. The results in **Table 3.2** show that the oxidation reactions had a higher selectivity for alcohol products compared to the ketone products. Amongst the alcohol products, the percentage yield for 1-octanol was the lowest followed by that of 3-octanol. The highest percentage yield was for the 2-

octanol product. It has been reported in literature [33] that in the catalytic oxidation of linear alkanes, the activation of the carbon atom at the second position was preferred to other positions and followed the order 2 > 3 > 4 >1. A different pattern though is found in the ketones formed with the yield of octan-2-one being lower than that of octan-3-one.

Comparison of TON for the two different substrates indicates that the activities of the catalysts on the different substrates were not significantly different. This shows that the reaction is not shape-selective. The catalysts are easily accessed by both the linear and cyclic alkane substrates. Tatsumi *et al.* [34] have however reported a large difference in TONs between n-hexane (TON = 7) and cyclohexane (TON = 0.37) and have attributed this large difference to substrate shape selectivity arising from the molecular sieving action of their titanosilicate catalyst.

3.2.2 Conclusions

The three dinuclear carboxylato-bridged complexes of osmium (**90**, **91** and **101**) were able to catalyse the oxidation of both cyclohexane and octane yielding their corresponding oxygenated products, albeit in low yields. The conversions were achieved under mild conditions (80 °C) and this is a very positive development in the light of the actual industrial process that uses homogeneous cobalt salts with operating temperatures above 150 °C and total conversion of 10-12 %. [35]. The alcohol : ketone ratio showed that the alcohol products are formed in higher proportions than the ketones.

3.3 Selective Isomerisation of 1-alkenes

This section describes results from selective 1-alkene isomerisation reactions. Some of this work has since been published as part of collaborative research project [36]. 1-Alkene isomerisation (see also Chapter 1) is a key step in many industrial processes, particularly in petrochemical refining, which involves various heterogeneous and homogeneous catalysts [37,38,39].

3.3.1 Results and Discussion

The complexes $[Os_2(CO)_6(\mu\text{-}O_2CMe)_2]$ (**4**) $[Ru(CO)_2(\mu\text{–}O_2CMe)_2]_n$ (**86**), $[Ru_2(CO)_4(\mu\text{-}O_2CMe)(\mu\text{-dppm})_2][PF_6]$ (**117**) and $[Ru_2(CO)_4(\mu\text{-}O_2CMe)_2(MeCN)_2]$ (**118**), were all tested as homogeneous catalysts for 1-alkene isomerisation reactions (see **Table 3.3**).

Table 3.3 Various catalysts tested for the isomerisation of 1-pentene to 2-pentene

Catalyst used	Experimental Conditions [a]	% Conversion (a mixture of cis- and trans- isomers)
$[Ru(CO)_2(\mu\text{–}O_2CMe)_2]_n$ (**86**)	10d, 80°C	66
$[Ru_2(CO)_4(\mu\text{-}O_2CMe)(\mu\text{-dppm})_2][PF_6]$(**117**)	10d, 80°C	35
$[Ru_2(CO)_4(\mu\text{-}O_2CMe)_2(MeCN)_2]$ (**118**)	5d, 80°C	100
$[Os_2(CO)_6(\mu\text{-}O_2CMe)_2]$ (**4**)	10d, 80°C	0
$[Ru_3(CO)_{12}]$ (**1**) [b]	3d, 80°C	100

[a] Toluene used as solvent. [b] See ref 36.

The highest catalytic activity was observed with the dinuclear carboxylato-bridged complex **118** while no activity was observed with complex **4.** The decreased activity of complex **117** could be attributed to steric effects. The catalytic activity of the polymeric complex **86** was lower than that of **118** and this could be a result of the compound being insoluble in aromatic solvents. Sivaramakrishna *et al.* [36] have reported that the parent cluster **1** was more efficient in the isomerisation reactions than these dinuclear compounds with a possible mechanistic pathway involving the dissociation of a CO ligand thus allowing for the coordination of the olefinic substrate to the cluster (See **Scheme 3.2**).

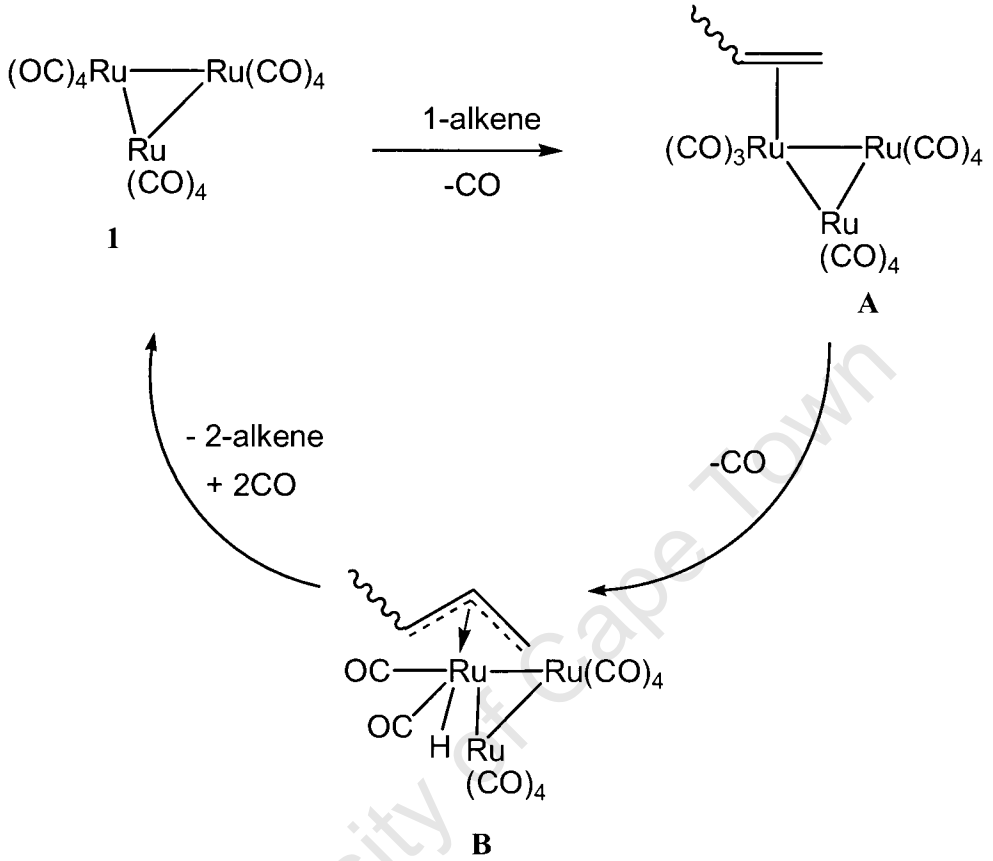

Scheme 3.2 [36]

The catalysis by the dinuclear complexes is expected to proceed mechanistically via the displacement of one axial ligand (using NCMe in **118** as an example) as reported by Salvini *et al.* [40]. The acetonitrile ligand is very labile and is displaced by the incoming 1-alkene substrate that coordinates to the metal centre. The mechanism is shown in **Scheme 3.3.** While the substrate is coordinated to the metal, isomerisation to give an internal olefin, possibly via an allyl hydride intermediate, takes place reducing its coordinating ability. The internal alkene formed is displaced by another terminal olefin.

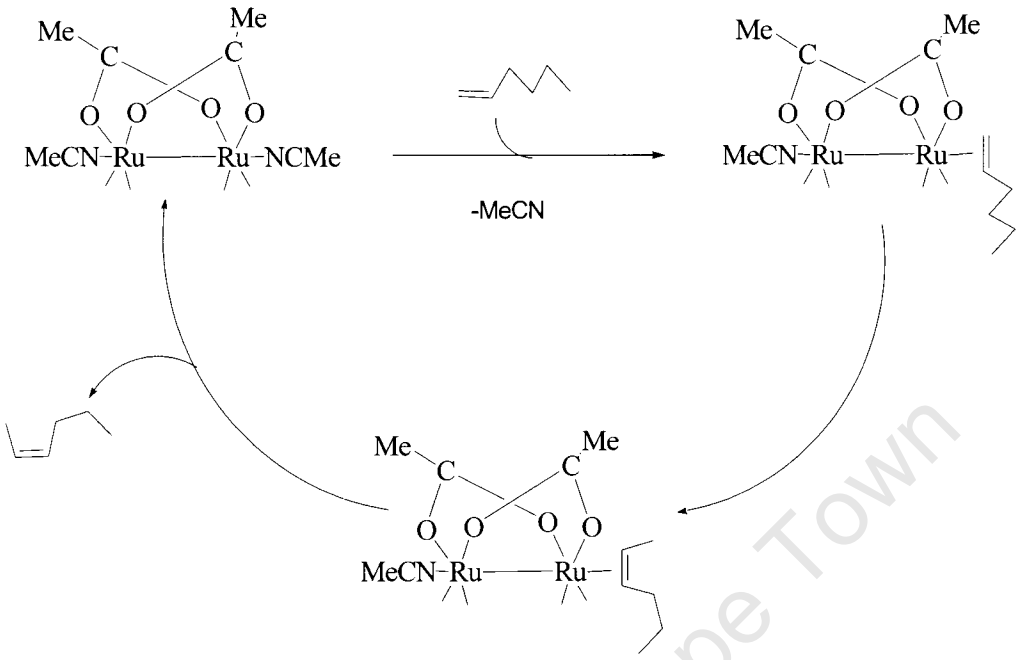

Scheme 3.3

3.3.2 Conclusions

The complexes $[Ru(CO)_2(\mu\text{–}O_2CMe)_2]_n$ (**86**), $[Ru_2(CO)_4(\mu\text{-}(O_2CMe)_2(MeCN)_2]$ (**118**), $[Ru_2(CO)_4(\mu\text{-}O_2CMe)(\mu\text{-}dppm)_2][PF_6]$ (**117**), $[Os_2(CO)_6(\mu\text{-}O_2CMe)_2]$ (**4**) have been shown to be catalysts for the isomerisation of 1-alkenes with $[Ru_2(CO)_4(\mu\text{-}(O_2CMe)_2(MeCN)_2]$ (**118**) being the most active of the three. The catalysis is expected to proceed via the displacement of one ligand from the metal centre providing a vacant site onto which the substrate can coordinate. Comparison with the activity of the parent cluster showed that the cluster was more efficient than the dinuclear systems.

3.4 Electrochemical studies

3.4.1 Results and discussion

The redox behaviour of the four complexes $[Ru_2(CO)_2(\mu\text{-}CO)_2(\mu\text{-}O_2CEt)(N\text{-}N)_2][PF_6]$ {N-N = 1,10-phen (**110**), 5-Me-1,10-phen (**111**), 4-Me-1,10-phen (**112**), 5-Cl-1,10-phen (**113**)} was investigated by cyclic voltammetry using dichloromethane solutions as the

complexes were not soluble in acetonitrile. **Table 3.4** shows the oxidation potentials, while **Figure 3.1** gives the cyclic voltammograms.

Table 3.4 Summary of cyclic voltammetric data [a] for the complexes **110-113**

Complex	E_a / V
110	+0.73
111	+0.72
112	+0.70
113	+0.77

[a] The cyclic voltammograms were recorded at a platinum disc electrode on *ca.* 1 mM dichloromethane solutions containing 0.1 M [n-Bu_4N][ClO_4] as the supporting electrolyte at room temperature. The potentials are given relative to the ferrocene / ferrocenium ion couple as a reference ($E_{1/2}$ = +0.20 V relative to the Ag/Ag^+ reference electrode).

All the complexes display a single irreversible anodic wave assigned to the $Ru^{I}{}_2/Ru^{I}Ru^{II}$ oxidation process [41] in the range +0.70 to +0.77 V. Comparison with an equimolar ferrocene system showed that the oxidation process involves only one electron transfer. The oxidation of one metal center strongly influences the electronic environment of the other metal centre, thus making the removal of an electron from the latter difficult.

The complex **110** with the unsubstituted 1,10-phenanthroline ligands is oxidized at a potential of +0.73 V. When substituents are introduced onto the ligand, small shifts in the oxidation potentials take place. The complex **113**, with an electron-withdrawing chloro-substituent at position 5, is oxidized at the higher potential of +0.77 V, while complexes **111** and **112**, with electron-donating methyl groups, are oxidized at slightly lower potentials of +0.72 and +0.70 V, respectively.

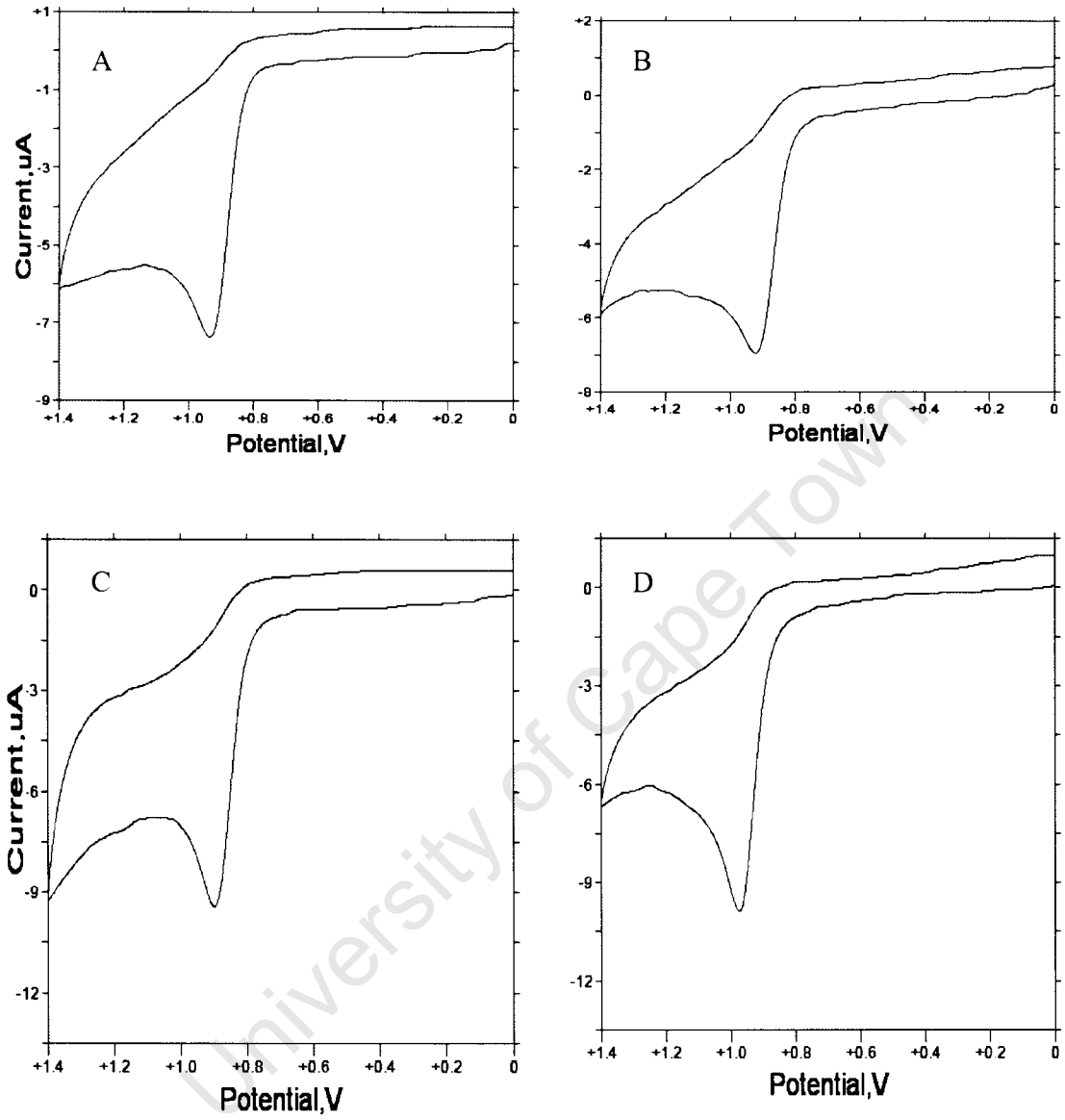

Figure 3.1 Cyclic voltammograms of **110** (A), **111** (B), **112** (C) and **113** (D) as recorded at 100 mV s^{-1} scan rate on a platinum disc electrode for ca. 1 mM analyte solutions in dichloromethane containing 0.1 M $[Bu_4N][ClO_4]$ as the supporting electrolyte. The potentials are given relative to the Ag/Ag^+ reference electrode. The $E_{1/2}$ for the ferrocene/ferrocenium ion couple under these conditions was +0.20 V.

The redox behaviour of the two ferrocenecarboxylato-bridged dinuclear osmium complexes $[Os_2(CO)_4(\mu\text{-}O_2CC_5H_4FeC_5H_5)_2L_2]$ {L = PPh_3 (**102**), py (**103**)} was also investigated. The two complexes undergo reversible oxidation of the ferrocene units followed by the irreversible oxidation of the diosmium core (see **Figure 3.2**). In each of the two complexes, both ferrocene units undergo reversible one-electron oxidation

simultaneously. Comparison of the oxidation current for the irreversible oxidation of the diosmium core, with that for the two one-electron oxidations of the ferrocene units shows that the irreversible oxidation of the metal centers involves two electrons. Auzias *et al.* [41] reported a different behaviour using the ruthenium analogues $[Ru_2(CO)_4(\mu\text{-}O_2CC_5H_4FeC_5H_5)_2(PPh_3)_2]$ (**119**) and $[Ru_2(CO)_4(\mu\text{-}O_2CC_5H_4FeC_5H_5)_2(py)_2]$ (**120**). The Ru_2-core was first oxidized followed by the ferrocene units when using **119** as the analyte, while **120** underwent oxidation of the ferrocene units followed by the irreversible oxidation of the Ru_2-core at higher potential. Here, too, both ferrocenyl groups were oxidized at the same potential.

A variation of oxidation potentials as a function of the axial ligand was observed [41]. In the triphenylphosphine-substituted complex **102**, the diosmium core (Os_2) is irreversibly oxidized at a potential of 0.50 V relative to the ferrocene / ferrocenium reference. An irreversible oxidation of the Os_2-core occurs at a higher potential of +0.66 V for the pyridine-substituted complex **103.** This behaviour is attributable to the different electron donating properties of the ligands. The triphenylphosphine ligand is a better electron donor than pyridine and therefore increases electron density on the Os_2-core facilitating its oxidation. The voltammogram of complex **102** is poorly resolved while that of **103** is well resolved (see **Figure 3.2**).

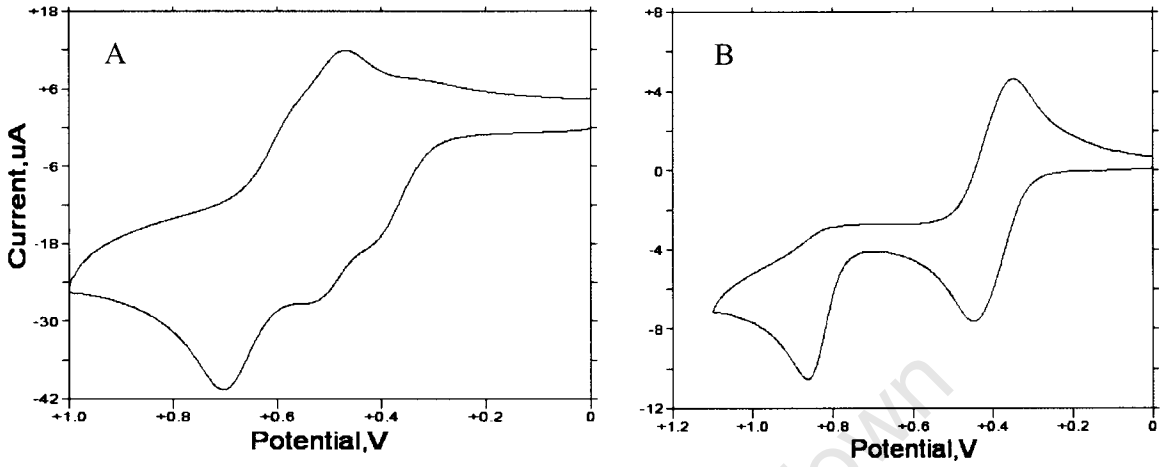

Figure 3.2 Cyclic voltammograms of **102** (A) and **103** (B) recorded at 100 mV s^{-1} scan rate on a platinum disc electrode for ca. 1mM analyte solutions in dichloromethane containing 0.1 M [n-Bu_4N][ClO_4] as the supporting electrolyte. The potentials are given relative to the Ag/Ag^+ reference electrode. The $E_{1/2}$ for the ferrocene/ferrocenium ion couple under these conditions was +0.20 V.

When [$Ru_2(\mu$-CO)$(CO)_4(dppm)_2$] (**114**) was used as the analyte, the voltammograms obtained were not well resolved. Two irreversible waves were observed at a higher scan rate of 500 mV s^{-1}, one at an oxidation potential of +0.02 V relative to the ferrocene/ferrocenium ion couple, attributed to the oxidation of the metal centers, and the other one at +0.66 V, which might be assigned to the oxidation of the diphosphine ligands. No firm conclusions can be drawn from the voltammograms due to their poor resolution using dichloromethane solutions of the analyte **114**. Comparison with other carboxylato-bridged complexes **102-103** and **110-113** shows that complex **114** is much easier to oxidize. This is due to the fact that the complex is electron rich with the ruthenium in the zero oxidation state.

3.4.2 Conclusions

All the complexes used in the electrochemical studies displayed irreversible oxidation of the di-metal centres.

The four complexes **110-113** displayed a single two-electron irreversible anodic wave in the range +0.70 to +0.77 V. The ferrocenecarboxylato-bridged dinuclear osmium complexes **102** and **103** underwent the reversible oxidation of the ferrocene units as well as the irreversible oxidation of the diosmium core. The complex **102** was oxidized at a lower potential (+0.50 V) than complex **103** (+0.66 V). This was attributed to differences in electron-donating properties of the axial ligands in the two complexes. This shows that by varying the axial ligands, the oxidation of metal centres and hence the reactivity of the complexes can be tuned. This may be particularly important in the designing of catalytic systems.

The complex **114** displayed two irreversible waves. The voltammograms for this complex were not well-resolved and therefore no firm conclusions could be made.

3.5 References

1. R. H. Crabtree, *J. Chem. Soc., Dalton Trans.,* 2001, 2437
2. B. L. Conley, W. J. Tenn III, K. J. H. Young, S. K. Ganesh, S. K. Meier, V. R. Ziatdinov, O. Mironov, J. Oxgaard, J. Gonzales, W. A. Goddard III, R. A. Periana, *J. Mol. Catal. A: Chem.,* 2006, **251**, 8
3. R. A. Periana, G. Bhalla, W.J. Tenn, K. J. H. Young, X. Y. Liu, O. Mironov, C. J Jones, V. R. Ziatdinov, *J. Mol. Catal. A: Chem.*, 2004, **220**, 7
4. J. A. Labinger, J. E. Bercaw, *Nature,* 2002, **417**, 507
5. E. P. Wasserman, C. B. Moore, R. G. Bergman, *Science,* 1992, **255**, 315
6. a) Y. Fujiwara, C. Jia, *Pure Appl. Chem.,* 2001, **73**, 319; b) A. Inagaki, T. Takemori, M. Tanaka, H. Suzuki, *Angew. Chem. Int. Ed. Engl.,* 2000, **39**, 404
7. J. A. Labinger, *J. Mol. Catal. A: Chem.,* 2004, **220**, 27
8. H. Suzuki, A. Inagaki, K. Matsubara, T. Takemori, *Pure Appl. Chem.,* 2001, **73**, 315
9. A. Miyashita, M. Hotta, Y. Saida, *J. Organomet. Chem.,* 1994, **473**, 353
10. R. H. Crabtree, *J. Organomet. Chem.,* 2004, **689**, 4083
11. M. Ayala, E. Torres, *Appl. Catal. A: General,* 2004, **272**, 1

12. M. C. Asplund, P. T. Snee, J. S. Yeston, M. J. Wilkens, C. K. Payne, H. Yang, K. T. Kotz, H. Frei, R. G. Bergman, C. B. Harris, *J. Am. Chem. Soc.,* 2002, **124**, 10605
13. S. S. Stahl, J. A. Labinger, J. E. Bercaw, *Angew. Chem. Int. Ed. Engl.,* 1998, **37**, 2180
14. A. J. Vetter, C. Flaschenriem, W. D. Jones, *J. Am. Chem. Soc.,* 2005, **127**, 12315
15. R. H. Crabtree, *Angew. Chem. Int. Ed. Engl.,* 1993, **32**, 789
16. T. O. Northcutt, D. D. Wick, A. J. Vetter, W. D. Jones, *J. Am. Chem. Soc.,* 2001, **123**, 7257
17. W. E. Billups, S. –C. Chang, R. H. Hauge, J. L. Margrave, *J. Am. Chem. Soc.,* 1993, **115**, 2039
18. H. Arakawa, M. Aresta, J. N. Armor, M. A. Barteau, E. J. Beckman, A. T. Bell, J. E. Bercaw, C. Creutz, E. Dinjus, D. A. Dixon, K. Domen, D. L. Dubois, J. Eckert, E. Fujita, D. H. Gibson, W. A. Goddard, D. W. Goodman, J. Keller, G. J Kubas, H. H. Kung, J. E. Lyons, L. E. Manzer, T. J. Marks, K. Morokuma, K. M. Nicholas, R. Periana, L. Que, J. Rostrup-Nielson, W. M. H. Sachtler, L. D. Schmidt, A. Sen, G. A. Somorjai, P. C. Stair, B. R. Stults, W. Tumas, *Chem. Rev.,* 2001, **101**, 953
19. A.S. Goldman, K.I. Golberg, ACS Symposium Series 885, *Activation and Functionalization of C-H Bonds,* 2004,1
20. W. Cui, B.B. Wayland, *J. Am. Chem. Soc.,* 2004, **126**, 8266
21. A. H. Janowicz, R. G. Bergman, *J. Am. Chem. Soc.,* 1982, **104**, 352
22. A. H. Janowicz, R. G. Bergman, *J. Am. Chem. Soc.,* 1983, **105**, 3929
23. W. D. Jones, F. J. Feher, *J. Am. Chem. Soc.,* 1986, **108**, 4814
24. M. E. Thompson, S. M. Baxter, A. R. Bulls, B. J. Burger, M. C. Nolan, B. D. Santarsiero, W. P. Schaefer, J. E. Bercaw, *J. Am. Chem. Soc.,* 1987, **109**, 203
25. A. Milet, A. Dedieu, G. Kapteijn, G. van Koten, *Inorg. Chem.,* 1997, **36**, 3223
26. D. H. R. Barton, E. Csuhai, N. Ozbalik, *Tetrahedron,* 1990, **46**, 3743
27. D. H. R. Barton, S. D. Beviere, W. Chavasiri, E. Csuhai, D. Doller, W. G. Liu, *J. Am. Chem. Soc.,* 1992, **114**, 2147.
28. H. C. Tung, C. Kang, D. T. Sawyer, *J. Am. Chem. Soc.,* 1992, **114**, 3445.
29. B. R. Cook, T. J. Reinert, K. S. Suslick, *J. Am. Chem. Soc.,* 1986, **108**, 7281.

30. J. B. Vincent, J. C. Huffman, G. Christou, Q. Li, M. A. Nanny, D. N. Hendrickson, R. H. Fong, R. H. Fish, *J. Am. Chem. Soc.,* 1988, **110**, 6898.
31. R. A. Leising, R. E. Norman, L. Que Jr., *Inorg. Chem.,* 1990, **29**, 2553.
32. U. Schuchardt, D. Cardoso, R. Sercheli, R. Pereira, R. S. da Cruz, M. C. Guerreiro, D. Mandelli, E. V. Spinacé, E. L. Pires, *Appl.Catal. A: General,* 2001, **211**, 1
33. P. R. Hari, A. V. Ramaswamy, *J. Chem. Soc., Chem. Commun.,* 1992, 1245
34. T. Tatsumi, M. Nakamura, S. Negishi, H. Tominaga, *J. Chem. Soc., Chem. Commun.,* 1990, 476
35. K.Weissermel, H.-J. Arpe, *Industrial Organic Chemistry, Second ed., VCH Press, Weinheim,* 1993
36. A. Sivaramakrishna, P. Mushonga, I. L. Rogers, F. Zheng, R. J. Haines, E. Nordlander, J. R. Moss, *Polyhedron*, 2008, **27**,1911.
37. a) W. A. Herman, M. Prinz, *A Text book on Homogeneous Catalysis,* 2002, pp 1119 and the references therein. b) N.R. Davis, *Rev. Pure Appl. Chem.,* 1967, **17**, 83
38. R. A. van Santen, P. W. N. M. van Leeuwen, J. A. Moulijn, B. A. Averill, *Catalysis: An Integrated Approach, 2nd ed., Elsevier Science, Amsterdam,* 1999.
39. C. A. Tolman, *J. Am. Chem. Soc.,* 1972, **94**, 2994. b) M. Mirza-Aghayan, R. Boukherroub, M. Bolourtchian, M. Hoseini, K. Tabar-Hydar, *J. Organomet. Chem.,* 2003, **678**, 1
40. A. Salvini, P. Frediani, F. Piacenti, J. *Mol. Catal. A: Chem.,* 2000, **159**, 185
41 M. Auzias, G. Süss-Fink, P. Štěpnička, J. Ludvík, *Inorg. Chim. Acta,* 2007, **360**, 2023

CHAPTER 4
CONCLUSIONS AND FUTURE WORK

4.1 Conclusions and future work

In this project, a series of dinuclear carboxylato-bridged complexes of ruthenium and osmium were synthesized and characterized. These include the new complexes **89-90**, **92**, **96-103** and **109-113**. The characterization data for these complexes supported their proposed structures.

The complexes $[Os_2(CO)_4(\mu\text{-}O_2CMe)_2(PCy_3)_2]$ (**90**), $[Os_2(CO)_4(\mu\text{-}O_2CMe)_2(PPh_3)_2]$ (**91**) and $[Os_2(CO)_4(\mu\text{-}O_2CMe)_2(4\text{-}H_2Npy)_2]$ (**101**) were investigated as catalysts for the oxidation of alkanes using cyclohexane and octane as substrates. The catalytic activities of these complexes were low. All the catalysts show a higher selectivity for the alcohol products than for the ketonic products.

The complexes $[Os_2(CO)_6(\mu\text{-}O_2CMe)_2]$ (**4**), $[Ru(CO)_2(\mu\text{-}O_2CMe)_2]_n$ (**86**), $[Ru_2(CO)_4\{\mu\text{-}O_2CMe)(\mu\text{-dppm})_2][PF_6]$ (**117**) and $[Ru_2(CO)_4(\mu\text{-}O_2CMe)_2(MeCN)_2]$ (**118**) were tested as catalysts for the isomerisation of the carbon-carbon double bonds in terminal alkenes. The complex $[Ru_2(CO)_4(\mu\text{-}O_2CMe)_2(MeCN)_2]$ (**118**) was found to be the most active. A mechanism of catalysis was proposed for the isomerisation reaction that involves the displacement of one of the axial ligands with the substrate molecules.

Cyclic voltammetric studies were carried out on seven complexes, **102-103** and **111-114.** All the complexes studied displayed a single anodic wave assigned to the $Ru_2^{I}/Ru^{I}Ru^{II}$ oxidation process with the exception of complexes **102** and **103** which contain the ferrocenecarboxylato bridges. It was shown that changing the type of ligand in the axial position influenced the potential at which irreversible oxidation of the metals took place. The diosmium core was irreversibly oxidized at a much lower potential (+0.50 V) in the triphenylphosphine-substituted complex **102** than in the pyridine-substituted complex **103** (+0.66 V) and this was attributed to the different electron donating properties of the ligands.

Future work in this area should include:

- Extending the catalytic work to other complexes with different ligands in order to develop catalytic systems that would give higher activities and selectivities for the oxidation of alkanes.
- Carrying out some investigation into the possible mechanism of the alkane oxidation reactions.
- Testing the complexes for catalysis of other organic transformations.

CHAPTER 5
EXPERIMENTAL SECTION

5.1 General experimental details

All manipulations were carried out under an atmosphere of nitrogen using standard Schlenk techniques unless stated otherwise. Solvents were dried and purified by heating at reflux under a nitrogen atmosphere in the presence of suitable drying agents. Benzene, toluene, tetrahydrofuran (THF), diethyl ether and hexane were dried over sodium wire and benzophenone. Alcohols were dried over magnesium and iodine. Dichloromethane and acetonitrile were distilled from phosphorus pentoxide. All other chemicals were used without further purification.

5.2 Instrumentation

Microanalysis data was obtained from the University of Cape Town's Microanalysis Laboratory using a Thermo Flash 1112 Series CHNS-O Analyser. Infrared spectroscopic data were recorded on a Perkin Elmer Spectrum One FT-IR spectrometer in solution cells using NaCl windows, as Nujol mulls or as potassium bromide disks.

NMR spectra were recorded on either a Varian Mercury 300MHz spectrometer or a Varian Unity 400MHz using deuterated solvents purchased from Aldrich. Tetramethylsilane (TMS) was used as the internal standard.

Carbonylation reactions were carried out in a 200mL Parr-type autoclave. The autoclave room was equipped with a Drager Multiwarn II gas detection device for monitoring concentrations of various gases in ambient air.

Gas Chromatographic analyses were performed on a Varian 3900 Gas Chromatograph equipped with a flame ionization detector (FID) and a 30 m x 0.32 mm CP-Wax 52 CB column (0.25 μm film thickness). The carrier gas was helium at 5.0 psi. The oven was programmed to hold at 32°C for 4 min and then to ramp to 200°C at 10 deg/min and hold 5 min. GC-MS analyses were performed using an Agilent 5973 Gas Chromatograph equipped with MSD and a 60 m x 0.25 mm Rtx-1 column (0.5 μm film thickness). The carrier gas was helium at 0.9 ml/min. The oven was programmed to hold at 50°C for 2 min and then ramp to 250°C at 10 deg/min and hold for 8 min.

5.3 Synthesis of complexes

5.3.1 Synthesis of $[Ru_3(CO)_{12}]$ (1)

$RuCl_3.3H_2O$ (2 g, 7.65 mmol) was added to 100 ml freshly dried methanol in a 200ml Parr autoclave. The autoclave was purged three times with carbon monoxide and then pressurized with the same gas to 5 MPa. The reactor was heated gradually to 125 °C causing the pressure to increase to about 7 MPa. The autoclave was kept at 125 °C and under continual stirring for eight hours. The reaction was then stopped and the autoclave allowed to cool slowly to room temperature overnight. The autoclave was vented. The orange $[Ru_3(CO)_{12}]$ crystals that had formed were filtered off using a Büchner funnel and washed repeatedly with dried methanol. The crystals were dried *in vacuo* for 2 h. Yield = 1.32 g, 81 %. IR (C_6H_{12}) cm^{-1}: (CO) 2061 vs, 2031 s, 2012 m.

5.3.2 Synthesis of $[Os_2(CO)_6(\mu\text{-}O_2CMe)_2]$ (4)

The dimer was prepared following the literature procedure [2]. $[Os_3(CO)_{12}]$ (**2**) (0.35 g, 0.39 mmol) was transferred into a thick-walled tube. Glacial acetic acid (7 mL) was added. Three cycles of freezing and thawing were carried out under vacuum to remove any air. The tube was filled with nitrogen gas and sealed. The tube was then heated at 185 °C for 8 h. The tube was allowed to cool overnight. A small amount of yellow crystals was filtered off and the solution evaporated under reduced pressure affording **4** as a white

product. Yield = 0.21 g, 55 %. Anal. Calc. for $C_{10}H_6O_{10}Os_2$: C, 18.02; H, 0.91. Found: C, 18.22; H, 0.88 %. IR (CCl_4) cm^{-1}: (CO) 2100 s, 2066 vs, 2014 s, 2000 vs, (OCO) 1573 s.

5.3.3 Synthesis of $[Ru(CO)_2(\mu\text{-}O_2CH)]_n$ (83)

The formate-bridged polymer was synthesized according to a literature procedure [2]. $[Ru_3(CO)_{12}]$ (**1**) (1.0 g, 1.56 mmol) was refluxed in formic acetic acid (50 mL) for 6 h. The resultant yellow precipitate was filtered off using a Büchner funnel and washed with formic acid (5 mL) followed by diethyl ether (3x5 mL). The product **83** was then dried under vacuum. Yield = 0.65 g, 68 %. Anal. Calc. for C_3HO_4Ru: C, 17.93; H, 0.50. Found: C, 17.93; H, 0.45 %. IR (CH_2Cl_2) cm^{-1}: (CO) 2067 s, 2038 vs, 2001sh, 1980 s, 1996 vs, (OCO) 1594 m, 1567 vs, 1463 vs.

5.3.4 Synthesis of $[Ru(CO)_2((\mu\text{-}O_2CMe)]_n$ (86)

The compound was prepared following the literature procedure [2]. $Ru_3(CO)_{12}$ (0.30 g, 0.47 mmol) was refluxed in glacial acetic acid (30 mL) for 12 h. The orange precipitate which formed was filtered off using a Büchner funnel and washed with acetic acid (5 mL) followed by diethyl ether (3x5 mL). The product **86** was then dried under vacuum. Yield = 0.21 g, 69 %. Anal. Calc. for $C_4H_3O_4Ru$: C, 22.23; H, 1.40. Found: C, 22.30; H, 1.36 %. IR (Nujol) cm^{-1}: (CO) 2050 s, 1990 vs, 1966 vs, (OCO) 1552 s.

5.3.5 Synthesis of $[Ru(CO)_2(\mu\text{-}O_2CEt)]_n$ (87)

This compound was prepared following the literature procedure [2]. $[Ru_3(CO)_{12}]$ (**2**) (1.0 g, 1.56 mmol) was refluxed in propionic acid (25 mL) for 7 h. The solvent was removed under reduced pressure. An orange residue was deposited and was washed with diethyl ether (5 mL). The product **87** was filtered off using a Büchner funnel and then dried under vacuum. Yield = 0.68 g, 63 %. Anal. Calc. for $C_{10}H_{10}O_8Ru_2$: C, 26.09; H,

2.19. Found: C, 26.23; H, 2.31. IR (CH_2Cl_2) cm^{-1}: (CO) 2033 vs, 1992 vs, 2014 s, (OCO) 1554 vs, 1463 vs, 1411vs, 1377 vs.

5.3.6 Synthesis of $[Ru_2(CO)_4(\mu\text{-}O_2CMe)_2(PPh_3)_2]$ (11)

The synthesis of this complex followed a published procedure [2]. A suspension of $[Ru(CO)_2(MeCO_2)]_n$ (0.15 g, 0.69 mmol) and triphenylphosphine (0.30 g, 1.14 mmol) in diethyl ether (10 mL) was heated under reflux until no further starting material could be observed. A yellow product was formed. The product **11** was filtered off, washed with diethyl ether and dried under vacuum. Yield = 0.23 g, 70 %. IR (CCl_4) cm^{-1}: (CO) 2027 vs, 1983 m, 1956 vs, 1927 w, (OCO) 1578 m, 1571 m, 1483 w. ^1H NMR (300 MHz, $CDCl_3$) δ = 7.56-7.52 ppm (m, 12H), 7.39-7.37 (m, 18H), 1.67 (s, 6H). $^{31}P\{1H\}$-NMR (121 MHz) δ = 14.67 ppm.

5.3.7 Synthesis of $[Ru_2(CO)_4(\mu\text{-}O_2CH)_2(PPh_3)_2]$ (14)

The complex was prepared following a literature procedure [2]. A suspension of $[Ru(CO)_2(HCO_2)]_n$ (0.10 g, 0.49 mmol) and triphenylphosphine (0.20 g, 0.76 mmol) in dry diethyl ether (10 mL) was heated to reflux for 5 h and a yellow product precipitated from the reaction solution. The product **14** was filtered off, washed with diethyl ether (5 mL) followed by hexane (2 x 5 mL). The complex was then dried *in vacuo*. Yield = 0.22 g, 96 %. Anal. Calc. for $C_{42}H_{32}O_8Ru_2$: C, 54.31; H, 3.47. Found: C, 53.97; H, 3.55 %. IR (CCl_4) cm^{-1}: (CO) 2031 vs, 1988 s, 1961 vs, (OCO) 1594 vs, 1573 w, 1483 w, 1435 s. ^1H-NMR (300 MHz, $CDCl_3$) : δ = 8.16 ppm (s, 2H), 7.57 (m, 12H), 7.41 (m, 18H); $^{31}P\{^1H\}$NMR (121 MHz, $CDCl_3$) : δ = 13.15 ppm (s).

5.3.8 Synthesis of $[Os_2(CO)_4(\mu\text{-}O_2CMe)_2(PPh_3)_2]$ (91)

The dinuclear complex was synthesized using a literature procedure [2]. A suspension of $[Os_2(CO)_6(\mu\text{-}O_2CMe)_2]$ (0.32 g, 0.48 mmol) and an excess of triphenylphosphine (0.30 g, 1.14 mmol) in dry benzene (10 mL) was heated under reflux for 3 h. The reaction was

allowed to cool and petroleum ether (60 – 80 °C) (10 mL) was added precipitating out the product. The product **91** was filtered off, washed with petroleum ether (60 – 80 °C) (2 x 5 mL) and dried *in vacuo*. Yield = 0.44 g, 81 %. Anal. Calc. for $C_{44}H_{36}O_8Os_2P_2$: C, 46.55; H, 3.20. Found: C, 46.63; H, 3.37 %. IR (CCl_4) cm^{-1}: (CO) 2018 vs, 1975 m, 1945 vs , (OCO) 1578 s, 1483 w, 1436 m. ^{1}H-NMR (300 MHz, $CDCl_3$): δ (ppm) = 7.49-7.54 (m, 12H), 7.38-7.41 (m, 18H), 1.61 (s, 6H) . ^{31}P{^{1}H-NMR} (121 MHz, $CDCl_3$) δ (ppm) = 18.01 (s).

5.3.9 Synthesis of $[Ru_2(CO)_4(O_2CCHPh_2)_2(PPh_3)_2]$ (92)

A solution of $[Ru_3(CO)_{12}]$ (0.30 g, 0.47 mmol) and diphenyl-acetic acid (0.80 g, 3.77 mmol) in dry tetrahydrofuran (20 mL) was heated under reflux for 3 h. The blood red solution that resulted was allowed to cool. Triphenylphosphine (0.80 g, 3.05 mmol) was added. The solution was heated at reflux for a further 1hr. The resulting solution was allowed to cool and the solvent was removed under reduced pressure. The oily residue was then recrystallised from a dichloromethane-ethanol mixture to give a light brown product **92**. Yield = 0.50 g, 56 %. Anal. Calc. for $C_{68}H_{52}O_8P_2Ru_2$: C, 64.76; H, 4.16. Found: C, 64.16; H, 4.38 %. IR (CH_2Cl_2) cm^{-1}: (CO) 2024 vs, 1980m, 1952 vs, (OCO) 1604 w, 1586 m, 1577 m, 1494 w, 1482 w. ^{1}H-NMR (300 MHz, acetone-d_6) δ (ppm) = 7.43 (m, 6H), 7.34 (dt, 24H, J = 2.6Hz, J = 7.0Hz), 7.12 (m, 12H), 6.88 (m, 8H), 4.70 (s, 2H). ^{31}P {^{1}H}-NMR (acetone-d_6) (121 MHz) δ (ppm) = 18.22 (s).

5.3.10 Synthesis of $[Ru_2(CO)_4(\mu\text{-}O_2CH)_2(PCy_3)_2]$ (89)

$[Ru(CO)_2(HCO_2)]_n$ (0.10 g, 0.49 mmol) and excess tricyclohexylphosphine (0.22 g, 0.78 mmol) were heated to reflux in dry diethyl ether (10 mL) for 2 h during which time a yellow solid formed. The reaction was allowed to cool to room temperature. The solid was filtered off, washed with petroleum ether (2 x 5 mL) and then dried in *vacuo*. Yield 0.14 g, 59 %. Anal. Calc. for $C_{42}H_{68}O_8P_2Ru_2$: C, 52.27; H, 7.10. Found: C, 52.32; H, 6.38 %. IR (CCl_4) cm^{-1}: (CO) 2018 vs, 1972 s, 1945 vs, (OCO) 1599 vs, 1447 w. ^{1}H-

NMR (300 MHz, $CDCl_3$) δ (ppm) = 8.18 (s, 2H), 2.21 (m, 6H), 1.99-1.72 (m, 30H), 1.61-1.56 (m, 12H), 1.24 (m, 18H). ^{31}P {^1H}-NMR (121 MHz, $CDCl_3$) δ (ppm) = 25.72 (s).

5.3.11 Synthesis of $[Os_2(CO)_4(\mu\text{-}O_2CMe)_2(PCy_3)_2]$ (90)

A solution of $[Os_2(CO)_6(MeCO_2)_2]$ (0.15 g, 0.23 mmol) and tricyclohexylphosphine (0.15 g, 0.53 mmol) in dry benzene (5 mL) was heated under reflux for 2 h. The reaction was allowed to cool to room temperature and a yellow solid formed. The solid **90** was filtered off and washed with petroleum ether. Yield = 0.12 g, 46 %. Anal. Calc. for $C_{44}H_{72}O_8Os_2P_2$: C, 45.11; H, 6.20. Found: C, 44.92; H, 6.14 %. IR (CCl_4) cm^{-1}: (CO) 2008 vs, 1962 w, 1931 vs , (OCO) 1581 m, 1444 m.

5.3.12 Synthesis of $[Ru_2(CO)_4(\mu\text{-}O_2CH)_2(py)_2]$ (93)

The complex was prepared according to the literature procedure [2]. A suspension of $[Ru(CO)_2(HCO_2)]_n$ (0.10 g, 0.49 mmol) and pyridine (2 mL) in dry benzene (5 mL) was heated under reflux for 3 h. The reaction was allowed to cool to room temperature and the volume of the solution was reduced to about 4mL under reduced pressure. Petroleum ether was then added precipitating out a yellow product. The product **93** was filtered off, washed with hexane (2 x 5 mL) and then dried *in vacuo*. Yield = 0.10 g, 73 %. Anal. Calc. for $C_{16}H_{12}N_2O_8Ru_2$: C, 34.17; H, 2.15; N, 4.98. Found: C, 34.57; H, 2.25; N, 4.77 %. IR (CH_2Cl_2) cm^{-1}: (CO) 2029 vs, 1977 s, 1945 vs, (OCO) 1597 vs, 1485 w, 1447 w. ^1H-NMR (300 MHz, $CDCl_3$) δ (ppm): 8.79 (d, 4H, J = 4.8 Hz), 8.36 (s, 2H), 7.87 (t, 2H, J = 7.6 Hz), 7.47 (m, 4H).

5.3.13 Synthesis of $[Ru_2(CO)_4(\mu\text{-}O_2CMe)_2(py)_2]$ (94)

$[Ru(CO)_2(MeCO_2)]_n$ (0.15 g, 0.69 mmol) suspended in diethyl ether (10 mL) was treated with pyridine (1.5 mL, 18.62 mmol). The suspension was then heated under reflux for 3 h during which time a colour change from orange to yellow was observed. The yellow solid **94** was filtered off and washed with diethyl ether (2 x 3 mL) and then dried under

vacuum. Yield = 0.15 g, 75 %. Anal. Calc. for $C_{18}H_{16}N_2O_8Ru_2$: C, 36.61; H, 2.71; N, 4.74. Found: C, 36.84; H, 2.74; N, 4.58 %. IR (CH_2Cl_2) cm^{-1}: (CO) 2024 vs, 1972 m, 1939 vs, (OCO) 1601 m, 1578 m, 1571 m, 1484 w, 1447 m. ^{1}H-NMR (300 MHz, $CDCl_3$) δ (ppm): 8.77 (m, 4H), 7.84 (m, 2H), 7.44 (ddd, 4H, *J* = 1.5 Hz, J = 4.8 Hz, *J* = 7.7 Hz), 2.07 (s, 6H).

5.3.14 Synthesis of $[Ru_2(CO)_4(\mu\text{-}O_2CEt)_2(py)_2]$ (95)

The synthesis of this complex followed the reported procedure [2]. A suspension of $[Ru(CO)_2(EtCO_2)]n$ (0.30 g, 1.30 mmol) and pyridine (2 mL, 24.82 mmol) in diethyl ether (10 mL) was heated under reflux until no further starting material could be observed. A yellow product was formed. The product **95** was filtered off and washed with diethyl ether and dried in vacuo. Yield = 0.29 g, 72 %. Anal. Calc. for $C_{20}H_{20}N_2O_8Ru_2$: C, 38.84; H, 3.26; N, 4.53. Found: C, 38.88; H, 3.45; N, 4.30 %.IR (CH_2Cl_2) cm^{-1}: (CO) 2023 vs, 1971 s, 1938 vs, (OCO) 1601 w, 1576 s, 1568 s, 1483 w, 1466 m, 1447 s. ^{1}H-NMR (300 MHz, $CDCl_3$) δ (ppm): 8.77 (m, 4H), 7.84 (m, 2H), 7.43 (ddd, 4H, *J* = 1.5 Hz, *J* = 4.8 Hz, *J* = 7.6 Hz), 2.30 (q, 4H, *J* = 7.6 Hz), 1.06 (t, 6H, *J* = 7.6 Hz).

5.3.15 Synthesis of $[Ru_2(CO)_4(\mu\text{-}O_2CH)_2(4\text{-}Phpy)_2]$ (96)

The polymer $[Ru(CO)_2(HCO_2)]n$ (0.10 g, 0.49 mmol) was suspended in diethyl ether (10 mL) and was treated with 4-phenylpyridine (0.09 g, 0.55 mmol). The mixture was heated to reflux for 12 h. The yellow solid that formed was filtered off and washed with diethyl ether. The product **96** was recrystallised from a dichloromethane-hexane mixture and dried under vacuum. Yield = 0.09 g, 50 %. Anal. Calc. for $C_{28}H_{20}N_2O_8Ru_2$: C, 47.06; H, 2.82; N, 3.92. Found: C, 46.53, H, 3.18, N, 3.53 %. IR (CH_2Cl_2) cm^{-1}: (CO) 2028 vs, 1977 s, 1945 vs, (OCO) 1610 sh, 1596 vs, 1485 w. ^{1}H-NMR (400 MHz, $CDCl_3$) δ (ppm): 8.83 (dd, 4H, *J* = 1.4 Hz, *J* = 5.1 Hz), 8.41 (s, 2H), 7.68 (m, 8H), 7.54 (m, 6H).

5.3.16 Synthesis of $[Ru_2(CO)_4(\mu\text{-}O_2CEt)_2(4\text{-}Phpy)_2]$ (97)

The polymer $[Ru(CO)_2(EtCO_2)]n$ (0.11 g, 0.48 mmol) was suspended in diethyl ether (10 mL) and was treated with 4-phenylpyridine (0.10 g, 0.64 mmol). The suspension was heated under reflux overnight. The yellow product that formed was filtered off and washed with diethyl ether (2 x 5 mL). The product **97** was recrystallised from dichloromethane-hexane mixture and then dried *in vacuo*. Yield 0.08 g, 43 %. Anal. Calc. for $C_{32}H_{28}N_2O_8Ru_2$: C, 49.87; H, 3.66; N, 3.61. Found: C, 49.36; H, 3.69; N, 3.21 %. IR (CH_2Cl_2) cm^{-1}: (CO) 2023 vs, 1971 s, 1938 vs, (OCO) 1610 m, 1571 s, 1484 w, 1466 w. ^{1}H-NMR (400 MHz, $CDCl_3$) δ (ppm): 8.80 (dd, 4H, J = 1.6 Hz, J = 5.0 Hz), 7.70 (m, 4H), 7.64 (dd, 4H, J = 1.6 Hz, J = 5.0 Hz), 7.52 (m, 6H), 2.34 (q, 4H, J = 7.6 Hz), 1.10 (t, 6H, J = 7.6 Hz).

5.3.17 Synthesis of $[Os_2(CO)_4(\mu\text{-}O_2CMe)_2(4\text{-}PhPy)_2]$ (100)

A solution of $Os_2(CO)_6(MeCO_2)_2$ (0.10 g, 0.15 mmol) and 4-phenylpyridine (0.06 g, 0.38 mmol) in dry benzene (5 mL) was heated under reflux for 4h. The reaction was allowed to cool to room temperature and a yellow product **100** precipitated out on addition of petroleum ether. The product was then filtered off and washed with petroleum ether (2 x 5 mL) and dried *in vacuo* for 1h. Yield = 0.07 g, 53 %. Anal. Calc. for $C_{30}H_{24}N_2O_8Os_2$: C, 39.12; H, 2.63; N, 3.04. Found: C, 38.93; H, 2.62; N, 2.52 %. IR (CH_2Cl_2) cm^{-1}: (CO) 2078 w, 2008 vs, 1956 s, 1921 vs, (OCO) 1612 s, 1577 vs, 1484 w, 1447 s. ^{1}H-NMR (400 MHz, $CDCl_3$) δ (ppm): 8.85 (ddd, 4H, J = 1.6 Hz, J = 5.1 Hz, J = 9.3 Hz), 7.68 (m, 8H), 7.55 (m, 6H), 2.10 (s, 6H, J = 4.5 Hz). The weak 2078 band possibly due to impurity.

5.3.18 Synthesis of $[Ru_2(CO)_4(\mu\text{-}O_2CMe)_2(4\text{-}Me_2Npy)_2]$ (98)

$[Ru(CO)_2(MeCO_2)]_n$ (0.12 g, 0.56 mmol) suspended in diethyl ether (10 mL) was treated with 4-dimethylaminopyridine (0.08 g, 0.65 mmol). The suspension was heated under reflux 5 h. The light orange solid formed was filtered off and washed with diethyl ether

(3mL). The product **98** was then dried under vacuum. Yield 0.14 g, 74 %. IR (CH_2Cl_2) cm^{-1}: (CO) 2020 vs, 1966 s, 1932 vs, (OCO) 1612 s, 1577 s, 1529 s, 1443 s. ^{1}H-NMR (400 MHz, $CDCl_3$) δ (ppm): 8.31 (dd, 4H, J = 1.4 Hz, J = 5.5 Hz), 6.56 (dd, 4H, J = 1.5 Hz, J = 5.5 Hz), 3.06 (s, 12H), 2.04 (s, 6H).

5.3.19 Synthesis of $[Ru_2(CO)_4(\mu\text{-}O_2CEt)_2(4\text{-}Me_2Npy)_2]$ (99)

The polymer $[Ru(CO)_2(EtCO_2)]n$ (0.13 g, 0.48 mmol) was suspended in diethyl ether (10 mL) and was treated with 4-dimethylaminopyridine (0.08 g, 0.65 mmol). This suspension was heated under reflux for 6 h. Yield = 0.13 g, 67 %. Anal. Calc. for $C_{24}H_{30}N_4O_8Ru_2$: C, 40.91; H, 4.29; N, 7.95. Found: C, 40.49; H, 4.32; N, 7.71 %. IR (CH_2Cl_2) cm^{-1}: (CO) 2018 vs, 1965 s, 1931 vs, (OCO) 1615 s, 1531 s, 1466 w. ^{1}H-NMR (400 MHz, $CDCl_3$) δ (ppm): 8.32 (dd, 4H, J = 1.4 Hz, J = 5.5 Hz), 6.55 (dd, 4H, J = 1.5 Hz, J = 5.5 Hz), 3.06 (s, 12H), 2.28 (q, 4H, J = 7.6 Hz), 1.07 (t, 6H, J = 7.5 Hz).

5.3.20 Synthesis of $[Os_2(CO)_4(\mu\text{-}O_2CMe)_2(4\text{-}H_2NPy)_2]$ (101)

A solution of $[Os_2(CO)_6(\mu\text{-}O_2CMe)_2]$ (0.15 g, 0.23 mmol) and 4-amino pyridine (0.05 g) in dry benzene (5 mL) was heated under reflux for 4 h. The yellow solid that separated out on adding petroleum ether was filtered off and washed with petroleum ether (2 x 5 mL) and dried in *vacuo* for 1 h. Yield = 0.13 g, 72 %. Anal. Calc. for $C_{18}H_{18}N_4O_8Os_2$: C, 27.02; H, 2.27; N, 7.01. Found: C, 27.11; H, 2.17; N, 6.50 %. IR (CH_2Cl_2) cm^{-1}: (CO) 2075 w, 1994 vs, 1943 s, 1906 vs, (OCO) 1638 s, 1615 m, 1567 s, 1514 m. ^{1}H-NMR (400 MHz, acetone-d_6) δ (ppm): 8.25 (dd, 4H, J = 1.4 Hz, J = 5.5 Hz), 6.72 (dd, 4H, J = 1.5 Hz, J = 5.4 Hz), 6.11 (s, 4H), 1.96 (s, 6H). The weak 2075 band possibly due to impurity.

5.3.21 Synthesis of $[Os_2(CO)_4(\mu\text{-}O_2CC_5H_4FeC_5H_5)_2(PPh_3)_2]$ (102)

The complex was synthesized according to a literature procedure [3]. A solution of $[Os_3(CO)_{12}]$ (0.15 g, 0.17 mmol) and ferrocene carboxylic acid (0.12 g, 0.52 mmol) in

dry tetrahydrofuran (20 mL) in a Schlenk tube was subjected to three cycles of freezing and thawing under vacuum to remove any air. The Schlenk tube was then heated at 160 ^{o}C 48 h. The solvent was removed under reduced pressure to give a brown residue. The residue was dissolved in dry tetrahydrofuran (20 mL) and triphenylphosphine (0.14 g, 0.53 mmol) was added. The solution was then heated under reflux for 4 h. The solvent volume was reduced to about 5 mL and hexane was added precipitating out an orange solid. The solid was filtered off, dissolved in dichloromethane, was subjected to a column chromatography on silica gel using dichloromethane as eluent. The first orange band was collected. The solvent was reduced to about 5 mL and hexane was added precipitating out the orange solid. The solid was recrystallised from THF-hexane mixture. Yield = 0.13 g, 35 %. Anal. Calc. for $C_{62}H_{48}Fe_2O_8P_2Os_2$: C, 50.48; H, 3.28. Found: C, 50.52; H, 4.13 %. IR (CH_2Cl_2) cm^{-1}: (CO) 2010 vs, 1966 m, 1935 vs, (OCO) 1548 s, 1485 s. ^{1}H-NMR (300 MHz, $CDCl_3$) δ (ppm): 7.67 (m, 12H), 7.47 (m, 18H), 4.06 (t, 4H), 3.97 (t, 4H), 3.91 (s, 10H). ^{31}P-NMR (121 MHz, $CDCl_3$) δ (ppm): 17.68 ppm (s).

5.3.22 Synthesis of $[Os_2(CO)_4(\mu\text{-}O_2CC_5H_4FeC_5H_5)_2(py)_2]$ (103)

This complex was synthesized in a manner similar to the one described in Section 5.3.21 using pyridine in place of triphenylphosphine. The orange solid obtained was dissolved in dichloromethane and subjected to a column chromatography on silica gel using dichloromethane as eluent. The first orange band was collected. The solvent was reduced to about 5 mL and hexane was added precipitating out the orange solid **103**. The solid was recrystallised from THF-hexane mixture. Yield 0.11 g, 39 %. IR (CH_2Cl_2) cm^{-1}: (CO) 2005 vs, 1953 m, 1918 s, (OCO) 1605 vs, 1555 m, 1487 m. ^{1}H-NMR (300 MHz, $CDCl_3$) δ (ppm): 9.00 (m, 4H), 7.98 (tt, 2H), 7.56 (m, 4H), 4.58 (m, 4H), 4.24 (m, 4H), 4.08 (s, 10H).

5.3.23 Synthesis of $[Ru_2(CO)_2(\mu\text{-}CO)_2(\mu\text{-}O_2CEt)(bipy)_2][PF_6]$ (109)

The cationic complex was prepared following the published procedure [4]. $[Ru_2(CO)_4(EtCO_2)_2(py)_2]$ (0.10 g, 0.16 mmol) and 2,2′-bipyridine (0.10 g, 0.64 mmol)

were suspended in methanol (20 mL). The suspension was heated under reflux for 24 h. The reaction was allowed to cool to room temperature and the volume concentrated to about 10 mL under reduced pressure. A solution of NH_4PF_6 (0.10 g, 0.61 mmol) in ethanol (2 mL) was added precipitating out a light orange solid. The solid **109** washed with diethyl ether and dried. Yield = 0.12 g, 86 %. Anal. Calc. for $C_{27}H_{21}F_6N_4O_6PRu_2$: C, 38.40; H, 2.51; N, 6.63. IR (CH_2Cl_2) cm^{-1}: (CO) 2025 vs, 1984 m, 1802 w, 1747 vs, (OCO) 1603 w, 1536 s, 1496 w, 1479 m, 1444 m. ^{1}H-NMR (400 MHz) δ (ppm): 10.08 (dd, 4H, J = 1.0 Hz, J = 5.5 Hz), 8.92 (d, 4H, J = 8.1 Hz), 8.49 (dt, 4H, J = 1.5 Hz, J = 7.8 Hz), 8.17 (m, 4H), 1.23 (q, 2H, J = 7.5 Hz), -0.08 (t, 3H, J = 7.5 Hz).

5.3.24 Synthesis of $[Ru_2(CO)_2(\mu\text{-}CO)_2(\mu\text{-}O_2CEt)(1,10\text{-phen})_2][PF_6]$ (110)

The complex was synthesized following the literature protocol [5]. $Ru_2(CO)_4(EtCO_2)_2(py)_2]$ (0.10 g, 0.16 mmol) and 1,10-phenanthroline (0.12 g, 0.67 mmol) were suspended in dry methanol (20 mL) in a Schlenk tube under nitrogen. The suspension was sonicated for about 5 min and the solution was stirred at 40 °C for 24 h. NH_4PF_6 (0.03 g, 0.18 mmol) dissolved in methanol (2 mL) was then added precipitating out a brown solid. The solid **110** was filtered off and washed with diethyl ether and then dried. Yield = 0.13 g, 88 %. Anal. Calc. for $C_{31}H_{21}F_6N_4O_6PRu_2$: C, 41.71; H, 2.37; N, 6.28. Found: C, 41.65; H, 2.67; N, 6.19 %. IR (CH_2Cl_2) cm^{-1}: (CO) 2024 vs, 1983 vw, 1803 vw, 1746 vs, (OCO) 1536 s, 1521 m. ^{1}H-NMR (400 MHz, acetone-d_6) δ (ppm): 10.63 (dd, 4H, J = 1.3 Hz, J = 5.0 Hz), 9.15 (dd, 4H, J = 1.3 Hz, J = 8.2 Hz), 8.58 (dd, 4H, J = 5.1 Hz, J = 8.1 Hz), 8.47 (s, 4H), 1.08 (q, 2H, J =7.5 Hz), -0.18 (t, 3H, J = 7.5 Hz).

5.3.25 Synthesis of $[Ru_2(CO)_2(\mu\text{-}CO)_2(\mu\text{-}O_2CEt)(5\text{-Me-}1,10\text{-phen})_2][PF_6]$ (111)

$[Ru_2(CO)_4(EtCO_2)_2(py)_2]$ (0.10 g, 0.16 mmol) and 5-methyl-1,10-phenanthroline (0.13 g, 0.67 mmol) were suspended in dry methanol (20 mL) in a Schlenk tube under nitrogen. The suspension was sonicated for about 5 min and the solution was stirred at 40 °C for 24 h. NH_4PF_6 (0.03 g, 0.18 mmol) dissolved in methanol (2 mL) was then added. The

suspension was refluxed for 3 h. The reaction was stopped and the solvent was reduced to about 5 mL. A light orange product precipitated out. The product **111** was filtered off and washed with diethyl ether and then dried. Yield = 0.08 g, 53 %. IR (CH_2Cl_2) cm^{-1}: (CO) 2024 vs, 1983 vw, 1802 vw, 1745 vs, 1712 vw, (OCO) 1605 vw, 1536 s. ^{1}H-NMR (400 MHz, acetone-d_6) δ (ppm): 10.60 (dd, 4H, J = 3.9 Hz, J = 37.3 Hz), 9.22 (d, 2H, J = 8.4 Hz), 9.01 (d, 2H, J = 8.1 Hz), 8.55 (m, 4H), 8.27 (s, 2H), 3.03 (s, 6H), 1.09 (q, 2H, J = 7.5 Hz), -0.17 (t, 3H, J = 7.5 Hz).

5.3.26 Synthesis of $[Ru_2(CO)_2(\mu\text{-}CO)_2(\mu\text{-}O_2CEt)(4\text{-}Me\text{-}1,10\text{-}phen)_2][PF_6]$ (112)

This complex was prepared following the method reported in literature [5]. $[Ru_2(CO)_4(EtCO_2)_2(py)_2]$ (0.10 g, 0.16 mmol) and 4-methyl-1,10-phenanthroline (0.13 g, 0.67 mmol) were suspended in dry methanol (20 mL) in a Schenk tube under nitrogen. The suspension was sonicated for about 5 min and the solution was stirred at 40 °C for 24 h. NH_4PF_6 (0.03 g, 0.18 mmol) dissolved in methanol (2 mL) was then added. The suspension was refluxed for three hours. The reaction was stopped and the solvent was removed under reduced pressure. The residue was dissolved in dichloromethane and an orange solid **112** precipitated out on adding methanol. Yield = 0.07 g, 47 %. Anal. Calc. for $C_{33}H_{25}F_6N_4O_6PRu_2$: C, 43.05; H, 2.74; N, 6.09. Found: C, 43.03; H, 2.71; N, 5.95 %. IR (CH_2Cl_2) cm^{-1}: (CO) 2023 vs, 1982 vw, 1801 vw, 1744 vs, (OCO) 1607 vw, 1536 s, 1523 s. ^{1}H-NMR (400 MHz, acetone-d_6) δ (ppm): 10.63 (d, 2H, J = 5.0 Hz), 10.46 (d, 2H, J = 5.2 Hz), 9.14 (d, 2H, J = 8.1 Hz), 8.51 (m, 8H), 3.15 (s, 6H), 1.09 (q, 2H, J = 7.4 Hz), -0.17 (t, 3H, J = 7.5 Hz).

5.3.27 Synthesis of $[Ru_2(CO)_2(\mu\text{-}CO)_2(\mu\text{-}O_2CEt)(5\text{-}Cl\text{-}1,10\text{-}phen)_2][PF_6]$ (113)

The synthesis of this complex also followed the published procedure [5]. $[Ru_2(CO)_4(\mu\text{-}O_2CEt)_2(py)_2]$ (0.10 g, 0.16 mmol) and 5-chloro-1,10-phenanthroline (0.14 g, 0.65 mmol) were suspended in dry methanol (20 mL) in a Schenk tube under nitrogen. The suspension was sonicated for about 5 min and the solution was stirred at 40 °C for 24 h. NH_4PF_6 (0.03 g, 0.18 mmol) dissolved in methanol (2 mL) was then added, precipitating

out a brown solid. The solid **113** was filtered off and washed with diethyl ether and then dried. Yield = 0.09 g, 56 %. IR (CH_2Cl_2) cm^{-1}: (CO) 2027 vs, 1986 vw, 1804 vw, 1748 vs, (OCO) 1605 vw, 1534 s, 1587 vw. ^{1}H-NMR (400 MHz, acetone-d_6) δ (ppm): 10.67 (dd, 4H, J = 5.0 Hz, J = 36.0 Hz), 9.34 (dd, 2H, J = 0.9 Hz, J = 8.4 Hz), 9.12 (d, 2H, J = 7.3 Hz), 8.74 (m, 4H), 8.61 (dd, 2H, J = 5.1 Hz, J = 8.1 Hz), 1.10 (q, 2H, J = 7.5Hz), -0.17 (t, 3H, J = 7.5 Hz).

5.3.28 Synthesis of [$Ru_2(CO)_5$(-dppm)$_2$] (114)

This complex was synthesized following the literature procedure [6]. [$Ru_3(CO)_{12}$] (0.64 g, 1.00 mmol) and dppm (1.16 g, 3.02 mmol) were placed in a 200 mL Parr-type reactor and toluene (100 mL) was added. The reactor was first purged three times with CO gas and pressurized with the same gas to 7 MPa. The reactor was heated to 125 °C and the reaction was stirred under these conditions for 16 h. The reaction was stopped and the reactor cooled to room temperature and vented. The reaction contents were transferred into a Schlenk flask and the volume reduced to about 50 mL. Hexane (200 mL) was added precipitating out a yellow air-sensitive solid. The solid **114** was recovered by filtration, washed with hexane and dried under reduced pressure. Yield = 1.08 g, 65 %. IR (Nujol) cm^{-1}: (CO) 1967 s, 1919 s, 1896 s, 1875 s, 1699 s.

5.3.29 Synthesis of [$Os_3(CO)_8$(-dppm)$_2$] (116)

The procedure described in Section 5.3.28 was followed in an attempt to prepare complex **115** using [$Os_3(CO)_{12}$] (0.50 g, 0.55 mmol) and dppm (0.64 g, 1.65 mmol). A higher temperature of 150 °C was used and reaction carried out for 24 h. The reaction was then stopped and the reactor was cooled to temperature and vented. The solution was left to stand for 36 h to allow an orange solid to precipitate out. The solid was filtered off, washed with hexane and dried under vacuum. Yield = 0.78 g, 90 %. The solid was identified as [$Os_3(CO)_8$(-dppm)$_2$] (**116**) based on elemental analysis, IR and NMR spectra. Anal. Calc. for $C_{58}H_{44}O_8P_4Os_3$: C, 44.55; H, 2.84. Found: C, 44.96; H, 2.80 %. IR (CH_2Cl_2) cm^{-1}: (CO) 2047 s, 1991 s, 1963 vs, 1938 s, 1896 w, 1483 w, 1435 m. ^{1}H-

NMR (300 MHz, $CDCl_3$) δ (ppm): 4.80 (t, 1H, J = 9.8 Hz). $^{31}P\{1H\}$-NMR (121 MHz, $CDCl_3$) δ (ppm): -21.81 (dd).

5.3.30 Synthesis of $[Ru_2CO)_4(\ -O_2CMe)(\ -dppm)_2][PF_6]$ (117)

A suspension of $[Ru(CO)_2(MeCO_2)]_n$ (0.66 g, 3.05 mmol)and dppm (1.14 g, 3.0 mmol) was stirred in refluxing ethanol (50 mL) for 2 h. The orange suspension was filtered through a sintered glass funnel and through Celite to remove unreacted polymer. A filtered solution of NH_4PF_6 (0.24 g, 1.50 mmol) in ethanol (5 mL) was added precipitating an air-stable yellow crystalline solid **117**. Yield = 0.99 g, 50 %. Anal. Calc. for $C_{56}H_{47}F6O_6Ru_2P_5$: C, 52.26; H, 3.68. Found: C, 51.98; H, 3.84 %. IR (CH_2Cl_2) cm^{-1}: (CO) 2024 s, 2005 vs, 1965 vs, 1935 m, (OCO) 1605 vw, 1543 m.

5.4 Catalytic alkane oxidation and alkene isomerisation reactions

5.4.1 General procedure for alkane oxidation

The alkane oxidation reactions were carried out using cyclohexane and octane as substrates and hydrogen peroxide (30 %) as oxidant following published procedures [7]. All reactions were carried out in duplicate in Schlenk tubes. The reactions were carried out in acetonitrile as solvent. In the runs carried out, a control experiment was run. Authentic samples of the oxygenated products were used as calibration standards in order to assign peaks in the chromatograms by comparison of retention times. The catalyst : substrate : oxidant ratio used was 1:1100:1100. The catalyst concentration was 7 x 10^{-4} M. The total volume was 10 mL and the reactions were carried out for 24 h at 80 °C. The samples were analyzed without workup.

5.4.2 General procedure for 1-alkene isomerisation reactions.

All the isomerisation reactions were carried out in sealed John-Young NMR tubes (Aldrich). The reaction mixture containing solvent, catalyst and olefin was cooled,

evacuated and heated in an oil bath thermostated at the prescribed temperature (± 1 °C). The reaction progress was monitored by ^{1}H-NMR analyses and then the products analyzed by GC and GC-MS to identify and quantify the final organic products. A Varian 3900 gas chromatograph equipped with an FID and a 30 m x 0.32 mm CP-Wax 52 CB column (0.25 μm film thickness) was used. The carrier gas was helium at 5.0 psi. The oven was programmed to hold at 32 °C for 4 min and then to ramp to 200 °C at 10 deg/min and hold 5 min. GC-MS analyses for peak identification were performed using an Agilent 5973 gas chromatograph equipped with MSD and a 60 m x 0.25 mm Rtx-1 column (0.5 μm film thickness). The carrier gas was helium at 0.9 ml/min. The oven was programmed to hold at 50 °C for 2 min and then ramp to 250 °C at 10 deg/min and hold for 8 min.

5.5 Electrochemistry

Cyclic voltammetry was performed at ambient temperature using a Bioanalytical Systems Inc. BAS 100W Electrochemical Analyser with a one-compartment three-electrode system comprising a platinum disk working electrode, a platinum wire auxiliary electrode and a Ag/Ag^+ reference electrode (0.01 M $AgNO_3$ and 0.1 M $[n\text{-}Bu_4N][ClO_4]$ in anhydrous acetonitrile). Measurements were made on anhydrous dichloromethane solutions which were 1 mM in sample and contained 0.1 M $[n\text{-}Bu_4N][ClO_4]$ as background electrolyte. IR compensation was employed for all measurements. Unless otherwise stated, the scan rate used was 100 mV s^{-1}. Under these conditions the ferrocene/ferrocenium couple, which was used as a reference, had an $E_{½}$ value of +0.20 V and E_p = 77 mV. All solutions were purged with argon and voltammograms were recorded under a blanket of argon. The platinum disk working electrode was polished between runs.

5.6 References

1. M. Bruce, C. Jensen, N, Jones, *Inorganic Synthesis*, 1990, **28**, 216
2. G. R. Crooks, B. F. G. Johnson, J. Lewis, I. G. Williams, G. Gamlen, *J. Chem. Soc. A*, 1969, 2761

3. M. Auzias, B. Therrien, G. Labat, H. Stoeckli-Evans, G. Süss-Fink, *Inorg. Chim. Acta,* 2006, **359**, 1012
4. M. Auzias, B. Therrien, G. Süss-Fink, P. Štěpnička, J. Ludvík, *J. Organomet. Chem.,* 2007, **692**, 755.
5. P. Pearson, C. M. Kepert, G. B. Deacon, L. Spiccia, A. C. Warden, B. W. Skeleton, A. H. White, *Inorg. Chem.,* 2004, **43**, 683.
6. G. M. Ferrence, P. E. Fanwick, C. P. Kubiak, R. J. Haines, *Polyhedron,* 1997, **16**, 1453